PATHOGENESIS OF MAMMARY CARCINOMAS ASSOCIATED WITH P53 AND RB DEFICIENCY

by Le Cheng

PATHOGENESIS OF MAMMARY CARCINOMAS ASSOCIATED WITH P53 AND RB DEFICIENCY

A Dissertation

Presented to the Faculty of the Graduate School

of Cornell University

In Partial Fulfillment of the Requirements for the Degree of

Doctor of Philosophy

by

Le Cheng

August 2010

PATHOGENESIS OF MAMMARY CARCINOMAS ASSOCIATED WITH P53 AND RB DEFICIENCY

Le Cheng, Ph. D.

Cornell University 2010

Alterations in *p53* and *Rb* tumor suppressors or their pathways are common in human breast cancer. We used newly generated *MMTV-Cre*105Ayn mice to inactivate *p53* and/or *Rb* strictly in the mammary epithelium. Inactivation of p53 led to formation of estrogen receptor positive raloxifene-responsive mammary carcinomas with features of luminal subtype B. Rb deficiency was insufficient to initiate carcinogenesis but accelerated formation of mammary carcinomas in combination with *p53* inactivation and promoted genomic instability. The recurrent amplification of the *cIAP1, cIAP2* and *Yap1* protooncogenes in the 9A1 locus was observed only in neoplasms associated with *p53* inactivation alone. However, all three genes remained overexpressed in carcinomas with *p53* and *Rb* inactivation due to elevated E2F expression and cooperated in carcinogenesis. To test involvement of the stem cell compartment in the initiation of mammary carcinogenesis we have isolated mammary stem cells (MRU; $CD24^{med}CD49f^{high}$), and their progeny (Ma-CFC, $CD24^{high}CD49f^{low}$). Loss of either *p53* or *Rb* led to an increase in the number and proliferation rate of Ma-CFC but not MRU. Both parameters were further increased in Ma-CFC pool deficient for both p53 and Rb. Notably, the resulting mammary neoplasms contained $CD24^{+}CD49f^{+}$ cells. Far fewer of $CD24^{+}CD49f^{+}$ cells were required for orthotopic transplantation, as compared to $CD24^{-}CD49f^{-}$ cell population. $CD24^{+}CD49f^{+}$ cells yielded carcinomas much

earlier and were able to reconstitute all tumor cell populations more efficiently than $CD24^{-}CD49f^{-}$ cells in secondary and tertiary transplantations. Thus, $CD24^{+}CD49f^{+}$ cells meet the definition of cancer stem cells (CSC). We have determined that CSC show higher genomic stability and are characterized by upregulation of Aldh1, cIAP1 and downregulation of microRNAs *miR-376b* and *miR-467b.* Importantly we have identified *cIAP1 and cIAP2* as targets of both miRNAs and shown that *miR-376b, miR-467b, cIAP1 and cIAP2* affect stem cell properties of CSC. Taken together, these findings establish a model of luminal subtype B mammary carcinoma, demonstrate that p53 and Rb cooperate in the maintenance of genomic integrity, identify critical role of cIAP1, cIAP2 and Yap co-expression in mammary carcinogenesis. Furthermore, our studies identify and characterize CSC and uncover miR-376b/miR-467b - cIAP1/2 pathway as a promising novel target for CSC-specific therapy.

BIOGRAPHICAL SKETCH

Le Cheng was born in Taiyuan, capital of Shanxi Province in central China. In 1997, he graduated from Taiyuan No.5 high school and entered Shanxi Medical University with major in clinical medicine. In July 2002, he graduated with a Bachelor of Science degree in clinical medicine. After two years of study he obtained Master of Science degree in watershed ecosystem graduate program at Trent University in Canada. In 2004, the author came to U.S. and enrolled into the Ph.D. program at Cornell University in the field of Environment Toxicology. He works in the laboratory of Dr. Alexander Nikitin in Department of Biomedical Sciences, and his research focuses on mammary carcinoma pathogenesis and cell biology.

ACKNOWLEDGMENTS

Any projects no matter how individual hard working, will almost certainly require input, assistance or encouragement from others, my project is no exception. I would like to thank several individuals for their intellectual, technical and emotional assistance and support in the preparation of this dissertation.

First and foremost, I am deeply grateful to my PhD advisor, Dr. Alexander Nikitin. He is an excellent mentor and a knowledgeable scientist. Thank you for giving me the opportunity to Cornell and to study such a fascinating field. Your enthusiasm, patience, motivation, and interest in my project encourage me to develop critical scientific thinking and confidence to complete scientific research and dissertation writing.

I would also like to thank my committee members: Dr. Tudorita Tumbar and Dr. David Putnam and Dr. Lee Kraus, for their excellent knowledge on study design, statistical analysis, data presentation, and valuable comments on my dissertation.

I appreciate both former and present Nikitin lab members who have been shaping a collaborative environment and memorable friendship. Much gratitude to Andrea Flesken-Nikitin, your assistance and support throughout my lab work was immeasurable. I would like to thank Dr. Zongxiang Zhou for everything he did for me. Thank you so much Anirudh Ramesh and Samantha Palmaccio for numerous help and critical discussion on my research. I would like to sincerely thank Wei Wang, Jinhyang Choi, David Corney, Chang-il Hwang, Gaofeng Jiang, Chieh-Yang Cheng and all my friends. Finally, I would like to thank our collaborators Dr. Thomas Reid and Dr.Jordi Camps for

helping us on genomic instability project.

Most importantly, I would like to thank my parents, my wife Yingying Zhao and my daughter Rebecca Xier Cheng for their encouragements and supports during all of my academic pursuits.

TABLE OF CONTENTS

LIST OF FIGURES

LIST OF TABLES

LIST OF ABBREVIATIONS

BrdU: bromodeoxyuridine

CGH: Comparative Genomic Hybridization

CK: CytoKeratin

CnSC: Cancer non Stem Cells

CSC: Cancer Stem Cells

DAPI: 4,6-diamidino 2-phenyl-indole

ERα: Estrogen Receptor α

ES: Embryonic Stem cell

FACS: Fluorescence Activated Cell Sorting

HE: Hematoxylin and Eosin

iPS: inducing Pluripotent Stem cells

Ma-CFC: Mammary Colony-Forming Cells

MaSC: Mammary Stem Cells

MEC: Mammary Epithelia Cell

MMTV: mouse mammary tumor virus

MRU: Mammary Repopulating Units

NOD/SCID: Non-Obese Diabetic/Severe Combined ImmunoDeficient

PR: Progesterone Receptor

RISC: RNA Induced Silencing Complex

SERM: Selective Estrogen Receptor Modulator

SKY: Spectral karyotyping RISC: RNA Induced Silencing Complex

SMA: Smooth Muscle Actin

UTR: Untranslated Region

WAP: Whey Acidic Protein

CHAPTER 1

INTRODUCTION*

1.1 Breast cancer etiology and pathogenesis

It is estimated that, in 2010, there will be a total of 1,529,560 new cancer cases and 569,490 cancer-related deaths in the United States, accounting for about 23% of all deaths (Jemal et al., 2010). Breast cancer is the most commonly diagnosed form of cancer and the second leading cause of cancer deaths in western women. One out of eight women will develop breast cancer during her lifetime. It is estimated that there will be approximately 207,090 new cases in the year 2010 in the U.S. alone (Jemal et al., 2010). Although our abilities to detect and treat breast cancer are improving, much remains to be understood about the pathogenesis and molecular basis of breast cancer.

The etiology of breast cancer is multifactorial and involves diet, reproductive factors, body weight, physical activity and related to hormonal imbalances. People with high caloric diet rich in animal fat and proteins, combined with a lack of physical exercise show a marked increase in incidence and mortality (Tavassoéli and Devilee, 2003). Comparative genomic hybridization (CGH) has indentified chromosomal subregions with increased DNA copy number, including 1q31-q32, 8q24, 16p13, 17q12, 17q22-24, and 20q13, and chromosomal subregions with decreased DNA copy number,

---

*Partially adopted from Cheng L et al., Toxicol Pathol. 2010;38(1):62-71. http://tpx.sagepub.com/content/38/1/62.long

including 1p32-36, 3p14-21, 7q31, 16q22, 17p13, and 18q21. A numbers of oncogenes have been found amplified, including *EFGR*, *FGFR1*, *c-MYC*, *CCND1*, and *ERBB2*. Some of tumor suppressors have been found based on DNA copy number loss, such as IGF2R, ST7, RB1CC1, CDH1, and P53 (Tavassoéli and Devilee, 2003). Regarding to familial risk of breast cancer, studies have found significantly elevated relative risks of breast cancer for female relatives of breast cancer patients. BRCA1 and BRCA2 explain about 20% of the overall familial risk of breast cancer (Tavassoéli and Devilee, 2003).

According to World Health Organization histological classification of breast tumors (a.k.a. tumors of the mammary gland), the types of breast cancer include invasive ductal carcinoma, invasive lobular carcinoma, tubular carcinoma, invasive cribriform carcinoma, medullary carcinoma, mucinous carcinoma, neuroendocrine tumors, invasive papillary carcinoma, apocrine carcinoma, and some other very rare types (Tavassoéli and Devilee, 2003).

Molecular expression profiling of breast cancers has revealed six main subtypes: luminal A, luminal B, luminal C, Erbb2 positive, basal like, and normal breast like (Hu et al., 2006; Sorlie et al., 2001; Sotiriou et al., 2003; Sotiriou and Pusztai, 2009). Luminal A subtype had the highest expression of the estrogen receptor α (ERα) gene, GATA binding protein 3, X-box binding protein 1, trefoil factor 3, hepatocyte nuclear factor 3α, and estrogen-regulated *LIV*-1**.** Luminal B subtype of tumors showed low to moderate expression of the luminal-specific genes including the ER cluster. Luminal subtype C was further distinguished from luminal subtypes A and B by the high expression of a novel set of genes whose coordinated function is unknown, which is a feature they share with the basal-like and ERBB2+ subtypes. The ERBB2+ subtype was

characterized by high expression of several genes in the ERBB2 amplicon at 17q22.24 including *ERBB2* and *GRB7.* The basal-like subtype was characterized by high expression of keratins 5 and 17, laminin, and fatty acid binding protein 7. The normal breast-like group showed the highest expression of many genes known to be expressed by adipose tissue and other nonepithelial cell types. These tumors also showed strong expression of basal epithelial genes and low expression of luminal epithelial genes (Sorlie et al., 2001; Sotiriou et al., 2003; Sotiriou and Pusztai, 2009). Importantly, *p53* mutations are most frequently associated with basal-like/ER negative (82%) ERBB2/HER2+ ER negative (71%) and luminal/ER positive luminal subtype B (40%) breast cancers (Sorlie et al., 2001) all of which have poor prognosis (Hu et al., 2006; Sorlie et al., 2001). These different subtypes may originate in distinct breast epithelial cells, or so called the cell of the origin. Better understanding of breast cancer heterogeneity and the nature of tumor initiation requires delineation of the mammary epithelial subtypes, including mammary stem cell, mammary progenitor cell, myoepithelial and luminal epithelia cells (Smalley and Ashworth, 2003).

1.2 Mammary stem cell

It is now generally accepted that the vast majority of, if not all, tissues have rare tissue-specific multipotent adult stem cells. The adult stem cell is capable of renewing itself and differentiating into one or more specialized cells (reviewed in Fuchs, 2009; reviewed in Orkin and Zon, 2008; Rossi et al., 2008). Proliferating progeny of stem cells fated for differentiation are usually named transit-amplifying cells (Smith, 2006) (Figure 1). At the same time, the

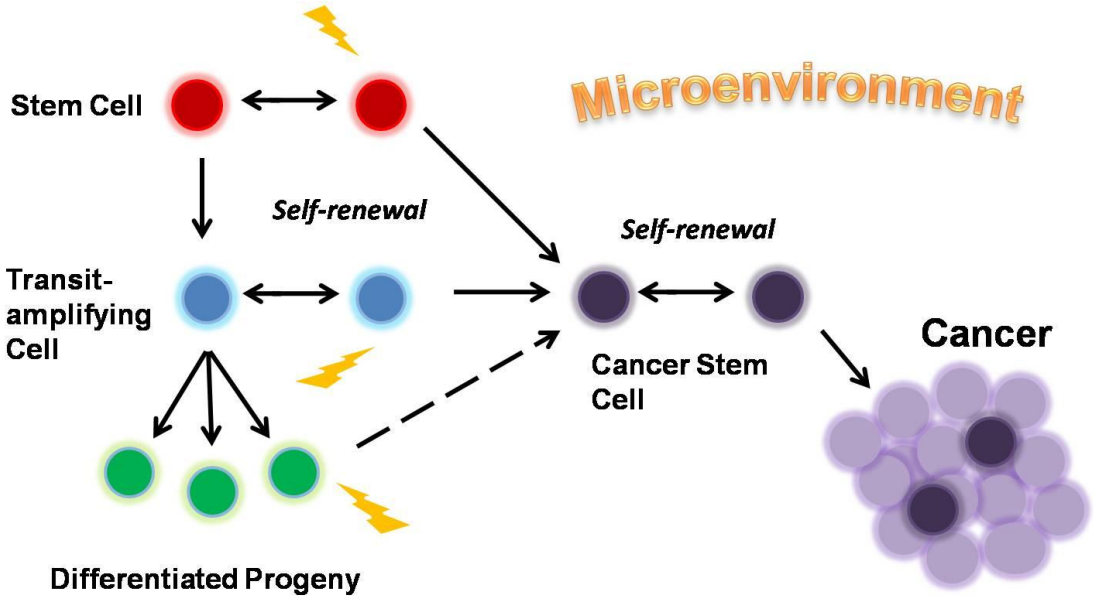

Figure 1.1 Cancer stem cell hypothesis.

Cancer stem cells (CSC, purple) have been defined as a subset of tumor cells with stem cell-like properties that are thought to be responsible for the growth, progression, metastasis, and recurrence of a tumor. Initiating mutation (yellow bolts) can occur in stem cells (red), transit-amplifying cells (blue) and possibly even their fully differentiated progeny (green).

“progenitor cell” term is commonly used to identify any dividing cell with the capacity to differentiate. This includes putative stem cells and transit-amplified cells in which presence of long-term self-renewal potential has not yet been determined or excluded, respectively.

Existence of putative mammary stem cells (MaSC) has been postulated for years due to the routine tissue renewal and massive expansions in epithelial tissue that occur in the mammary gland during pregnancy and lactation (Smalley and Ashworth, 2003). Mouse MaSC are thought to give rise to either of two progenitor cells, one which gives rise to myoepithelial cells and the second which gives rise to luminal cells, and are responsible for much of the amplification in cell number that is observed during pregnancy and lactation (Smalley and Ashworth, 2003). Recently, considerable progress has been made in the field of mammary stem cell biology, and some of approaches used in other systems have been applied to the mouse mammary gland. The mouse MaSC has been prospectively isolated by Shackleton et al. (2006) and Stingl et al. (2006), which give rise the opportunity to investigate the cell of origin of mammary cancer. Mammary repopulating units (MRU, $CD24^{med}CD49f^{high}$) are MaSC, and their progeny mammary colony-forming cells (Ma-CFC, $CD24^{high}CD49f^{low}$) are mammary progenitors (Stingl et al., 2006). Cleared mammary fat pad transplantations have been a standard technique in mammary gland biology. In this experiment, the mammary epithelium is cleared from a young mouse, leaving only the fat pad. Cells transplanted into this fat pad can regenerate the lobulo-alveolar mammary tree after 4 weeks (Smalley and Ashworth, 2003).

1.3 Cancer stem cell

The concept of cancer stem cells (CSC) or tumor initiating cells can be traced back to the “embryonal rest” theory proposed by Conheim and Durante in 19th century (reviewed in Sell, 2004). The modern version stipulates that CSC represent a subpopulation of neoplastic cells which may be responsible for cancer initiation and/or progression (reviewed in Cho and Clarke, 2008; Clarke and Fuller, 2006; reviewed in Matoso et al., 2008; Nafus and Nikitin, 2009; Visvader and Lindeman, 2008; Wicha et al., 2006).

CSC have stem cell-like properties that include the active expression of telomerase and common stem cell genes, the activation of antiapoptotic pathways, and an increased ability to migrate and metastasize. Furthermore, CSC may remain relatively quiescent and have mechanisms enhancing their survival and multi-drug resistance, enabling them to evade traditional cancer therapies that target rapidly dividing cells (reviewed in Matoso et al., 2008; reviewed in Visvader and Lindeman, 2008).

It is important to emphasize that the term CSC does not refer to the cell of origin. Rather, CSC have been named as such in reference to the properties that CSC share with normal stem cells (Wicha et al., 2006). CSC may originate from mutated stem, transit-amplifying, or differentiated cells (Figure 1). It is also possible that an initial mutation occurs within a stem cell, but subsequent mutations occur in its downstream progeny that gain stem cell properties during neoplastic transformation and function as CSC.

Traditionally, CSC have been identified through sphere formation in culture with matrigel or extra-low attachment conditions and serial transplantation of cellular subpopulation isolated with a Fluorescence Activated Cell Sorting (FACS) into animal models (reviewed in Nafus and

Nikitin, 2009). Both assays are designed to determine the self-renewal and differentiation potential of a cell population and are adapted from adult stem cell research, where they have been used to characterize adult stem cells (Shackleton et al., 2006) in neural tissues (Doetsch et al., 1999) the prostate (Tsujimura et al., 2002; Xin et al., 2003), and the mammary gland (Shackleton et al., 2006; Stingl et al., 2006). After transplantation of the CSC population and subsequent tumor formation, the primary tumor is expected to mirror the phenotypic heterogeneity of the original tumor and exhibit the ability to self-renewal in serial transplantations. It is commonly anticipated that they have higher tumorigenicity as compared to other neoplastic cells (reviewed in Nafus and Nikitin, 2009). The tumorigenic potential is usually tested by transplantations of serially diluted cell populations.

To date, in humans, CSC have been identified in a number of malignancies, including leukemia (Bonnet and Dick, 1997; Lapidot et al., 1994), breast cancer (Al-Hajj et al., 2003), prostate cancer (Collins et al., 2005), brain tumors (Bao et al., 2006), ovarian cancer (Alvero et al., 2009; Szotek et al., 2006; Zhang et al., 2008b) and colon cancer (O'Brien et al., 2007; Ricci-Vitiani et al., 2007) (Table 1). These studies typically rely upon xenotransplantation of the CSC subpopulation of a human tumor into mice with a compromised immune system (typically non-obese diabetic/severe combined immunodeficient (NOD/SCID) mice). Albeit useful, these systems do not accurately reflect such critical for carcinogenesis factors as microenvironment and the immune response (Frese and Tuveson, 2007). Consistent with these limitations of xenotransplantations, a recent study by Quintana and colleagues (Quintana et al., 2008) demonstrated that by using severely immunocompromised (IL2rγ null NOD/SCID) mice about 25% of

Table 1.1 Identification and characterization of human and mouse stem cells

Organ	Human/mouse model	Markers	% of CSC	Assays	References
Brain	Human	$CD133^+$	3.5-46.3	Sphere formation; xenograft (brain); serial transplantation	Singh et al. 2003; Singh et al. 2004
	Ptc$^{+/-}$ mouse	$CD15^+$	~15-20	Transplantation	Read et al. 2009
	p53$^{+/-}$, *Nf1*$^{flox/flox}$, *hGFAP-Cre* mouse	$GFAP^+$	N/A*	Lineage tracing; anatomic location	Y. Zhu et al. 2005
Intestine	Human	$CD133^+$	2.5 ± 1.4	Sphere formation; xenograft (subcutaneous; renal); serial transplantation	O'Brien et al. 2007; Ricci-Vitiani et al. 2007
	Lgr5-CreER^{T2}, *Apc*$^{flox/flox}$ mouse	$Lgr5^+$	N/A	Lineage tracing; anatomic location	Barker et al. 2009
	Bmi1Cre-ER/+ Ctnnb1$^{lox(ex3)}$ mouse	$Bmi1^+$	N/A	Lineage tracing; anatomic location	Sangiorgi and Capecchi 2008
	Prom1$^{+/C\text{-}L}$ *Ctnnb1*$^{lox(ex3)}$ mouse	$CD133^+$	N/A	Lineage tracing; anatomic location, clone formation	L. Zhu et al. 2009
Mammary gland	Human	$CD44^+$ $CD24^{-/low}$ $CD326^+$; $CD133^+$	2-4	Sphere formation; xenograft (mammary fat pad); serial transplantation	Al-Hajj et al. 2003
	p53$^{-/-}$ mouse	$CD24^{hi}$ $CD29^{hi}$	5-10	Sphere formation; serial transplantation; serial dilution	S. Zhang et al. 2008
	MMTV-Wnt1 mouse	Thy^+ $CD24^+$	1-4	Serial transplantation; serial dilution	Cho et al. 2008
	MMTV-Wnt1 mouse	$CD29^{low}$ $CD24^+$ $CD61^+$	~15	Serial transplantation; serial dilution	Vaillant et al. 2008
Ovary	Human	$CD44^+$	6.3-19	Sphere formation; xenograft (subcutaneous); serial transplantation	Alvero et al. 2009
	MISRII-TAg and LSL-K-ras$^{G12D/+}$ *Pten*$^{flox/flox}$ *mice*	Hoechst 33342^{low} $Bcrp1^+$	6.28	Transplantation	Szotek et al. 2006
Prostate	Human	$CD44^+$ $\alpha2\beta1^{hi}$ $CD133^+$	0.1	Colony-formation; long-term serial culture	Collins et al. 2005
	Probasin-Cre, Pten$^{flox/flox}$ mouse	$Sca1^+$, $BCL2^+$	N/A	Anatomic location	Wang et al. 2006
	Probasin-Cre, p53$^{flox/flox}$*Rb*$^{flox/flox}$ mouse	$Sca1^+$, $CK8^+$/Syn^+	N/A	Anatomic location	Zhou, Flesken-Nikitin, and Nikitin 2007

Abbreviations: N/A, not available

unselected melanoma cells formed tumors as compared to 0.1-0.0001% of cells able to form tumors in less immunocompromised NOD/SCID mice.

In animal model, the CSC subpopulation has been described in several mouse models of mammary carcinogenesis using different cell surface markers (Cho et al., 2008; Vaillant et al., 2008; Zhang et al., 2008a). For example, in the *MMTV-Wnt1* mouse model of mammary cancer, a $Thy1^{+}CD24^{+}$ cancer cell population was found to be highly enriched for CSC relative to the non $Thy1^{+}CD24^{+}$ population (Cho et al., 2008). In the *p53*-null mammary tumor model described by Zhang and colleagues (Zhang et al., 2008a), a subpopulation of cells expressing high levels of CD24 and CD29 ($Lin^{-}CD24^{H}CD29^{H}$), which accounts for 5-10% of total mammary epithelial cell population, has been identified as CSC by limiting dilution in cell culture mammosphere assays and subsequent transplantation *in vivo*. However, it should be noted that all experiments in this study were performed on tumors derived by transplantation of p53-null mammary epithelium cells into cleared mammary fat pads. Thus, it remains to be demonstrated if observed results can be reproduced in an autochthonous sporadic mouse model of mammary carcinogenesis.

1.4 Tumor suppressor genes p53 and Rb

Cancer formation, including breast carcinogenesis, is a multistep process. Many of these steps involve inactivation of tumor suppressor genes or activation of oncogenes, followed by sequential accumulation of genetic alternations (Fialkow, 1974; Nowell, 1976). p53 and Rb are central to these processes and they are frequently altered in the breast cancer. p53 is evolutionally ancient transcription factor, the primordial function of which in

early metazoans may have been to coordinate transcriptional responses to stress and damage (Junttila and Evan, 2009). Initially, p53 was considered to be a tumor oncogene with transforming abilities. Only during the late 1980s, it was revealed that p53 acts as an important tumor suppressor (Nigro et al., 1989). Since then, evidences demonstrated that either it or its attendant upstream or downstream pathways are functionally inactivated in virtually all cancers, and 20-40% of sporadic breast carcinomas have mutation in the *p53* gene (Brosh and Rotter, 2009); (Borresen-Dale, 2003). *p53* regulates genes critical for cell cycle, apoptosis, senescence, and DNA repair, thus preventing genomic instability (Meek, 2009, Riley, 2008 #35; Riley et al., 2008). In normal unstressed cells, p53 activity is maintained at low levels, which mediates many physiological functions. These low levels are primarily maintained by the ubiquitin-mediated degradation of p53, a process regulated by E3 ubiquitin ligase MDM2 and the related protein MDM4 (Brosh and Rotter, 2009). Activation of p53 by DNA damage is principally mediated through post-translational modification (phosphorylation). The phosphorylation of p53 impairs interactions between p53 and MDM2 and MDM4, inhibiting the capacity of MDM2 and MDM4 to suppress p53 transcription and promote p53 degradation (Junttila and Evan, 2009).

Mice homozygous for the *p53* null allele ($p53^{-/-}$) develop lymphomas or sarcomas within the first 3 month after birth (Donehower et al., 1992; Jacks et al., 1994). Development of some mammary tumors was observed in $p53^{+/-}$ mice, but only on the BALB/c background (Kuperwasser et al., 2000). With the development of Cre-*LoxP* technology, spontaneous mammary tumor development was observed after inactivation of wild-type *p53* by either its deletion (Lin et al., 2004; Liu et al., 2007) or expression of dominant negative

form carrying *p53.R270H* point mutation (Wijnhoven et al., 2005). Unfortunately, the interpretation of experiments has been somewhat complicated by formation of lymphomas and/or other neoplasms due to expression of Cre transgene in lymphocytes and other tissues.

Rb is essential for cell cycle control and exerts diverse effects on cell proliferation, survival and differentiation (Burkhart and Sage, 2008). More recently the role of Rb in control of genomic instability has been demonstrated in cell culture experiments and mouse model of liver neoplasia (Reed et al., 2009; Seeley et al., 2007). Transcription factor E2F family is primary downstream effectors of the Rb. In mammals, the E2F family includes eight genes (E2F1-8), which give rise to nine different proteins. E2F1, E2F2, and E2F3a, which interact only with Rb, are mainly transcription activators and have been referred to as activator E2F. E2F4-8 are largely transcription repressor and have been referred to as repressor E2Fs.

The observation that *Rb* is inactivated in 20-35% of human breast cancers suggests that it has an important role in the pathogenesis of these neoplasms (Bosco et al., 2007; Scambia et al., 2006). Additionally, other defects of *Rb* pathway components, such as *Cyclin D1* overexpression, and $p16^{INK4A}$ loss are frequently observed in human breast cancer (Geradts and Wilson, 1996; Roy and Thompson, 2006). However, in serial transplantations of *Rb* mutant mammary anlagen no significant differences were found in outgrowth of pRb-deficient and wild-type epithelia (Robinson et al., 2001). At the same time, transgenic mice expressing cyclin D1 in the mammary gland, hence deprived of functional Rb family proteins (Rb, p107 and p130), develop mammary neoplasms adenocarcinoma (Wang et al., 1994). Accordingly, It has been reported that inactivation of the whole Rb family by T_{121m} a fragment of

SV40 T antigen, leads to development of mammary tumors (Simin et al., 2004). It is known that *p107* and *p130* could play overlapping roles of *Rb* in many cell types of mouse (Dannenberg et al., 2000; Luo et al., 1998; Robanus-Maandag et al., 1998; Sage et al., 2000). Nevertheless, *Rb* itself also has distinct functions that are not compensated by *p107* and *p130*. Unlike $Rb^{-/-}$ mice which die during embryonic development (Clarke et al., 1992; Jacks et al., 1992; Lee et al., 1992), simultaneous disruption of *p107* and *p130* is compatible with embryonic development up to birth (Cobrinik et al., 1996). The earlier lethal outcome of germline *Rb* mutation indicates that *Rb* possesses indispensable functions. Furthermore, *Rb* family members have different binding capacities for E2F-binding sites (Dyson, 1998), indicating these genes can repress different subsets of genes. Finally, mutations in *Rb* but not in p107 and p130 genes are found in many types of human cancers (Weinberg, 1995). The tumor suppressor function that distinguishes *Rb* from other pocket proteins may originate from the biochemical properties of *Rb* or the nature of the cell in which *Rb* functions. All these evidences suggest the distinct function of *Rb*. However, the exact function of *Rb* itself in mammary carcinogenesis is still not clear, because of lacking mouse model with specifically inactivation of *Rb* in mammary gland epithelium.

There is extensive crosstalk between p53 and Rb, which influences vital cellular decisions. Rb-E2F acts both upstream and downstream of the Arf-p53 pathway (Sherr and McCormick, 2002). While the cooperation of p53 and Rb in restricting carcinogenesis and activating many apoptotic genes may vary in different cellular context. Because mutation of *p53 and Rb* pathway often coexist in human breast carcinoma, to investigate the interactions between *Rb* and *p53* signaling pathways in breast epithelial cell are critical for

understanding the formation and development of breast cancer. A mouse model with conditional loss both *p53* and *Rb* in the mammary epithelium may significantly facilitate addressing this issue.

1.5 p53, Rb and stem cells

To date, *p53* has been shown to induce differentiation of embryonic stem cells and to limit the capacity of stem cells to self-renew (Lin et al., 2005; Qin et al., 2006; Rosso et al., 2006), mediate the onset of senescence of endothelial progenitor cells (Rosso et al., 2006) and negatively regulate proliferation and survival of neural stem cells (Meletis et al., 2006). More recently, it was reported that reducing the activity of p53 in mouse embryonic fibroblasts improves the efficiency and kinetics of generating inducing pluripotent stem (iPS) cells, even in the absence of Myc retrovirus, and using only Oct4 and Sox2 (Hong et al., 2009; Kawamura et al., 2009; Li et al., 2009; Marion et al., 2009; Utikal et al., 2009).

Rb also plays a prominent role in controlling several aspects of stem cell biology, including control stem cell cycle progression, senescence and tissue homeostasis (Galderisi et al., 2006; Wenzel et al., 2007; Wildwater et al., 2005). Mouse fibroblasts lacking *Rb* function form spheres and undergo reprogramming to a cancer stem cell phenotype (Liu et al., 2009). In spite of these studies, the potential functions for *p53* and *Rb* in MaSC have not been yet addressed. Since *p53* and *Rb* mutations are common in breast carcinoma, it is of particular interest to study if molecular mechanisms controlling MaSCs self-renewal and mammary cancer initiation and progression are shared.

1.6 microRNAs

microRNAs (miRNAs) are short (around 22 nucleotides) endogenous, single-stranded RNA molecules that regulate gene expression. Like transcription factors, miRNAs regulate diverse cellular pathways and most biological processes. The first miRNA *lin-4* (22 nucleotides) was discovered by Ambros and colleagues in a screen for genes required for post embryonic development in *C.elegans* in 1993 (Bartel, 2004). The *lin-4* locus produces a single strand RNA that is partially complementary to sequence in the 3' Untranslated Region (UTR) of its regulatory target, the lin-14 mRNA (Ghildiyal and Zamore, 2009). Initially thought to represent a rare class of regulatory molecules, the number of identified miRNA is now over 110 in *C.elegans*, 140 in the Drosophila, and 400 in humans-numbers that approach about 1-2% of the number of protein –coding genes in these respective species (Bartel, 2009).

miRNA genes are typically transcribed by RNA polymerase II into primary miRNA transcripts (pri-miRNA), and their transcription is sensitive to the polymerase II inhibitor α-amanitin treatment. The pri-miRNA is then endonucleolytically cleaved by the nuclear micro-processor complex, consisting of RNase III enzyme Drosha and the RNA binding protein Pasha, to generate a precursor-miRNA (pre-miRNA) which has stem-loop secondary structure about 70bp in size (Ghildiyal and Zamore, 2009; Winter et al., 2009). Pre-miRNA is exported to the cytoplasm by an exportin-5 mediated complex. Once in the cytoplasm, pre-miRNA is cleaved by the RNase III Dicer, generating a roughly 22 nucleotide miRNA duplex with two nucleotides protruding as overhangs at each 3' end. Double-strand miRNA needs to be separated into functional guides strand, and passenger strand. The mature

miRNA (functional guides strand) is selectively recruited into the RNA Induced Silencing Complex (RISC). The passenger strand is subsequently degraded. This functional asymmetry depends on the thermodynamic stability of the base pairs at the two ends of the strand: the miRNA strand with the less stable base pair at its 5' end is loaded into RISC. The RISC-miRNA complex is able to bind to the 3' UTR of target mRNA (Winter et al., 2009).

The mechanism by which a miRNA regulates its mRNA target reflects both the specific Argonaut protein into which the small RNA is loaded and the extent of complementarily between the miRNA and the mRNA. Most miRNA pair with their targets through only a limited region of sequence nucleotides 2-8 at the 5' end of the miRNA are designed the seed sequence. The seed is primary specificity determinant for target selection (Bartel, 2009). The canonical binding sites are described as 7mer-A1, 7mer-m8, and 8mer, which respectively refer to an Adenine at site 1 of the mRNA and matches at nucleotides 2-7, 2-8, and 2-8 with an Adenine at site 1. 3' supplementary of compensatory sites may also have a role in predicting the targets of miRNA (Bartel, 2009). More often, though, the 3' end of the miRNA is involved in binding with the Argonaut protein that is a part of the RISC[13]. This information was used to develop programming algorithms to create databases for miRNA targets based on conservation across species and stringency of seed sequence binding to 3' UTRs (Bartel, 2009). The miRNA repress translation and direct degradation of their mRNA. The small size of the seed means that a single miRNA can regulate many, even hundreds of different genes.

Several miRNAs have been identified as being biologically significant. miRNA have been linked to roles in differentiation and development. Expression of *miR-181b* in hematopoietic stem cells initiates differentiation into

the B-cell lineage (Chen et al., 2004). *miR-375* has been shown to decrease insulin secretion in pancreatic β cells (Poy et al., 2004). Several miRNAs have been shown to act as tumor suppressors and oncogenes (sometimes called an onco-miRNA). Clear examples of tumor suppressor miRNAs are *miR-15a* and *miR-16-1.* Deletion of *miR-15a* and *miR-16-1* increased the levels of the anti-apoptotic protein BCL2 in B cells resulting in a dysregulation of negative selection of B cells via apoptosis (Cimmino et al., 2005).

Some miRNAs are targets of important cellular transcription factors, indicating significant co-evolution between these two classes of regulatory molecules. For example, the transcription factor forkhead box P3 (FOXP3), which is involved in the development and function of T regulatory cells, can upregulate the expression of *miR-155 (Lodish et al., 2008)*. Finally, it was recently shown in our lab and in other labs, that the transcription factor p53 is able to upregulate the *miR-34* family expression in response to DNA stress and damage (Corney et al., 2007). The *miR-34* family is predicted to repress genes that promote the cell cycle. As a consequence, an increase in *miR-34* expression correlates to increased senescence and apoptosis (He et al., 2007). It has also been shown that miR-34 inhibits CD44+/CD133+ pancreatic cancer stem cell self-renewal *in vitro* and tumor-initiation *in vivo* (Ji et al., 2009). Michael Clark's group recently found that three clusters, miR-200c-141, miR-200b-200a-429, and miR-183-96-182 were downregulated in human breast cancer stem cells, normal human and murine mammary stem/progenitor cells, and embryonal carcinoma cells. miR-200c strongly suppressed the ability of normal mammary stem cells to form mammary ducts and tumor formation driven by human breast CSC in vivo (Shimono et al., 2009).

Given the important role of miRNAs, it is worth to further find the novel miRNAs that are important for cancer formation, and CSC self-renewal and differentiation. Mouse model of mammary carcinoma will certainly accelerate the discovery of such miRNAs.

1.7 Mouse model of mammary carcinoma

The biology of the mouse mammary gland has been studied for many years. The normal development, lactation related changes and spontaneous tumors in the mouse mammary gland are well characterized. Better models of xenotransplantation that employs a humanized mouse may alleviate some pitfalls. For example, in some xenotransplantation models, human cytokines are exogenously administered or human stromal cells are co-injected to provide the transplanted CSC with a more native growth environment (reviewed in Pearson and Sanchez Alvarado, 2008). However, the complete understanding of cancer pathogenesis, particularly its earliest stages, is impossible without accurate autochthonous immunocompetent mouse models of human cancer. Recent advances in genetic engineering and genomics have provided the necessary tools to generate genetically defined mouse models which replicate such essential features of human cancers as molecular and histological characteristics, the process of cancer initiation and progression, and response to therapeutics (Table 1, reviewed in Frese and Tuveson, 2007; Jonkers and Berns, 2002; Van Dyke and Jacks, 2002).

The first generation of mouse models of breast cancer occurred between 1920 and 1960. Mammary tumors were induced by the treatment of certain genetic hormonal and environmental factors (e.g. mouse mammary tumor virus (MMTV), chemical carcinogens) to the mice (Allred and Medina,

2008; Borowsky, 2007). The second generation roughly starts from 1980 to 1995, and is based on overexpression of specific oncogenes or deletion of specific tumor suppressor genes transgenic mice. Genes, including c-myc, p53, c-neu, SV40LT, TGFα, H-ras, cyclin D1, etc., have been studied, and over 100 mouse models have been generated (Allred and Medina, 2008; Borowsky, 2007; Cardiff et al., 2000). The third generation starts around 1997 and includes conditional models prepared by activating or deleting specific genes in the mammary gland at a specific time. The commonly used promoters for mammary epithelium-specific gene expression are mouse mammary tumor virus long terminal repeat (MMTV-LTR), the whey acidic protein (WAP), and the beta-lactoglobin promoter (Allred and Medina, 2008; Borowsky, 2007).

Nevertheless, there are several important limitations in these models. For example, one limitation is that the promoters used in these models usually lead to gene mutation or overexpression in the majority of mammary epithelial cells, and this is in contrast to low frequency stochastic mutations in the human sporadic cancers. It would be ideal to have specific promoter target a low percentage of the specific cell population (stem cells, progenitors, differentiated cells). Furthermore, few of models accurately represent ER positive or progesterone receptor dependent human breast cancer, which account for over 70% or 50% human breast cancer, respectively. In addition, because of insufficient tissue specificity of used promoters, mice often develop other types of tumors, for example lymphomas, in addition to mammary neoplasms. Thus the next generation of models allowing introduction of genetic alterations restricted to the mammary epithelium and occurring in stochastic manner is required.

1.8 Concluding remarks and project overview

Due to heterogeneity in morphology, genetic lesions, molecular profiles, cell surface markers, cell proliferation kinetics, and response to therapy, studies of pathogenesis of breast cancer have been challenging, thereby leading to insufficient development of advanced diagnostic and treatment approaches. Modeling human cancer of the mammary gland in mouse provides unique opportunities for studying the nature of the disease, as well as for testing new diagnostic tools, drugs, therapeutic approaches, and strategies for prevention and control.

In this study, I generated a mouse model of mammary cancer by Cre-*loxP*-mediated conditional inactivation of *p53* and *Rb* specifically in mammary epithelial cells. In chapter 2, the generation of a mouse mammary cancer will be described in detail. My studies demonstrated that *p53* inactivation led to formation of estrogen receptor positive raloxifene-responsive mammary carcinomas with features of luminal subtype B. Rb deficiency was insufficient to initiate carcinogenesis but promoted genomic instability and growth rate of neoplasms associated with *p53* inactivation. I identified critical role of cIAP1, cIAP2 and Yap co-expression in mammary carcinogenesis and provided an explanation for the lack of recurrent amplifications of *cIAP1*, *cIAP2* and *Yap1.*

In chapter 3, I isolated and functionally proved the existence of CSC in our mouse model of mammary carcinoma associated with *p53* and/or Rb deficiency using the mammary stem cell markers CD24 and CD49f. I demonstrated that CSC have less percentage of comet tail positive cell and lower expression of Mad2 than cancer non stem cells (CnSC), indicating that CSC may have more stable genome than CnSC. Accordingly, CSC have less DNA damage after γ irradiation as compared to CnSC. To test involvement of

the stem cell compartment in the initiation of mammary carcinogenesis I have isolated mammary stem cells (MRU; $CD24^{med}CD49f^{high}$), and their progeny (Ma-CFC, $CD24^{high}CD49f^{low}$). I found that loss of either *p53* or *Rb* leads to an increase in the number and proliferation rate of Ma-CFC but not MRU. Both parameters are further increased in Ma-CFC pool deficient for both p53 and Rb. These results demonstrate that mammary progenitor cells may be the principle targets for malignant transformation, and indentify expansion of progenitor cell pool as a novel cooperative effect of *p53* and *Rb* inactivation on carcinogenesis.

In chapter 4, I studied the role of miRNA in CSC. I identified that miR-376b and miR-467b, the most downregulated in both CSC and Mammary Stem Cells (MaSC) as compared to CnSC and normal differentiated mammary epithelial cells. I demonstrated that cIAP1 and cIAP2 are direct targets of miR-376b and miR-467b. Furthermore, I showed that miR-376b and miR-467b reconstitution, as well as cIAP1/2 siRNA-mediated knockdown decrease mammosphere formation. These studies indicate that miR-376b/ miR-467b - cIAP1/2 pathway is important for CSC self-renewal and may represent a new target for development of new therapeutic approaches.

Finally I summarized the studies and outline the future directions in chapter 5.

REFERENCES

Al-Hajj, M., Wicha, M. S., Benito-Hernandez, A., Morrison, S. J., and Clarke, M. F. (2003). Prospective identification of tumorigenic breast cancer cells. Proc Natl Acad Sci U S A *100*, 3983-3988.

Allred, D. C., and Medina, D. (2008). The relevance of mouse models to understanding the development and progression of human breast cancer. J Mammary Gland Biol Neoplasia *13*, 279-288.

Alvero, A. B., Chen, R., Fu, H. H., Montagna, M., Schwartz, P. E., Rutherford, T., Silasi, D. A., Steffensen, K. D., Waldstrom, M., Visintin, I., and Mor, G. (2009). Molecular phenotyping of human ovarian cancer stem cells unravels the mechanisms for repair and chemoresistance. Cell Cycle *8*, 158-166.

Bao, S., Wu, Q., McLendon, R. E., Hao, Y., Shi, Q., Hjelmeland, A. B., Dewhirst, M. W., Bigner, D. D., and Rich, J. N. (2006). Glioma stem cells promote radioresistance by preferential activation of the DNA damage response. Nature *444*, 756-760.

Bartel, D. P. (2004). MicroRNAs: genomics, biogenesis, mechanism, and function. Cell *116*, 281-297.

Bartel, D. P. (2009). MicroRNAs: target recognition and regulatory functions. Cell *136*, 215-233.

Bonnet, D., and Dick, J. E. (1997). Human acute myeloid leukemia is organized as a hierarchy that originates from a primitive hematopoietic cell. Nat Med *3*, 730-737.

Borowsky, A. (2007). Special considerations in mouse models of breast cancer. Breast Dis *28*, 29-38.

Borresen-Dale, A. L. (2003). TP53 and breast cancer. Hum Mutat *21*, 292-300.

Bosco, E. E., Wang, Y., Xu, H., Zilfou, J. T., Knudsen, K. E., Aronow, B. J., Lowe, S. W., and Knudsen, E. S. (2007). The retinoblastoma tumor suppressor modifies the therapeutic response of breast cancer. J Clin Invest *117*, 218-228.

Brosh, R., and Rotter, V. (2009). When mutants gain new powers: news from the mutant p53 field. Nat Rev Cancer *9*, 701-713.

Burkhart, D. L., and Sage, J. (2008). Cellular mechanisms of tumour suppression by the retinoblastoma gene. Nat Rev Cancer *8*, 671-682.

Cardiff, R. D., Anver, M. R., Gusterson, B. A., Hennighausen, L., Jensen, R. A., Merino, M. J., Rehm, S., Russo, J., Tavassoli, F. A., Wakefield, L. M.*, et al.* (2000). The mammary pathology of genetically engineered mice: the consensus report and recommendations from the Annapolis meeting. Oncogene *19*, 968-988.

Chen, C. Z., Li, L., Lodish, H. F., and Bartel, D. P. (2004). MicroRNAs modulate hematopoietic lineage differentiation. Science *303*, 83-86.

Cho, R. W., and Clarke, M. F. (2008). Recent advances in cancer stem cells. Curr Opin Genet Dev *18*, 48-53.

Cho, R. W., Wang, X., Diehn, M., Shedden, K., Chen, G. Y., Sherlock, G., Gurney, A., Lewicki, J., and Clarke, M. F. (2008). Isolation and molecular characterization of cancer stem cells in MMTV-Wnt-1 murine breast tumors. Stem Cells *26*, 364-371.

Cimmino, A., Calin, G. A., Fabbri, M., Iorio, M. V., Ferracin, M., Shimizu, M., Wojcik, S. E., Aqeilan, R. I., Zupo, S., Dono, M.*, et al.* (2005). miR-15 and miR-16 induce apoptosis by targeting BCL2. Proc Natl Acad Sci U S A *102*, 13944-13949.

Clarke, A. R., Maandag, E. R., van Roon, M., van der Lugt, N. M., van der

Valk, M., Hooper, M. L., Berns, A., and te Riele, H. (1992). Requirement for a functional Rb-1 gene in murine development. Nature *359*, 328-330.

Clarke, M. F., and Fuller, M. (2006). Stem cells and cancer: two faces of eve. Cell *124*, 1111-1115.

Cobrinik, D., Lee, M. H., Hannon, G., Mulligan, G., Bronson, R. T., Dyson, N., Harlow, E., Beach, D., Weinberg, R. A., and Jacks, T. (1996). Shared role of the pRB-related p130 and p107 proteins in limb development. Genes Dev *10*, 1633-1644.

Collins, A. T., Berry, P. A., Hyde, C., Stower, M. J., and Maitland, N. J. (2005). Prospective identification of tumorigenic prostate cancer stem cells. Cancer Res *65*, 10946-10951.

Corney, D. C., Flesken-Nikitin, A., Godwin, A. K., Wang, W., and Nikitin, A. Y. (2007). MicroRNA-34b and MicroRNA-34c are targets of p53 and cooperate in control of cell proliferation and adhesion-independent growth. Cancer Res *67*, 8433-8438.

Dannenberg, J. H., van Rossum, A., Schuijff, L., and te Riele, H. (2000). Ablation of the retinoblastoma gene family deregulates G(1) control causing immortalization and increased cell turnover under growth-restricting conditions. Genes Dev *14*, 3051-3064.

Doetsch, F., Caille, I., Lim, D. A., Garcia-Verdugo, J. M., and Alvarez-Buylla, A. (1999). Subventricular zone astrocytes are neural stem cells in the adult mammalian brain. Cell *97*, 703-716.

Donehower, L. A., Harvey, M., Slagle, B. L., McArthur, M. J., Montgomery, C. A., Jr., Butel, J. S., and Bradley, A. (1992). Mice deficient for p53 are developmentally normal but susceptible to spontaneous tumours. Nature *356*, 215-221.

Dyson, N. (1998). The regulation of E2F by pRB-family proteins. Genes Dev *12*, 2245-2262.

Fialkow, P. J. (1974). The origin and development of human tumors studied with cell markers. N Engl J Med *291*, 26-35.

Frese, K. K., and Tuveson, D. A. (2007). Maximizing mouse cancer models. Nat Rev Cancer *7*, 645-658.

Fuchs, E. (2009). The tortoise and the hair: slow-cycling cells in the stem cell race. Cell *137*, 811-819.

Galderisi, U., Cipollaro, M., and Giordano, A. (2006). The retinoblastoma gene is involved in multiple aspects of stem cell biology. Oncogene *25*, 5250-5256.

Geradts, J., and Wilson, P. A. (1996). High frequency of aberrant p16(INK4A) expression in human breast cancer. Am J Pathol *149*, 15-20.

Ghildiyal, M., and Zamore, P. D. (2009). Small silencing RNAs: an expanding universe. Nat Rev Genet *10*, 94-108.

He, L., He, X., Lim, L. P., de Stanchina, E., Xuan, Z., Liang, Y., Xue, W., Zender, L., Magnus, J., Ridzon, D.*, et al.* (2007). A microRNA component of the p53 tumour suppressor network. Nature *447*, 1130-1134.

Hong, H., Takahashi, K., Ichisaka, T., Aoi, T., Kanagawa, O., Nakagawa, M., Okita, K., and Yamanaka, S. (2009). Suppression of induced pluripotent stem cell generation by the p53-p21 pathway. Nature *460*, 1132-1135.

Hu, Z., Fan, C., Oh, D. S., Marron, J. S., He, X., Qaqish, B. F., Livasy, C., Carey, L. A., Reynolds, E., Dressler, L.*, et al.* (2006). The molecular portraits of breast tumors are conserved across microarray platforms. BMC Genomics *7*, 96.

Jacks, T., Fazeli, A., Schmitt, E. M., Bronson, R. T., Goodell, M. A., and Weinberg, R. A. (1992). Effects of an Rb mutation in the mouse. Nature *359*,

295-300.

Jacks, T., Remington, L., Williams, B. O., Schmitt, E. M., Halachmi, S., Bronson, R. T., and Weinberg, R. A. (1994). Tumor spectrum analysis in p53-mutant mice. Curr Biol *4*, 1-7.

Jemal, A., Siegel, R., Xu, J., and Ward, E. Cancer Statistics, 2010. CA Cancer J Clin. *in press*.

Ji, Q., Hao, X., Zhang, M., Tang, W., Yang, M., Li, L., Xiang, D., Desano, J. T., Bommer, G. T., Fan, D*., et al.* (2009). MicroRNA miR-34 inhibits human pancreatic cancer tumor-initiating cells. PLoS One *4*, e6816.

Jonkers, J., and Berns, A. (2002). Conditional mouse models of sporadic cancer. Nat Rev Cancer *2*, 251-265.

Junttila, M. R., and Evan, G. I. (2009). p53--a Jack of all trades but master of none. Nat Rev Cancer *9*, 821-829.

Kawamura, T., Suzuki, J., Wang, Y. V., Menendez, S., Morera, L. B., Raya, A., Wahl, G. M., and Belmonte, J. C. (2009). Linking the p53 tumour suppressor pathway to somatic cell reprogramming. Nature *460*, 1140-1144.

Kuperwasser, C., Hurlbut, G. D., Kittrell, F. S., Dickinson, E. S., Laucirica, R., Medina, D., Naber, S. P., and Jerry, D. J. (2000). Development of spontaneous mammary tumors in BALB/c p53 heterozygous mice. A model for Li-Fraumeni syndrome. Am J Pathol *157*, 2151-2159.

Lapidot, T., Sirard, C., Vormoor, J., Murdoch, B., Hoang, T., Caceres-Cortes, J., Minden, M., Paterson, B., Caligiuri, M. A., and Dick, J. E. (1994). A cell initiating human acute myeloid leukaemia after transplantation into SCID mice. Nature *367*, 645-648.

Lee, E. Y., Chang, C. Y., Hu, N., Wang, Y. C., Lai, C. C., Herrup, K., Lee, W. H., and Bradley, A. (1992). Mice deficient for Rb are nonviable and show

defects in neurogenesis and haematopoiesis. Nature *359*, 288-294.

Li, H., Collado, M., Villasante, A., Strati, K., Ortega, S., Canamero, M., Blasco, M. A., and Serrano, M. (2009). The Ink4/Arf locus is a barrier for iPS cell reprogramming. Nature *460*, 1136-1139.

Lin, S. C., Lee, K. F., Nikitin, A. Y., Hilsenbeck, S. G., Cardiff, R. D., Li, A., Kang, K. W., Frank, S. A., Lee, W. H., and Lee, E. Y. (2004). Somatic mutation of p53 leads to estrogen receptor alpha-positive and -negative mouse mammary tumors with high frequency of metastasis. Cancer Res *64*, 3525-3532.

Lin, T., Chao, C., Saito, S., Mazur, S. J., Murphy, M. E., Appella, E., and Xu, Y. (2005). p53 induces differentiation of mouse embryonic stem cells by suppressing Nanog expression. Nat Cell Biol *7*, 165-171.

Liu, X., Holstege, H., van der Gulden, H., Treur-Mulder, M., Zevenhoven, J., Velds, A., Kerkhoven, R. M., van Vliet, M. H., Wessels, L. F., Peterse, J. L.*, et al.* (2007). Somatic loss of BRCA1 and p53 in mice induces mammary tumors with features of human BRCA1-mutated basal-like breast cancer. Proc Natl Acad Sci U S A *104*, 12111-12116.

Liu, Y., Clem, B., Zuba-Surma, E. K., El-Naggar, S., Telang, S., Jenson, A. B., Wang, Y., Shao, H., Ratajczak, M. Z., Chesney, J., and Dean, D. C. (2009). Mouse fibroblasts lacking RB1 function form spheres and undergo reprogramming to a cancer stem cell phenotype. Cell Stem Cell *4*, 336-347.

Lodish, H. F., Zhou, B., Liu, G., and Chen, C. Z. (2008). Micromanagement of the immune system by microRNAs. Nat Rev Immunol *8*, 120-130.

Luo, R. X., Postigo, A. A., and Dean, D. C. (1998). Rb interacts with histone deacetylase to repress transcription. Cell *92*, 463-473.

Marion, R. M., Strati, K., Li, H., Murga, M., Blanco, R., Ortega, S., Fernandez-

Capetillo, O., Serrano, M., and Blasco, M. A. (2009). A p53-mediated DNA damage response limits reprogramming to ensure iPS cell genomic integrity. Nature *460*, 1149-1153.

Matoso, A., Zhou, Z., Hayama, R., Flesken-Nikitin, A., and Nikitin, A. Y. (2008). Cell lineage-specific interactions between Men1 and Rb in neuroendocrine neoplasia. Carcinogenesis *29*, 620-628.

Meek, D. W. (2009). Tumour suppression by p53: a role for the DNA damage response? Nat Rev Cancer *9*, 714-723.

Meletis, K., Wirta, V., Hede, S. M., Nister, M., Lundeberg, J., and Frisen, J. (2006). p53 suppresses the self-renewal of adult neural stem cells. Development *133*, 363-369.

Nafus, M. G., and Nikitin, A. Y. (2009). Cancer stem cells in solid tumours, In Stem Cell Biology in Health and Disease, T. Dittmar, and K. Zänker, eds. Springer, Springer, Dordrecht, p. 295-326.

Nigro, J. M., Baker, S. J., Preisinger, A. C., Jessup, J. M., Hostetter, R., Cleary, K., Bigner, S. H., Davidson, N., Baylin, S., Devilee, P., and et al. (1989). Mutations in the p53 gene occur in diverse human tumour types. Nature *342*, 705-708.

Nowell, P. C. (1976). The clonal evolution of tumor cell populations. Science *194*, 23-28.

O'Brien, C. A., Pollett, A., Gallinger, S., and Dick, J. E. (2007). A human colon cancer cell capable of initiating tumour growth in immunodeficient mice. Nature *445*, 106-110.

Orkin, S. H., and Zon, L. I. (2008). Hematopoiesis: an evolving paradigm for stem cell biology. Cell *132*, 631-644.

Pearson, B. J., and Sanchez Alvarado, A. (2008). Regeneration, stem cells,

and the evolution of tumor suppression. Cold Spring Harb Symp Quant Biol *73*, 565-572.

Poy, M. N., Eliasson, L., Krutzfeldt, J., Kuwajima, S., Ma, X., Macdonald, P. E., Pfeffer, S., Tuschl, T., Rajewsky, N., Rorsman, P., and Stoffel, M. (2004). A pancreatic islet-specific microRNA regulates insulin secretion. Nature *432*, 226-230.

Qin, H., Yu, T., Qing, T., Liu, Y., Zhao, Y., Cai, J., Li, J., Song, Z., Qu, X., Zhou, P.*, et al.* (2006). Regulation of apoptosis and differentiation by p53 in human embryonic stem cells. J Biol Chem *282*, 5842-52

Quintana, E., Shackleton, M., Sabel, M. S., Fullen, D. R., Johnson, T. M., and Morrison, S. J. (2008). Efficient tumour formation by single human melanoma cells. Nature *456*, 593-598.

Reed, C. A., Mayhew, C. N., McClendon, A. K., Yang, X., Witkiewicz, A., and Knudsen, E. S. (2009). RB has a critical role in mediating the in vivo checkpoint response, mitigating secondary DNA damage and suppressing liver tumorigenesis initiated by aflatoxin B1. Oncogene *28*, 4434-4443.

Ricci-Vitiani, L., Lombardi, D. G., Pilozzi, E., Biffoni, M., Todaro, M., Peschle, C., and De Maria, R. (2007). Identification and expansion of human colon-cancer-initiating cells. Nature *445*, 111-115.

Riley, T., Sontag, E., Chen, P., and Levine, A. (2008). Transcriptional control of human p53-regulated genes. Nat Rev Mol Cell Biol *9*, 402-412.

Robanus-Maandag, E., Dekker, M., van der Valk, M., Carrozza, M. L., Jeanny, J. C., Dannenberg, J. H., Berns, A., and te Riele, H. (1998). p107 is a suppressor of retinoblastoma development in pRb-deficient mice. Genes Dev *12*, 1599-1609.

Robinson, G. W., Wagner, K. U., and Hennighausen, L. (2001). Functional

mammary gland development and oncogene-induced tumor formation are not affected by the absence of the retinoblastoma gene. Oncogene *20*, 7115-7119.

Rossi, D. J., Jamieson, C. H., and Weissman, I. L. (2008). Stems cells and the pathways to aging and cancer. Cell *132*, 681-696.

Rosso, A., Balsamo, A., Gambino, R., Dentelli, P., Falcioni, R., Cassader, M., Pegoraro, L., Pagano, G., and Brizzi, M. F. (2006). p53 Mediates the accelerated onset of senescence of endothelial progenitor cells in diabetes. J Biol Chem *281*, 4339-4347.

Roy, P. G., and Thompson, A. M. (2006). Cyclin D1 and breast cancer. Breast *15*, 718-727.

Sage, J., Mulligan, G. J., Attardi, L. D., Miller, A., Chen, S., Williams, B., Theodorou, E., and Jacks, T. (2000). Targeted disruption of the three Rb-related genes leads to loss of G(1) control and immortalization. Genes Dev *14*, 3037-3050.

Scambia, G., Lovergine, S., and Masciullo, V. (2006). RB family members as predictive and prognostic factors in human cancer. Oncogene *25*, 5302-5308.

Seeley, S. L., Bosco, E. E., Kramer, E., Parysek, L. M., and Knudsen, E. S. (2007). Distinct roles for RB loss on cell cycle control, cisplatin response, and immortalization in Schwann cells. Cancer Lett *245*, 205-217.

Sell, S. (2004). Stem cell origin of cancer and differentiation therapy. Crit Rev Oncol Hematol *51*, 1-28.

Shackleton, M., Vaillant, F., Simpson, K. J., Stingl, J., Smyth, G. K., Asselin-Labat, M. L., Wu, L., Lindeman, G. J., and Visvader, J. E. (2006). Generation of a functional mammary gland from a single stem cell. Nature *439*, 84-88.

Sherr, C. J., and McCormick, F. (2002). The RB and p53 pathways in cancer.

Cancer Cell *2*, 103-112.

Shimono, Y., Zabala, M., Cho, R. W., Lobo, N., Dalerba, P., Qian, D., Diehn, M., Liu, H., Panula, S. P., Chiao, E.*, et al.* (2009). Downregulation of miRNA-200c links breast cancer stem cells with normal stem cells. Cell *138*, 592-603.

Simin, K., Wu, H., Lu, L., Pinkel, D., Albertson, D., Cardiff, R. D., and Van Dyke, T. (2004). pRb inactivation in mammary cells reveals common mechanisms for tumor initiation and progression in divergent epithelia. PLoS Biol *2*, E22.

Smalley, M., and Ashworth, A. (2003). Stem cells and breast cancer: A field in transit. Nat Rev Cancer *3*, 832-844.

Smith, A. (2006). A glossary for stem-cell biology. Nature *441*, 1060.

Sorlie, T., Perou, C. M., Tibshirani, R., Aas, T., Geisler, S., Johnsen, H., Hastie, T., Eisen, M. B., van de Rijn, M., Jeffrey, S. S.*, et al.* (2001). Gene expression patterns of breast carcinomas distinguish tumor subclasses with clinical implications. Proc Natl Acad Sci U S A *98*, 10869-10874.

Sotiriou, C., Neo, S. Y., McShane, L. M., Korn, E. L., Long, P. M., Jazaeri, A., Martiat, P., Fox, S. B., Harris, A. L., and Liu, E. T. (2003). Breast cancer classification and prognosis based on gene expression profiles from a population-based study. Proc Natl Acad Sci U S A *100*, 10393-10398.

Sotiriou, C., and Pusztai, L. (2009). Gene-expression signatures in breast cancer. N Engl J Med *360*, 790-800.

Stingl, J., Eirew, P., Ricketson, I., Shackleton, M., Vaillant, F., Choi, D., Li, H. I., and Eaves, C. J. (2006). Purification and unique properties of mammary epithelial stem cells. Nature *439*, 993-997.

Szotek, P. P., Pieretti-Vanmarcke, R., Masiakos, P. T., Dinulescu, D. M., Connolly, D., Foster, R., Dombkowski, D., Preffer, F., Maclaughlin, D. T., and

Donahoe, P. K. (2006). Ovarian cancer side population defines cells with stem cell-like characteristics and Mullerian Inhibiting Substance responsiveness. Proc Natl Acad Sci U S A *103*, 11154-11159.

Tavassoéli, F.A., Devilee, P. (2003). Pathology and Genetics of Tumours of the Breast and Female Genital Organs: The International Agency for Research on Cancer Press, Lyon, France, 432.

Tsujimura, A., Koikawa, Y., Salm, S., Takao, T., Coetzee, S., Moscatelli, D., Shapiro, E., Lepor, H., Sun, T. T., and Wilson, E. L. (2002). Proximal location of mouse prostate epithelial stem cells: a model of prostatic homeostasis. J Cell Biol *157*, 1257-1265.

Utikal, J., Polo, J. M., Stadtfeld, M., Maherali, N., Kulalert, W., Walsh, R. M., Khalil, A., Rheinwald, J. G., and Hochedlinger, K. (2009). Immortalization eliminates a roadblock during cellular reprogramming into iPS cells. Nature *460*, 1145-1148.

Vaillant, F., Asselin-Labat, M. L., Shackleton, M., Forrest, N. C., Lindeman, G. J., and Visvader, J. E. (2008). The mammary progenitor marker CD61/beta3 integrin identifies cancer stem cells in mouse models of mammary tumorigenesis. Cancer Res *68*, 7711-7717.

Van Dyke, T., and Jacks, T. (2002). Cancer modeling in the modern era: progress and challenges. Cell *108*, 135-144.

Visvader, J. E., and Lindeman, G. J. (2008). Cancer stem cells in solid tumours: accumulating evidence and unresolved questions. Nat Rev Cancer *8*, 755-768.

Wang, T. C., Cardiff, R. D., Zukerberg, L., Lees, E., Arnold, A., and Schmidt, E. V. (1994). Mammary hyperplasia and carcinoma in MMTV-cyclin D1 transgenic mice. Nature *369*, 669-671.

Weinberg, R. A. (1995). The retinoblastoma protein and cell cycle control. Cell *81*, 323-330.

Wenzel, P. L., Wu, L., de Bruin, A., Chong, J. L., Chen, W. Y., Dureska, G., Sites, E., Pan, T., Sharma, A., Huang, K.*, et al.* (2007). Rb is critical in a mammalian tissue stem cell population. Genes Dev *21*, 85-97.

Wicha, M. S., Liu, S., and Dontu, G. (2006). Cancer stem cells: an old idea--a paradigm shift. Cancer Res *66*, 1883-1890; discussion 1895-1886.

Wijnhoven, S. W., Zwart, E., Speksnijder, E. N., Beems, R. B., Olive, K. P., Tuveson, D. A., Jonkers, J., Schaap, M. M., van den Berg, J., Jacks, T.*, et al.* (2005). Mice expressing a mammary gland-specific R270H mutation in the p53 tumor suppressor gene mimic human breast cancer development. Cancer Res *65*, 8166-8173.

Wildwater, M., Campilho, A., Perez-Perez, J. M., Heidstra, R., Blilou, I., Korthout, H., Chatterjee, J., Mariconti, L., Gruissem, W., and Scheres, B. (2005). The RETINOBLASTOMA-RELATED gene regulates stem cell maintenance in Arabidopsis roots. Cell *123*, 1337-1349.

Winter, J., Jung, S., Keller, S., Gregory, R. I., and Diederichs, S. (2009). Many roads to maturity: microRNA biogenesis pathways and their regulation. Nat Cell Biol *11*, 228-234.

Xin, L., Ide, H., Kim, Y., Dubey, P., and Witte, O. N. (2003). In vivo regeneration of murine prostate from dissociated cell populations of postnatal epithelia and urogenital sinus mesenchyme. Proc Natl Acad Sci U S A *100 Suppl 1*, 11896-11903.

Zhang, M., Behbod, F., Atkinson, R. L., Landis, M. D., Kittrell, F., Edwards, D., Medina, D., Tsimelzon, A., Hilsenbeck, S., Green, J. E.*, et al.* (2008a). Identification of tumor-initiating cells in a p53-null mouse model of breast

cancer. Cancer Res *68*, 4674-4682.

Zhang, S., Balch, C., Chan, M. W., Lai, H. C., Matei, D., Schilder, J. M., Yan, P. S., Huang, T. H., and Nephew, K. P. (2008b). Identification and characterization of ovarian cancer-initiating cells from primary human tumors. Cancer Res *68*, 4311-4320.

CHAPTER 2

RB INACTIVATION ACCELERATES NEOPLASTIC GROWTH AND SUBSTITUTES FOR RECURRENT AMPLIFICATION OF CIAP1, CIAP2 AND YAP1 IN SPORADIC MAMMARY CARCINOMA ASSOCIATED WITH P53 DEFICIENCY*

2.1 Abstract

Genetically defined mouse models offer an important tool to identify critical secondary genetic alterations with relevance to human cancer pathogenesis. We used newly generated *MMTV-Cre*105Ayn mice to inactivate *p53* and/or *Rb* strictly in the mammary epithelium and to determine recurrent genomic changes associated with deficiencies of these genes. *p53* inactivation led to formation of estrogen receptor positive raloxifene-responsive mammary carcinomas with features of luminal subtype B. Rb deficiency was insufficient to initiate carcinogenesis but promoted genomic instability and growth rate of neoplasms associated with *p53* inactivation. Genome-wide analysis of mammary carcinomas identified a recurrent amplification at chromosome band 9A1, a locus orthologous to human 11q22, which contains protooncogenes *cIAP1 (Birc2), cIAP2 (Birc3)* and *Yap1.* Interestingly, this amplicon was preferentially detected in carcinomas carrying wild-type *Rb*. However, all three

---

* Accepted for publication as **Cheng L,** et al., *Rb* inactivation accelerates neoplastic growth and substitutes for recurrent amplification of the *Birc2, Birc3 and Yap1* in sporadic mammary carcinoma associated with p53 deficiency. Oncogene, *in press*

genes were overexpressed in carcinomas with *p53* and *Rb* inactivation, likely due to E2F-mediated transactivation, and cooperated in carcinogenesis according to gene knockdown experiments. These findings establish a model of luminal subtype B mammary carcinoma, identify a critical role of *cIAP1, cIAP2* and *Yap1* co-expression in mammary carcinogenesis and provide an explanation for the lack of recurrent amplifications of *cIAP1*, *cIAP2* and *Yap1* in some tumors with frequent Rb-deficiency, such as mammary carcinoma.

2.2 Introduction

Breast cancer is the most commonly diagnosed malignancy and the second leading cause of cancer-related deaths among women in the US (Jemal et al., 2010). *p53* and *Rb* and their pathways are frequently altered in breast cancer. *p53* is a transcription factor that regulates genes critical for cell cycle, apoptosis, senescence, and DNA repair, thus preventing genomic instability (Meek, 2009; Riley et al., 2008). Mutation of *p53* is the most common genetic abnormality found in human cancer, and occurs in 20-40% of sporadic breast carcinomas (Borresen-Dale, 2003). Furthermore, *p53* is mutated in individuals with Li-Fraumeni syndrome, a heritable condition in which early-onset breast cancers are the most prevalent cancer types (Malkin, 1994). According to gene expression profiling, *p53* mutations are most frequently associated with basal-like/ER negative (82%), ERBB2/HER2 overexpressing/ER negative (71%) and luminal/ER positive subtype B (40%) breast cancers (Sorlie et al., 2001) all of which have poor prognosis (Hu et al., 2006; Sorlie et al., 2001).

Mice homozygous for the *p53* null allele ($p53^{-/-}$) develop lymphomas or sarcomas within first three months (Donehower et al., 1992; Jacks et al.,

1994). Development of some mammary tumors has been observed in *p53*$^{+/-}$ mice, but only on the BALB/c background (Kuperwasser et al., 2000). With the development of Cre-*loxP* technology, spontaneous mammary carcinogenesis has been observed after inactivation of wild-type *p53* by either its deletion (Lin et al., 2004; Liu et al., 2007) or expression of a dominant negative form carrying a *p53.R270H* point mutation (Wijnhoven et al., 2005). Unfortunately, the interpretation of experiments has been somewhat complicated by formation of lymphomas and/or other neoplasms due to expression of the Cre transgene in lymphocytes and other tissues.

Rb is essential for cell cycle control and exerts diverse effects on cell proliferation, survival and differentiation (Burkhart and Sage, 2008). More recently the role of Rb in control of genomic instability has been demonstrated in cell culture experiments and in a mouse model of liver neoplasia (Knudsen et al., 2006; Reed et al., 2009). The observation that *Rb* is inactivated in 20-35% of human breast cancers, suggests that it has an important role in the pathogenesis of these neoplasms (Bosco et al., 2007; Scambia et al., 2006). Additionally, other defects in *Rb* pathway components, such as *Cyclin D1* overexpression, and *p16*^{INK4A} loss are frequently observed in human breast cancer (Geradts and Wilson, 1996; Roy and Thompson, 2006). However, in serial transplantations of *Rb* mutant mammary anlagen no significant differences were found in outgrowth of Rb-deficient and wild-type epithelia (Robinson et al., 2001). At the same time, transgenic mice expressing cyclin D1 in the mammary gland, hence deprived of functional Rb family proteins (Rb, p107 and p130), develop mammary neoplasms (Wang et al., 1994). Accordingly, it has been reported that inactivation of the whole Rb family by T_{121m}, a fragment of SV40 T antigen, also leads to mammary carcinogenesis

(Simin et al., 2004).

In agreement with the potential cooperation between *p53* and *Rb* inactivation, p53 deficiency results in acceleration of mammary carcinogenesis in the T_{121m} model (Simin et al., 2004) as well as in transgenic mice expressing SV40 large T antigen (Li et al., 2000) which inactivates both p53 and all proteins of Rb family. However, it remains unclear if selective inactivation of *Rb* has any effect on cancer initiation or progression.

To ensure mammary epithelium-restricted Cre expression, we have established a new FVB/N *MMTV-Cre* transgenic mouse line (*MMTV-Cre*105Ayn) which does not express Cre in lymphocytes and other tissues. Using this line we demonstrate that conditional inactivation of *p53* results in ER-positive mammary carcinomas which carry recurrent amplification of cellular inhibitor of apoptosis (cIAP)1, cIAP2 and *Yap1*. *Rb* inactivation alone is insufficient to initiate mammary carcinogenesis but promotes genetic instability and accelerates neoplastic growth. Interestingly, lack of Rb suppresses genomic amplification of *cIAP1*, *cIAP2* and *Yap1*. However, expression levels of these genes remain elevated and their knockdown decreases tumorigenicity, thereby indicating critical importance of the *cIAP1*, *cIAP2* and *Yap1* in mammary carcinogenesis.

2.3 Materials and methods

Generation of transgene. To generate the mouse mammary tumor virus-long terminal repeat *(MMTV-LTR)-Cre-Methallothionein-I (MT-I) pA* plasmid, a HindIII-XhoI DNA fragment containing the 1.48 kb *MMTV-LTR* from pMAM (Clontech, Palo Alto, CA, USA) and XhoI-EcoRI fragment containing the 3.7 kb *Cre-MT-I* from pBS185 (Invitrogen, Carlsbad, CA, USA) were

simultaneously cloned into HindIII-EcoRI restricted pBluescript. The 5.18 kb KpnI digested *MMTV-Cre* transgene was isolated with GELase (Epicentre Technologies, Madison, WI, USA) and injected into pronuclei of fertilized oocytes of superovulated FVB/N mice at a concentration of 2 ng/ml.

Mouse breeding. Male *MMTV-Cre* transgenic mice were crossed with female $p53^{floxP/floxP}$ $(p53^{L/L})$, $Rb^{floxP/floxP}$ $(Rb^{L/L})$ or $p53^{floxP/floxP}Rb^{floxP/floxP}$ $(p53^{L/L}Rb^{L/L})$ mice to achieve, respectively, inactivation of *p53* or *Rb* alone or together in the mammary epithelium. The resulting *MMTV-Cre*, $p53^{L/L}$, *MMTV-Cre*, $Rb^{L/L}$ and *MMTV-Cre*, $p53^{L/L}$ $Rb^{L/L}$ mice, were designated as $p53^{ME-/-}$, $Rb^{ME-/-}$, and $p53^{ME-/-}$ $Rb^{ME-/-}$, respectively. Reporter mice *Gt(ROSA)26SorTM1sor* (Chai et al., 2000) were obtained from the Jackson Laboratory (Bar Harbor, Maine, USA). Mice carrying conditional alleles for *p53* (floxed exon 2-10) and/or *Rb* (floxed exon 19) were described elsewhere (Jonkers et al., 2001; Marino et al., 2000). All mice were placed on FVB/N genetic background by at least 10 backcrosses and only nulliparous females were used. All mice were maintained identically, following recommendations of the Institutional Laboratory Animal Use and Care Committee.

Genotyping. $p53^{L/L}$ *and* $Rb^{L/L}$ mice were identified as described (Flesken-Nikitin et al., 2003). *MMTV-Cre* transgenic mice have been identified by primers Cre5' (5' GGA CAT GTT CAG GGA TCG CCA GGC G 3') and Cre3' (5' GCA TAA CCA GTG AAA CAG CAT TGC TG 3'). PCR amplification of Cre results in 296 bp DNA fragment. The PCR temperature profile was 94^{o}C for 30 seconds, 60^{o}C for 1 minute, and 72^{o}C for 2 minutes with extension of the last cycle for 10 minutes at 72^{o}C.

Pathological evaluation. Mice were euthanized when mammary tumors reached 1 cm in diameter, at 700 days of age or after becoming

moribund. Animals were evaluated grossly during necropsy and subjected to the systematic pathological assessment as descried earlier (Flesken-Nikitin et al., 2003; Zhou et al., 2006; Zhou et al., 2007). All lesions were identified according to the Classification of Neoplasia of Genetically Engineered Mice (Cardiff et al., 2000) endorsed by the Mouse Models of Human Cancer Consortium (NIH/NCI).

Histochemical analyses. Immunohistochemical analysis of paraffin sections of paraformaldehyde-fixed tissue was done by a modified avidin-biotin-peroxidase (ABC, Vector Laboratories, Burlingame, CA, USA) technique with antigen retrieval as described earlier (Zhou et al., 2006). Primary antibodies to the following antigens were used: cytokeratin 5 (CK5, Covance, Berkeley, CA, USA, 1:1000), CK6, (Covance, 1:300), CK8 (Developmental Studies Hybridoma Bank, University of Iowa, 1:50), Ki67 (Novocastra Laboratories, Bannockburn, IL, USA, 1:1000), smooth muscle actin (SMA, Spring Bioscience, Fermont, CA, USA, 1:300), ERα (Santa Cruz, Santa Cruz, CA, USA, 1:200), and progesterone receptor (PR; Santa Cruz, 1:200). Enzymatic detection of bacterial β-galactosidase was performed as previously described (Flesken-Nikitin et al., 2003; Zhou et al., 2007). All quantitative analyses were performed on digitally captured images as described in (Zhou et al., 2006).

Western blotting analyses. Proteins were determined using Western blotting, as described previously (Matoso et al., 2008). Briefly, cells were rinsed twice on ice with ice-cold PBS, extracted in lysis buffer and total protein (30 µg) was separated on 6%-10% SDS-PAGE gels in Mini-Protean II cell (BioRad, Hercules, CA, USA). Following transfer to polyvinylidene difluoride membranes, proteins were blocked with 5% milk (w/v), 0.1% Tween 20 in TBS

for 1 hours, followed by exposure to the before exposure to the primary antibody to ERα (1:200, Santa Cruz), PR (1:200, Santa Cruz), E2F1 (1:500, Cell Signaling, Danvers, MA, USA), E2F3 (1:200, Santa Cruz), Mad2 (1:200, Santa Cruz), Yap1 (1:300, Cell Signaling), cIAP1 (1:300, Abcam, Cambridge, MA, USA) and Gapdh (1:1000, Advanced immunochemical Inc, Long Beach, CA, USA) overnight at 4°C. After incubation with secondary horseradish peroxidase–conjugated antibody (Santa Cruz), the filters were incubated with SuperSignal® West Pico Chemiluminescent Substrate (Pierce, Rockford, IL, USA). To normalize for differences in loading, the blots were stripped and reprobed with mouse anti-Gapdh monoclonal antibody.

Cell culture. To prepare mammary epithelial cells, mammary glands were dissected from 3-6 months old females. The tissue was placed in EpiCult-B medium (StemCell Technologies, Vancouver, BC, Canada) with 5% fetal bovine serum (FBS, Sigma, St. Louis, MO, USA), 300 U/ml collagenase (StemCell Technologies) and 100U/ml hyaluronidase (StemCell Technologies) for 8 hours at 37^{o}C. The dissociated tissue fragments were resuspended in 0.64% NH_4Cl for lysis of the red blood cells. The further dissociation of fragments was obtained by their gentle pipetting in 0.25% Trypsin (Cellgro, Manassas, VA, USA) for 2 min, followed by placing into 5 mg/ml dispase (StemCell Technologies) and 0.1 mg/ml DNase (StemCell Technologies) for 3 min and filtration through a 40-µm mesh. Derivation of MCN1, MCN2, MCN3 and MCN9 cells is described in Table 2.3. Cells were cultured in HAM's medium DMEM/F12, 50/50 Mix; Cellgro), supplemented with 5% fetal bovine serum, 2 mM L-Glutamine, 1 mM Na-Pyruvate, 5 µg/ml Insulin. MCF7 (ATCC, Manassas, VA), a human breast cancer cell line, was cultured in DMEM containing 10% fetal bovine serum and 10 µg/ml Insulin. All cell lines were

maintained in 5% CO_2 atmosphere at 37°C.

Mammary fat pad transplantation, raloxifene and siRNA treatment. The number 4 pair of mammary glands of anaesthetized, 3-week-old female FVB mice were surgically exposed under sterile condition. 10^6 tumor cells in 100 µl sterile PBS were injected into the cleared fat pad using a Hamilton syringe and 25 gauge needle and tumor formation was monitored daily. Tumors were measured in three dimensions with a caliper, and the volume was calculated using the formula: $V = \pi/ 6 (L \times W \times H)$. Raloxifene (10 µg/g body weight in DMSO) was applied s.c. to mice every two days from second day after cell transplantation. For siRNA treatment, 100 µl 5 µM siRNA was mixed with 100 µl atelocollagen (AteloGene™ Systemic Use; Koken, Tokyo, Japan) and administered locally as described (Minakuchi et al., 2004). All mice were monitored daily and the experiments were terminated after tumors reached volume 0.8 cm^3.

Proliferation and apoptosis assays. One day before the raloxifene (Sigma) or *cIAP1*, *cIAP2*, and *Yap1* siRNAs (Dharmacon, Lafayette, CO, USA) treatment, tumor cells were passaged to 12-well culture plates. Next day, after tumor cells reached around 80% confluence, they were treated with raloxifene in DMSO or 100 nM of siRNAs for 24 hours in 5% CO_2 at 37°C. After 24 hours, tumor cells were incubated with 3 µg/ml bromodeoxyuridine (BrdU, Sigma) for 2 hours at 37°C, and BrdU was detected by staining with anti-BrdU antibody (1:50, Becton Dickinson, Franklin Lakes, NJ, USA) as described previously (Nikitin and Lee, 1996). Apoptosis was detected by staining of cells with anti-cleaved Caspase 3 antibody (Cell Signaling, 1:200). All quantitative analyses were performed on digitally captured images as described in (Zhou et al., 2006). For estimation of proliferating and apoptotic cells, 10 images with

area 10,384 μm^2 each were analyzed in each sample. Approximately 2,000 cells were analyzed in a single experiment. Experiments were performed in triplicate.

Comparative genomic hybridization assay. Genomic DNA of mammary tumors from *p53*$^{ME-/-}$ and *p53*$^{ME-/-}$*; Rb*$^{ME-/-}$ mice was assayed by comparative genomic hybridization. Genomic DNA from FVB female mice was used as a control. Genomic DNA was extracted using DNeasy Tissue Kit (Qiagen, Valencia, CA, USA). Mouse BAC genomic arrays, each composed of 6500 RPCI-23 or PRCI-24 clones, were prepared in the Roswell Park Cancer Institute Microarray Core Facility (Buffalo, NY, USA). Data were analyzed as previously described (Zhou et al., 2006).

Spectral karyotyping (**SKY).** Metaphase chromosomes for SKY were prepared after exposure of the tumor cells (passages 2-6) to colcemid (Roche, Indianapolis, IN) for 1–3 hours at a final concentration of 0.1 μg/ml. The cells were lysed in hypotonic solution (0.075 M KCl), and the nuclei were fixed in methanol and acetic acid (3:1). SKY was performed as described by Liyanage et al. (Liyanage et al., 1996). For protocol details, please refer to Padilla-Nash et al. (Padilla-Nash et al., 2007). Differentially labeled chromosome-specific painting probes were hybridized simultaneously onto metaphase chromosomes. Images were acquired with a custom-designed triple-pass filter using the SpectraCube SD200 (Applied Spectral Imaging, Vista, CA, USA) connected to an epifluorescence microscope (DMRXA, Leica Microsystems, Wetzlar, Germany). At least 10 metaphases and corresponding inverted 4,6-diamidino 2-phenyl-indole (DAPI) images were analyzed for each tumor, and karyotypes were defined using the nomenclature rules from the International Committee on Standardized Genetic Nomenclature for Mice (Davisson, 1994).

Neutral comet and centrosome assays. Cells were processed for comet tail formation using neutral comet assay condition according to the manufacturer's instructions (Trevigen, Gaithersburg, MD, USA). Briefly, cells were mixed with LMAgarose at a ratio of 1:10 (v/v) and then plated onto CometSlides at 4°C in the dark for 10 min. Slides were immersed in prechilled lysis solution at 4°C for 30 min, and then transferred to a horizontal electrophoresis apparatus at 20V for 10 min. Finally, slides were stained with SYBR Green I, and imaged by fluorescence microscopy. Centrosomes were detected with mouse monoclonal γ-tubulin antibody (1:5000, Sigma), followed by FITC-conjugated anti-mouse secondary antibodies (Jackson ImmunoResearch Laboratories, West Grove, PA, USA) and DAPI (10 µg/ml Sigma) nuclear counterstaining.

AdCre, E2F1 knockdown and doxorubicin treatment assays. Cells were treated with AdCre or blank adenovirus ($6x10^7$ pfu/ml at MOI 200, the University of Iowa Gene Transfer Vector Core, Iowa City, IA, USA) for 2 hours in 5% CO_2 atmosphere at 37°C and cultured for a further 48 hours and processed for mRNA isolation. In order to knockdown E2F1, cells were transfected with *E2F1* siRNAs (Dharmacon) for 24 hours in 5% CO_2 at 37°C and then processed for mRNA isolation. For doxorubicin treatment assay, cells were treated with 2 µg/ml doxorubicin for 12 hours, followed by RNA isolation and analysis.

Real-time PCR and RT-PCR. Quantitative PCR analysis was carried out on an ABI 7500 HT Real-time PCR System (Applied Biosystems, Foster City, CA, USA). The primers for quantification of gene copy number are described in (Zender et al., 2006). Quantification of mRNA expression of *cIAP1*, *cIAP2*, *Yap1, E2F1* and *Mad2* was performed using TaqMan probes

(Applied Biosystems). Samples were normalized to the level of *Gapdh*.

Statistical Analyses. All statistical analyses in this study were done using InStat 3.06 and Prism 5.01 software (GraphPad, Inc., San Diego, CA, USA) as described previously (Zhou et al., 2006).

2.4 Results

Generation of *MMTV-Cre* transgenic mice. To avoid genetic background variations and frequent lymphomas due to Cre expression in lymphocytes and other tissues we generated mice expressing *Cre* under the control of *MMTV-LTR* (Fig 2.1A) and screened founders for exclusive expression of Cre in the mammary epithelium after their crosses with *Gt(ROSA)26SorTM1sor* reporter mice. One out of five tested lines, FVB/N *Tg(MMTV-Cre)105Ayn* expressed Cre selectively in the mammary epithelium (Table 2.1 and Fig 2.2) Furthermore, no lymphomas or other non-mammary neoplasms were observed in crosses of this line with $p53^{floxP/floxP}$ mice. Therefore, it has been chosen for all subsequent experiments and will be described as *MMTV-Cre.*

Inactivation of *p53* in mammary epithelium leads to neoplastic lesions and *Rb* loss accelerates carcinogenesis. Conditional inactivation of *p53* was sufficient for mammary carcinogenesis in our model. Eight out of 16 (50%) $p53^{ME-/-}$ mice (see Materials and Methods for abbreviations) and none out of eight (0%) $Rb^{ME-/-}$ mice developed mammary neoplasms by 700 days of age (Fig 2.1B). Fifteen out of 17 (88%) $p53^{ME-/-}$ $Rb^{ME-/-}$ mice developed mammary neoplasms. All neoplasms arising in $p53^{ME-/-}$ and $p53^{ME-/-}$ $Rb^{ME-/-}$ mice have lost both copies of *p53* and *p53* and *Rb*, respectively (Fig 2.3). The median tumor-free survival of $p53^{ME-/-}$ $Rb^{ME-/-}$ mice was significantly shorter

Figure 2.1 Generation and characterization of a mouse model of mammary carcinoma associated with p53 and Rb deficiency.

A, Generation and characterization of *MMTV-Cre* transgenic mice. (Top) The *MMTV-Cre* transgene consists of the 1.48 kb *MMTV-LTR* promoter followed by the 1.1 kb *Cre* gene and the 1.2 kb *MT-1* polyadenylation site. (Bottom) Identification of *MMTV-Cre* transgenic mice by PCR genotyping. 296 bp and 194 bp fragments are diagnostic for the *Cre* gene and mouse *Rb* gene, respectively. *MMTV-Cre* founder mice are identified in lanes 1, 4, 5, 7, and 8 (lines *MMTV-Cre*104Ayn, 105Ayn, 106Ayn, 107Ayn, 108Ayn, respectively). B, Survival of mice with mammary-specific inactivation of *p53* (n=16, median 669 days), *Rb* alone (n=8, median 700 days) or *p53* and *Rb* together (n=17, median 504 days). P for log-rank comparisons of survival curves of $p53^{ME-/-}$ and $p53^{ME-/-}Rb^{ME-/-}$ mice is 0.0058. C, Neoplasms of the mammary epithelium in $p53^{ME-/-}$ and $p53^{ME-/-}Rb^{ME-/-}$ mice. (Top) Mammary carcinomas with mainly (Left) solid pattern of growth (arrow) and dense fibrous stroma (arrowhead), (Middle) glandular pattern (arrow), (Right) spindle cell pattern with diverse cell types (arrow). H&E stain. (Middle) Lung metastasis of mammary carcinoma (arrow) (Left), H&E stain. Expression of CK8, CK5 and smooth muscle actin (SMA) in carcinoma cells (arrows) (Middle and Right). (Bottom) Expression of Mad2, ER and PR in carcinoma cells (arrows). ABC Elite method, hematoxylin counterstaining. Calibration bar for all images: 100 µm.

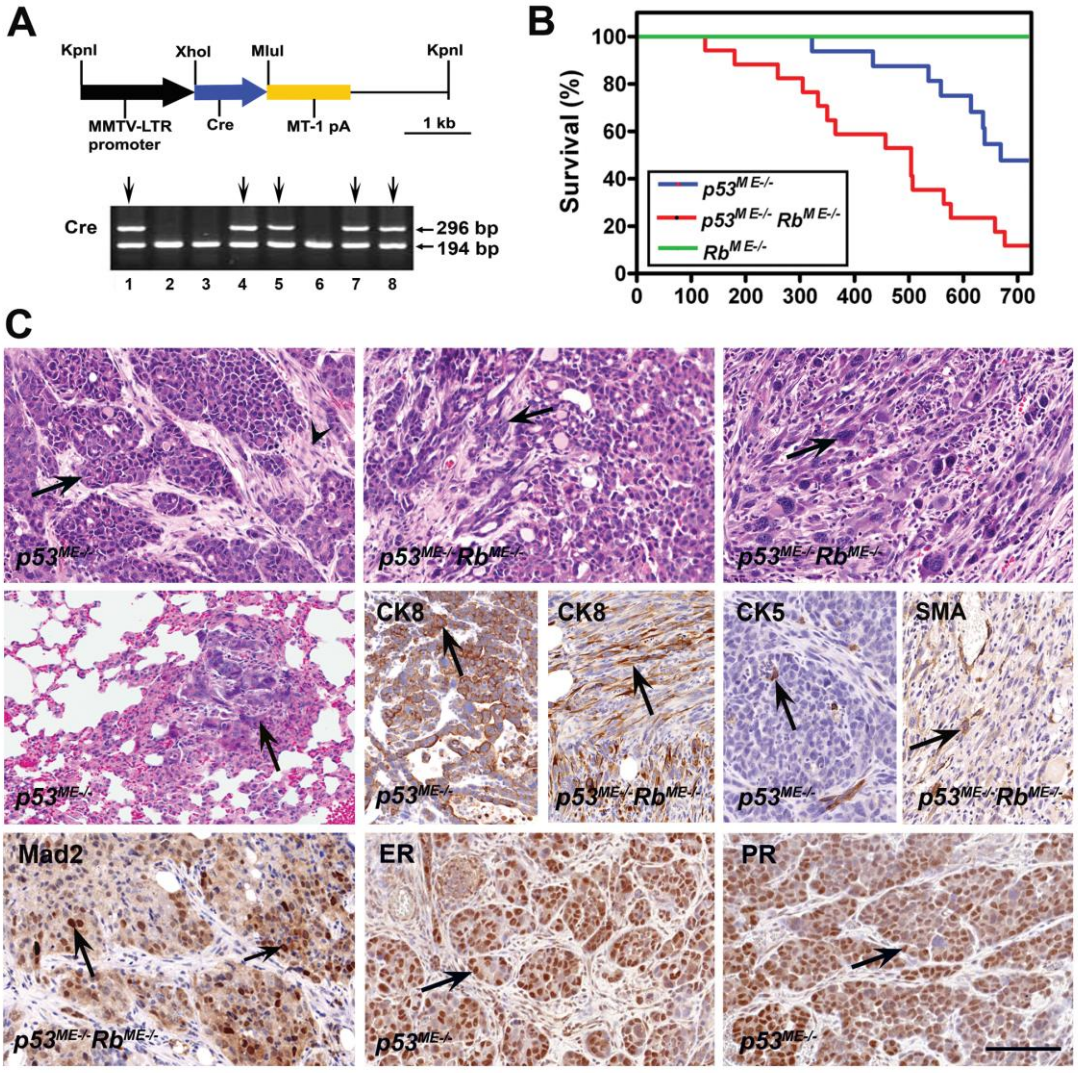
A
KpnI
XhoI
MluI
KpnI
MMTV-LTR promoter
Cre
MT-1 pA
1 kb
Cre
296 bp
194 bp
1 2 3 4 5 6 7 8
B
Survival (%)
100
80
60
40
20
0
0 100 200 300 400 500 600 700
p53ME-/-
p53ME-/- RbME-/-
RbME-/-
C
p53ME-/-
p53ME-/-RbME-/-
p53ME-/-RbME-/-
p53ME-/-
CK8
p53ME-/-
CK8
p53ME-/-RbME-/-
CK5
p53ME-/-
SMA
p53ME-/-RbME-/-
Mad2
p53ME-/-RbME-/-
ER
p53ME-/-
PR
p53ME-/-

Table 2.1 Characterization of *Cre* activity in 5 *MMTV-Cre* mouse lines*.

Lines / Tissues	104A	105	106	107	108
Lung	0**	0	0	0	<0.1
Liver	0	0	0	0	0
Spleen	<0.1	<0.1	0	0	5-10
Nulliparous mammary gland	<1	1	0	0	5
Multiparous mammary gland	NA***	30-60	NA	NA	30-50

* *MMTV-Cre* mice were crossed to *Gt(ROSA)26SorTM1sor* reporter mice.

** % of positive cells was determined by counting of at least 300 cells in 5 random fields of view (9 x 10^3 μm^2 area each).

*** NA, not available.

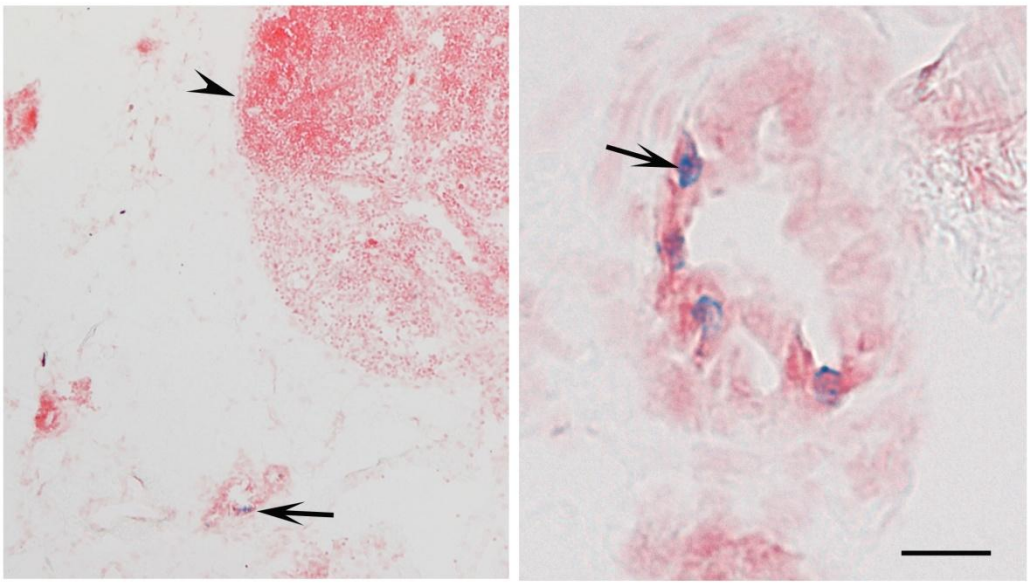

Figure 2.2 *Cre* expression in the mammary glands of *Tg(MMTV-Cre)*, *Gt(ROSA)26SorTM1sor* mice.

Only mammary epithelial cells contain β-galactosidase (arrow, green color). No *Cre* expression is detected in lymphocytes of the inguinal lymph node (left, arrowhead). Counterstaining with nuclear fast red. Calibration bar: (Left) 200 µm, (Right) 30 µm.

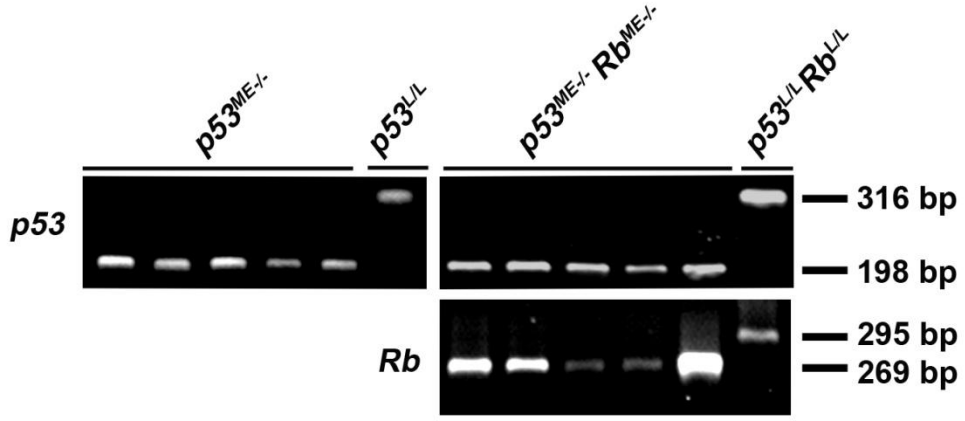

Figure 2.3 PCR analysis of p53 and Rb gene structures in mammary carcinoma (*p53*$^{ME-/-}$ and *p53*$^{ME-/-}$*Rb*$^{ME-/-}$ lanes) and normal cells (*p53*$^{L/L}$ and *p5*$^{L/L}$*Rb*$^{L/L}$ lanes).

Cells were isolated from dissociated tissues by magnetic purification with CD31 (endothelial cell), CD45 (hematopoietic cells), Ter119 (hematopoietic cells), and CD140a (stromal cells) antibodies using CELLection Biotin Binder Kit (Invitrogen). 198-bp and 316-bp fragments are diagnostic for the excised and floxed alleles of the *p53* gene, respectively. 269-bp and 295-bp fragments are diagnostic for the excised and floxed alleles of the *Rb* gene, respectively.

than that of *p53*$^{ME-/-}$ mice (P=0.0058). Thus, although *Rb* inactivation alone is insufficient for initiation of mammary carcinogenesis, *p53* and *Rb* cooperate in suppression of carcinogenesis.

In agreement with the low frequency (1% of cells) of Cre expression in the mammary glands, the majority of mice developed only one mammary tumor (Table 2.2). Eleven (3 out of 27) and 10 (4 out of 40) percent of *p53*$^{ME-/-}$ and *p53*$^{ME-/-}$ *Rb*$^{ME-/-}$ mice, respectively developed lung metastasis. Eight out of 27 (30%) and 10 out of 43 (23%) neoplasms in *p53*$^{ME-/-}$ and *p53*$^{ME-/-}$ *Rb*$^{ME-/-}$ trabecular patterns and were separated by desmoplastic stroma. One tumor in each group was an adenosquamous carcinoma. The remaining tumors were poorly differentiated carcinomas and consisted of CK8 positive epithelioid, spindle or polygonal, frequently pleomorphic, cells. The degree of pleomorphism was particularly notable in two out of 18 (11%) and nine out of 32 (28%) neoplasms from *p53*$^{ME-/-}$ and *p53*$^{ME-/-}$ *Rb*$^{ME-/-}$ mice respectively. The frequency of poorly differentiated carcinomas of *p53*$^{ME-/-}$ *Rb*$^{ME-/-}$ mice was also somewhat higher than that of *p53*$^{ME-/-}$ mice (67% vs. 75%). However, both parameters were not statistically significant (Fisher's exact test two-sided P=0.2866 and 0.579, respectively). Seven out of 32 poorly differentiated neoplasms of *p53*$^{ME-/-}$ *Rb*$^{ME-/-}$ mice but none out of 18 those of *p53*$^{ME-/-}$ mice contained significant (over 5%) areas of solid or glandular differentiation (Fisher's exact test two-sided P=0.04). SMA, CK5 or CK6 positive cells were present in one third of neoplasms but did not exceed 3-5% of tumor cells. As expected from the loss of Rb function, neoplastic cells deficient for both p53 and Rb proliferated significantly faster than cells with p53 deficiency alone in histologically comparable areas (Fig. 2.4). In agreement with mice, respectively, were relatively well differentiated carcinomas (Fig 2.1C and Table

Table 2.2 Neoplasms in *p53*$^{ME-/-}$ and *p53*$^{ME-/-}$ *Rb*$^{ME-/-}$ mice.

Genotype	*p53*$^{ME-/-}$	*p53*$^{ME-/-}$ *Rb*$^{ME-/-}$
No of tumors per tumor bearing mouse	1.12 (27/24)*	1.13 (43/42)
Well differentiated carcinoma, %	30 (8/27)	23 (10/43)
Poorly differentiated carcinoma, %	67 (18/27)	75 (32/43)
Adenosquamous carcinoma, %	3 (1/27)	2 (1/43)
Lung metastasis, %	11 (3/27)	10 (4/43)

* Numbers in parentheses indicate number of mice with neoplasm out of total number of tumor bearing mice.

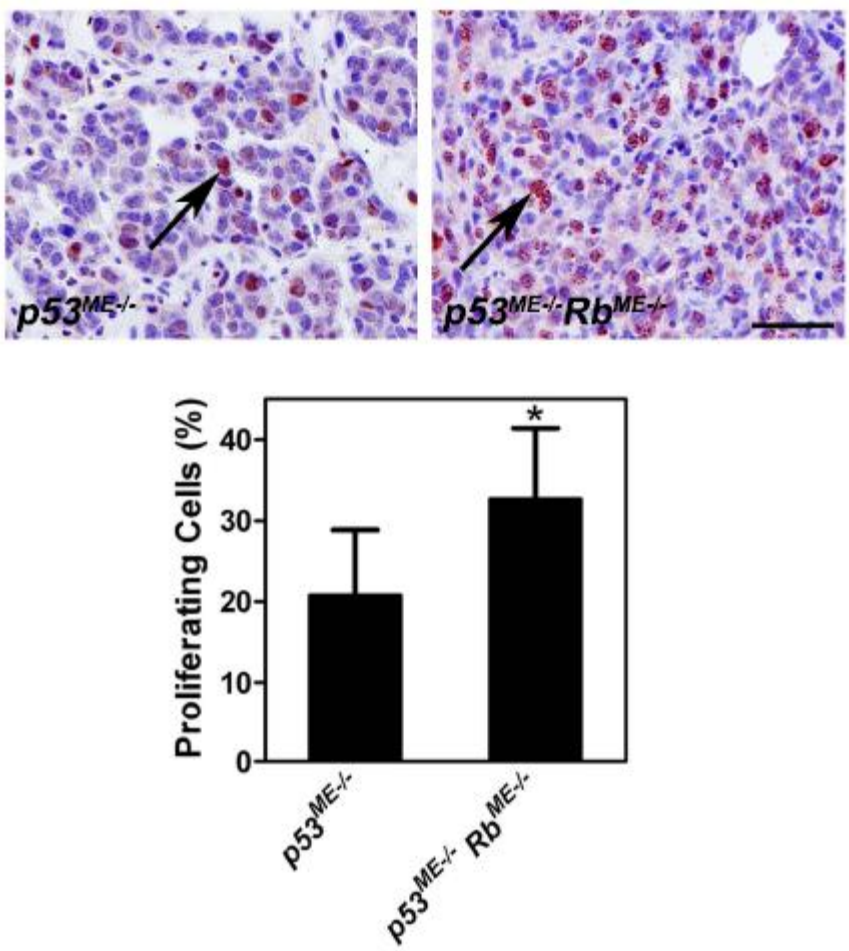

Figure 2.4 Cell proliferation in mammary carcinomas of *p53*$^{ME-/-}$ and *p53*$^{ME-/-}$ *Rb*$^{ME-/-}$ mice.

(Top) immunohistochemical detection of Ki67 (arrows). Counterstaining with hematoxylin. Calibration bar, 50 µm. (Bottom) Quantitative analysis of Ki67 immunostaining demonstrates that neoplastic cells in mammary carcinomas associated with p53 and Rb deficiency proliferate faster as compared to mammary carcinoma cells with p53 deficiency alone (Mean ± SD, 32.58 ± 8.8 vs 20.67 ± 8.15, ten tumors of comparable histological types per each group, P=0.0023).

2.2). In these tumors neoplastic cells formed solid, glandular and preferentially luminal differentiation of the neoplasms, all of them (10 out of 10 in each group) expressed ERα in at least 25% of cells (Fig 2.1C). All tumors also expressed a downstream target of ERα, PR. At the same time, as characteristic for luminal subtype B carcinomas (Hu et al., 2006), all tumors expressed mitotic checkpoint protein Mad2.

Mammary neoplasms respond to hormone therapy with a selective estrogen receptor modulator. In addition to detection of ER and PR in all mammary carcinomas by immunohistochemical analysis (Fig 2.1C), we confirmed their expression in the cell lines MCN1, MCN2 and MCN3 established from those tumors (Fig 2.5A and Table 2.3). To determine if tumors respond to hormone therapy, effects of raloxifene, a selective estrogen receptor modulator (SERM), which competes with endogenous estrogen for ERα binding (Sporn et al., 2004), were tested in all three mammary carcinoma cell lines. According to the BrdU incorporation assay, raloxifene treatment resulted in a dose dependent cell proliferation decrease in all three cell lines within concentration range from 10 nM to 1 μM ($P<0.05$ in all treatments and cell lines, Fig 2.5B). Raloxifene also significantly delayed the neoplastic growth after mammary fat pad transplantation of MCN1 ($P=0.0132$) and MCN2 ($P=0.0088$; Fig 2.5C). Taken together, these results confirm functional status of ERα in $p53^{ME-/-}$ and $p53^{ME-/-}$ $Rb^{ME-/-}$mouse models of mammary carcinoma.

***Rb* inactivation affects the pattern of secondary genetic alterations and increases genomic instability of mammary cancer associated with *p53* deficiency.** To determine whether there were any specific genetic aberrations associated with mammary carcinomas in our models, comparative genomic hybridization array (aCGH) analyses were performed on DNA

Figure 2.5 Mammary neoplasms respond to hormone therapy with raloxifene.

A, Western blot of ERα, and PR in MCN1, MCN2, MCN3 and MCF7 cell lines. To normalize for differences in loading, the blots were stripped and reprobed with mouse anti-Gapdh monoclonal antibody. B, Effects of raloxifene on proliferation of mammary carcinoma cells as determined by BrdU incorporation and compared to control (Mean ± SD, n=3 in each group, $P < 0.05$, indicated as *). All MCN cell lines are *p53* null and have either two (+/+) or no (-/-) functional copies of the *Rb* gene. C, Effects of raloxifene on tumor growth *in vivo*. MCN1 and MCN2 cells (10^6) were transplanted to cleared fad pad of 4 weeks old FVB mice. According to the tumor volume measurements 12 days after transplantation, raloxifene (raloxifene +) significantly delays the tumor growth of MCN1 (P=0.0132) and MCN2 (P=0.0088) cells as compared to control group without raloxifene treatment (raloxifene -).

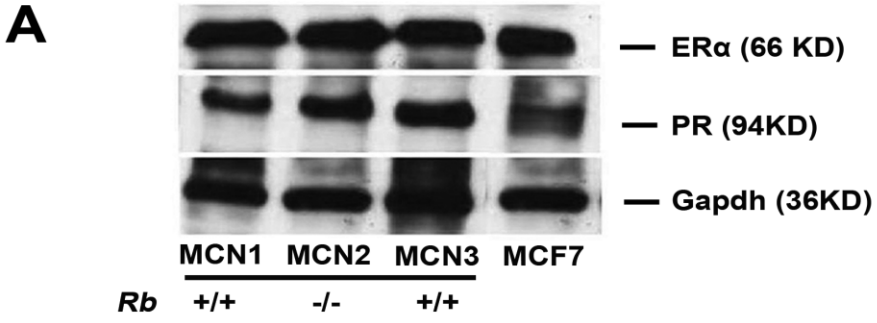
A
ERα (66 KD)
PR (94KD)
Gapdh (36KD)
MCN1
MCN2
MCN3
MCF7
Rb
+/+
-/-
+/+

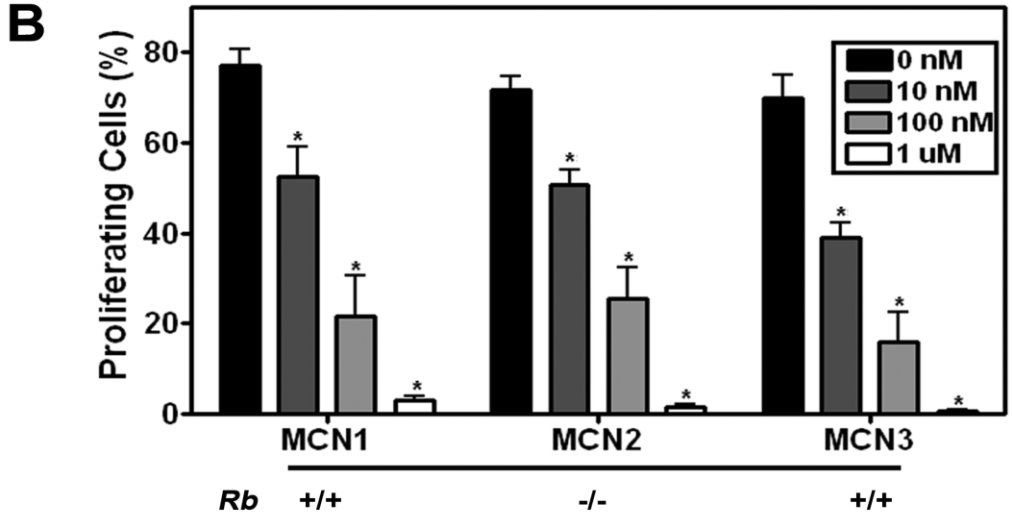
B
Proliferating Cells (%)
0
20
40
60
80
0 nM
10 nM
100 nM
1 uM
MCN1
MCN2
MCN3
Rb
+/+
-/-
+/+

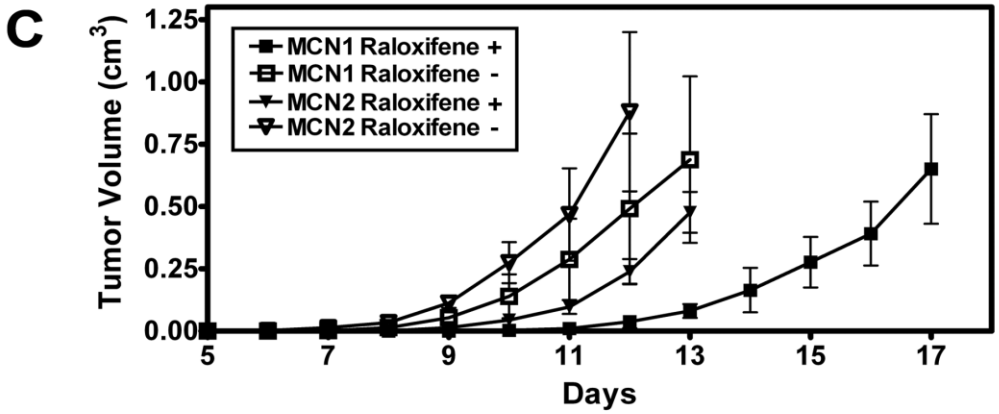
C
Tumor Volume (cm3)
0.00
0.25
0.50
0.75
1.00
1.25
MCN1 Raloxifene +
MCN1 Raloxifene -
MCN2 Raloxifene +
MCN2 Raloxifene -
5
7
9
11
13
15
17
Days

Table 2.3 Mammary carcinoma cell lines.

Cell line	Mouse genotype	Mouse age (days)	Tumor type	p53/Rb status
MCN1	$p53^{ME-/-}$	473	Poorly differentiated carcinoma	$p53^{-/-}Rb^{+/+}$
MCN2	$p53^{ME-/-}$ $Rb^{ME-/-}$	506	Poorly differentiated carcinoma	$p53^{-/-}Rb^{-/-}$
MCN3	$p53^{ME-/-}$	434	Solid carcinoma	$p53^{-/-}Rb^{+/+}$
MCN9	$p53^{ME-/-}$ $Rb^{ME-/-}$	508	Solid carcinoma	$p53^{-/-}Rb^{-/-}$

Figure 2.6. Genomic alterations in mammary carcinomas of *p53*$^{ME-/-}$ and *p53*$^{ME-/-}$ *Rb*$^{ME-/-}$ mice.

A, The log2 ratios for each chromosome in order from 1p to Xqter. (Top) Chromosomal regions with consistent gene copy number alterations (5 out of 6 samples, arrows). Carcinomas of *p53*$^{ME-/-}$ mice: significant gain and loss are mapped to the chromosomal bands 9A1 and 12C2 - 12F1, respectively. Carcinomas of *p53*$^{ME-/-}$ *Rb*$^{ME-/-}$ mice: significant gain at 6A1 and 6A2. B, Spectral Karyotyping analysis of chromosome metaphase spreads of primary tumor cells (Top, *p53*$^{ME-/-}$; Bottom, *p53*$^{ME-/-}$ *Rb*$^{ME-/-}$). Karyotype of metaphase spread with classification pseudo-color and its corresponding inverted-DAPI. Arrow, net gain of chromosome 9A1 in tumors of *p53*$^{ME-/-}$ mice. C, (Left) Comparison of aCGH profiles of tumors from *p53*$^{ME-/-}$ and *p53*$^{ME-/-}$ *Rb*$^{ME-/-}$ mice. (Right) Chi-square test of the number of BAC in altered chromosome region of tumors from *p53*$^{ME-/-}$ and *p53*$^{ME-/-}$ *Rb*$^{ME-/-}$ mice.

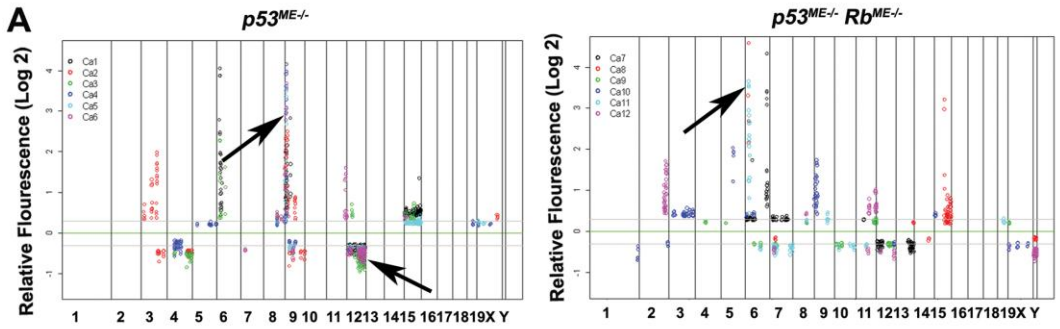

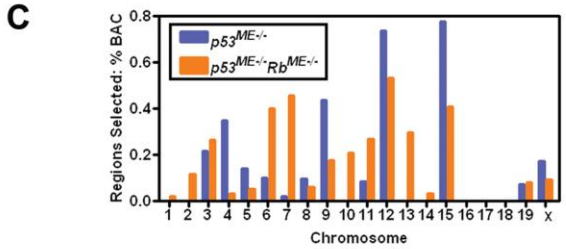

Number of Bac in Regions	$p53^{ME-/-}$	$p53^{ME-/-}$ $Rb^{ME-/-}$
Changed	978	1218
Unchanged	5529	5289
Total	6507	6507
Chi-square test p value	2.22E-08	

isolated from these neoplasms (Fig 2.6). The genome of p53 deficient tumors was characterized by a recurrent amplification (5 out of 6 tumors) at chromosomal band 9A1. Additionally, chromosome bands 12C2 - 12F1 were deleted in 5 out of 6 mammary tumors from *p53*$^{ME-/-}$ mice. Interestingly, in mammary tumors from *p53*$^{ME-/-}$ *Rb*$^{ME-/-}$ mice (Fig 2.6 A), only 1 out of 6 tumors had a genomic amplification of 9A1 and none carried the deletion at 12C2 - 12F1. At the same time, 5 out of 6 (83%) mammary tumors from *p53*$^{ME-/-}$*Rb*$^{ME-/-}$ mice had amplification at chromosome 6A1 and 6A2, while only 2 out of 6 (33%) mammary tumors from *p53*$^{ME-/-}$ mice had amplification of these regions. Analysis by SKY showed chromosomal aberrations that resulted in a net gain of chromosome 9A1 (Fig 2.6B).

aCGH data also demonstrated that neoplasms from *p53*$^{ME-/-}$ *Rb*$^{ME-/-}$ mice contained 20% more genomic imbalances compared to those in *p53*$^{ME-/-}$ mice (Fig 2.6C). Consistently, SKY analysis demonstrated a high degree of aneuploidy and an increased rate of structural chromosomal instability (P=0.0213) in carcinomas from *p53*$^{ME-/-}$ *Rb*$^{ME-/-}$ mice. This was measured as the presence of *de novo* non-clonal chromosome aberrations per cell (Fig 2.6B and Table 2.4).

Previous studies demonstrated that E2F family, one of the main Rb downstream effectors, mediates DNA double strand break accumulation and contribute to mitotic defects and genomic instability (Pickering and Kowalik, 2006) at least in part by activating Mad2 expression (Hernando et al., 2004). Consistently with those observations, higher levels of E2F1, E2F3 and Mad 2 were found in primary tumors from *p53*$^{ME-/-}$ *Rb*$^{ME-/-}$ mice as compared to *p53*$^{ME-/-}$ mice (Fig 2.7A). Accordingly, tumor cells deficient for both p53 and Rb contained higher subpopulation with multiple centrosomes (Fig 2.7B) and

Table 2.4 Summary of SKY analysis.

Genotype	Modal number	Ploidy	Metaphases analyzed	# of metaphases w/ modal number	Clonal aberrations	Non-clonal aberrations	Rate of structural instability
$p53^{-/-}$	74	4n-	10	3	3	7	0.7
$p53^{-/-}$	100	5n	10	3	6	6	0.6
$p53^{-/-}$	71	4n-	10	3	10	8	0.8
$p53^{-/-}Rb^{-/-}$	84	4n+	10	2	2	12	1.2
$p53^{-/-}Rb^{-/-}$	71	4n-	10	5	9	11	1.1
$p53^{-/-}Rb^{-/-}$	68	3n+	6	2	5	10	1.6

Figure 2.7 *Rb* inactivation promotes genomic instability.

A, (Left) Western blot of E2F1, E2F3, and Mad2 in primary tumor cells from $p53^{ME-/-}$ and $p53^{ME-/-}$ $Rb^{ME-/-}$ mice. (Right) Relative Mad2 mRNA expression in carcinomas of $p53^{ME-/-}$ and $p53^{ME-/-}$ $Rb^{ME-/-}$ mice (Mean ± SD, 2.9 ± 2.1 versus 6.3 ± 4.0, n=10, P = 0.0411, indicated as *). B, (Top) Immunofluorescence staining (γ-tubulin) of centrosomes in primary tumor cells from $p53^{ME-/-}$ and $p53^{ME-/-}$ $Rb^{ME-/-}$ mice. (Bottom Left) Percentage of cells with more than 2 centrosomes is higher in cells from $p53^{ME-/-}$ $Rb^{ME-/-}$ mice, as compared to that in cells from $p53^{ME-/-}$ mice (75.8 ± 9.0 versus 49.6 ± 12.0, n=10, P = 0.0083). (Bottom Right) Tumor cells from $p53^{ME-/-}$ $Rb^{ME-/-}$ mice have higher average number of centrosomes per cell than that from $p53^{ME-/-}$ mice (4.96 ± 0.76 versus 3.34 ± 0.90, n=10, P=0.0152,). C, (Left) Representative images of neutral comet assay with primary tumor cells from $p53^{ME-/-}$ and $p53^{ME-/-}$ $Rb^{ME-/-}$ mice. (Right) Tumor cells from $p53^{ME-/-}$ $Rb^{ME-/-}$ mice have higher percentage of cells with comet tail as compared to $p53^{ME-/-}$ (18.9 ± 1.3 versus 11.5 ± 3.3, n=10, P = 0.0232).

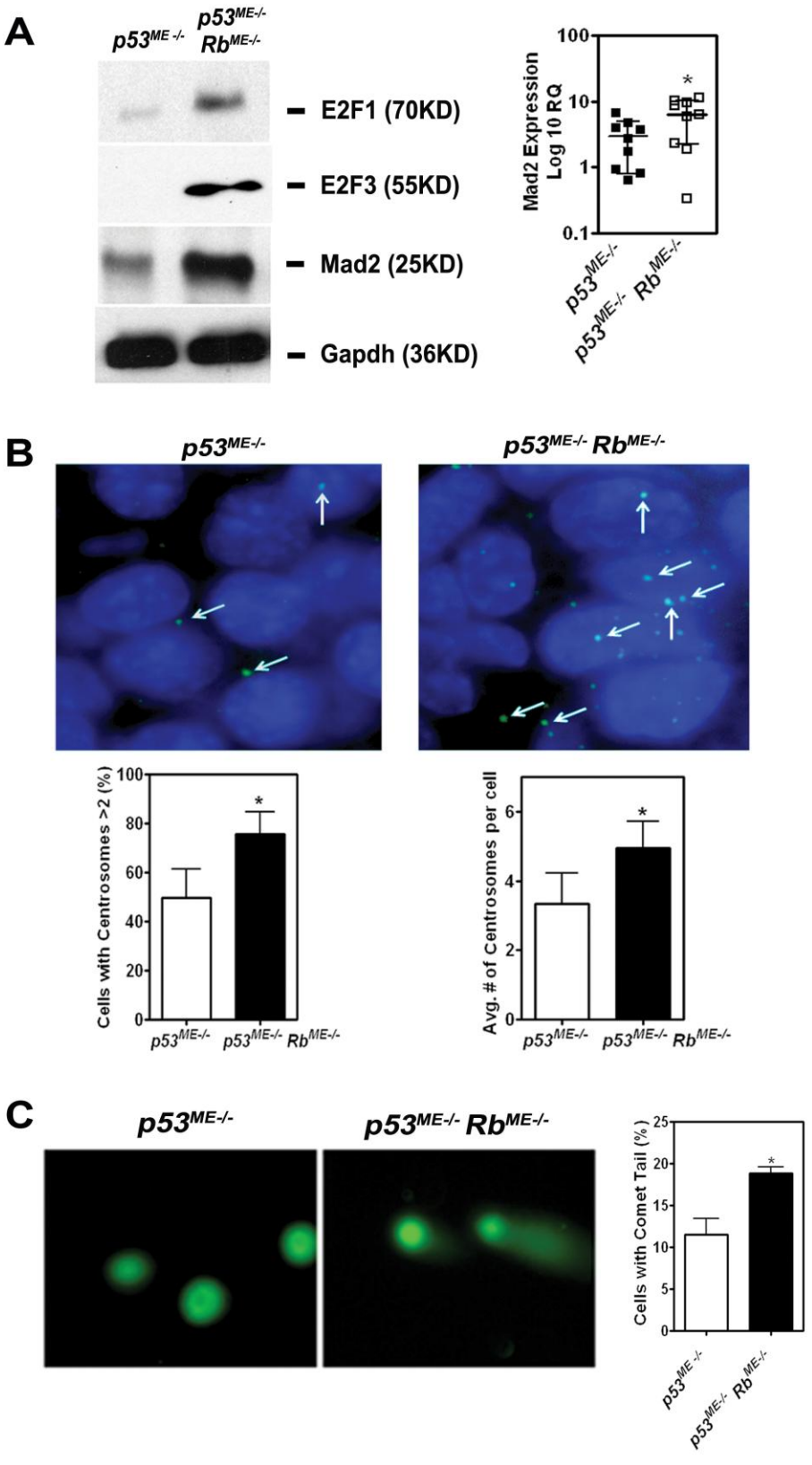
A
p53ME -/-
p53ME-/- RbME-/-
E2F1 (70KD)
E2F3 (55KD)
Mad2 (25KD)
Gapdh (36KD)
Mad2 Expression Log 10 RQ
100
10
1
0.1
*
p53ME-/-
p53ME-/- RbME-/-
B
p53ME-/-
p53ME-/- RbME-/-
Cells with Centrosomes >2 (%)
100
80
60
40
20
0
*
p53ME-/-
p53ME-/- RbME-/-
Avg. # of Centrosomes per cell
6
4
2
0
*
p53ME-/-
p53ME-/- RbME-/-
C
p53ME-/-
p53ME-/- RbME-/-
Cells with Comet Tail (%)
25
20
15
10
5
0
*
p53ME-/-
p53ME-/- RbME-/-

double strand breaks (Fig 2.7C) according to γ-tubulin staining and neutral comet assays, respectively.

***cIAP1, cIAP2 and Yap1* are regulated by *E2F* and cooperate in mammary carcinogenesis.** The chromosome band 9A1 is orthologous to human chromosome band 11q22, which is frequently amplified in human cancers (Overholtzer et al., 2006) and contains the protooncogenes *cIAP1 (Birc2), cIAP2 (Birc3)* and *Yap1*. Given the potential importance of these genes for human cancer we fine mapped the extent of the amplicon by demonstrating lack of amplification of the flanking genes *Tmem123* (*Porimin*) and *Pgr* (*PR*) genes by quantitative real time PCR (qPCR) in tumors from $p53^{ME-/-}$ mice (Fig 2.8A). At the same time, qPCR was also used to confirm the aCGH results indicating lack of recurrent amplification of *cIAP1*, *cIAP2* and *Yap1* in carcinomas of $p53^{ME-/-}$ $Rb^{ME-/-}$ mice.

Notably, mRNA expression analyses demonstrated that all three genes were similarly overexpressed in carcinomas of both $p53^{ME-/-}$ and $p53^{ME-/-}$ $Rb^{ME-/-}$ mice (Fig 2.8B). Since promoter regions of all three genes contain E2F binding sites (Fig 2.9), E2F regulation of *cIAP1*, *cIAP2* and *Yap1* expression was tested by *E2F1* knockdown. Consistent with the Rb/E2F regulation model, knockdown of *E2F1* by siRNA in mammary carcinoma cell lines resulted in significant ($P<0.05$) downregulation of *cIAP1*, *cIAP2* and *Yap1* 24 hours after transfection (Fig 2.8C). *Cre-loxP*-mediated inactivation of *Rb* alone or together with *p53* in primary mammary epithelial cells resulted in increased expression of *cIAP1* and *cIAP2* at 24 hours followed by further increase at 72 hours (Fig 2.8C). Inactivation of *p53* alone had only marginal effect on expression of *cIAP1* and led to decreased expression of *cIAP2*. Furthermore, induction of

Figure 2.8 Copy number and expression of *cIAP1*, *cIAP2* and *Yap1* in mammary carcinomas of $p53^{ME-/-}$ and $p53^{ME-/-}$ $Rb^{ME-/-}$ mice.

A, (Top) The map of the genes in the chromosome 9A1 region under study. (Bottom) Mammary carcinomas from $p53^{ME-/-}$ mice have higher *cIAP1*, *cIAP2* and *Yap1* gene copy number than those from $p53^{ME-/-}$ $Rb^{ME-/-}$ mice (Mean±SD, n=10 in each group). *cIAP1:* 17.6±19.2 versus 3.1±3.1; *cIAP2:* 20.3±19.7 versus 3.1±2.4 and *Yap1:* 19.03±17.96 versus 4.08±2.95, respectively. * indicates P<0.05. DNA copy number of *Tmem123* and *Pgr* is similar between the cells from these two different types of mice (*Tmem123:* 1.88±1.36 versus 1.78±1.41 and *Pgr*: 1.87±1.6 versus 1.72±1.32). B, (Left) Overexpression of *cIAP1*, *cIAP2* and *Yap1* in mammary carcinomas from both $p53^{ME-/-}$ and $p53^{ME-/-}Rb^{ME-/-}$ mice as compared to the wild-type (WT) mammary epithelium (Mean±SD, n=10 in each group) *cIAP1:* 7.80±8.61 ($p53^{ME-/-}$), 12.30±15.30 ($p53^{ME-/-}$ $Rb^{ME-/-}$) versus 1.05±0.13 (WT); *cIAP2:* 6.31±10.89 ($p53^{ME-/-}$), 5.73±6.72 ($p53^{ME-/-}$ $Rb^{ME-/-}$) versus 1.06±0.18 (WT), and *Yap1:* 18.29±27.12 ($p53^{ME-/-}$), 19.12±20.15 ($p53^{ME-/-}$ $Rb^{ME-/-}$) versus 1.16±0.19 (WT), * indicates P<0.05. (Right) Western blot of *cIAP1* and *Yap1* in MCN1, MCN2, MCN3 cells and primary culture of wild type mammary epithelium (WT). C, Expression of *E2F1*, *cIAP1*, *cIAP2*, and *Yap1* after *E2F1* knockdown by *E2F1* siRNA as compared to scrambled siRNA control (Mean±SD, n=4 in each group; P<0.05 is indicated as*). All MCN cell lines are *p53* null and have either two(+/+) or no(-/-) functional copies of the *Rb* gene (Top Left). Relative expression (Mean±SD, n=4 in each group) of *cIAP1* (Top Right)*, cIAP2 (*Bottom Left*)* and *Yap1* (Bottom Right) collected at 24 and 72 hours after treatment of mammary epithelium cells from floxed *p53* ($p53^{L/L}$), *Rb* ($Rb^{L/L}$), or $p53^{L/L}Rb^{L/L}$ mice with blank Adenovirus (Blank) or *AdCre* (P<0.05 is indicated as *).

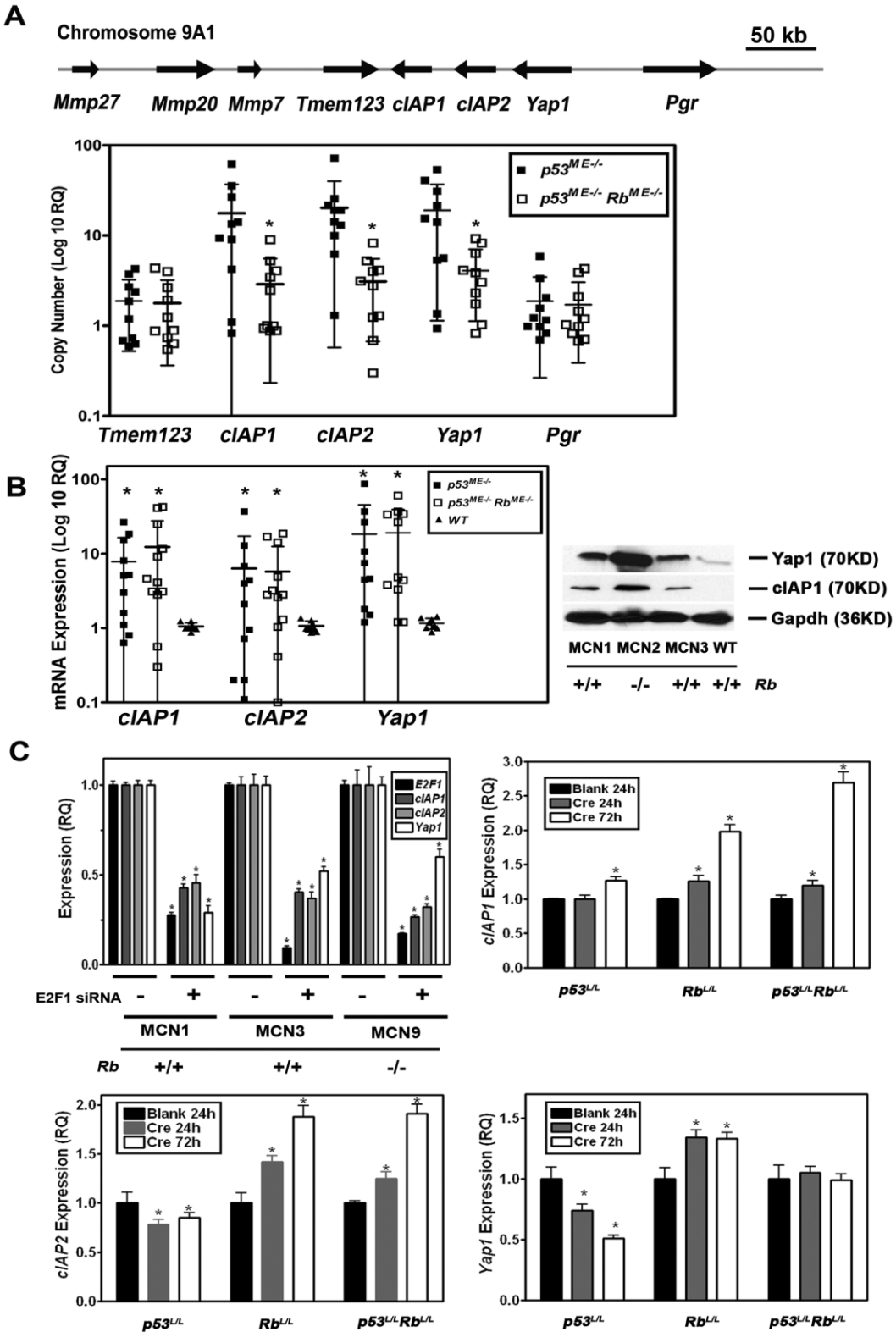
A
Chromosome 9A1
50 kb
Mmp27
Mmp20
Mmp7
Tmem123
cIAP1
cIAP2
Yap1
Pgr
Copy Number (Log 10 RQ)
p53ME-/-
p53ME-/- RbME-/-
Tmem123
cIAP1
cIAP2
Yap1
Pgr
B
mRNA Expression (Log 10 RQ)
p53ME-/-
p53ME-/- RbME-/-
WT
cIAP1
cIAP2
Yap1
Yap1 (70KD)
cIAP1 (70KD)
Gapdh (36KD)
MCN1 MCN2 MCN3 WT
+/+ -/- +/+ +/+ Rb
C
Expression (RQ)
E2F1
cIAP1
cIAP2
Yap1
E2F1 siRNA - + - + - +
MCN1
MCN3
MCN9
Rb +/+ +/+ -/-
cIAP1 Expression (RQ)
Blank 24h
Cre 24h
Cre 72h
p53L/L
RbL/L
p53L/LRbL/L
cIAP2 Expression (RQ)
Yap1 Expression (RQ)

p53 expression by treatment with doxorubicin did not result in decreased expression of *cIAP1* and *cIAP2* as compared to p53 deficient cells (Fig 2.10). *Yap1* expression also increased after *Rb* inactivation but lacked significant increase immediately after simultaneous inactivation of *p53* and *Rb* genes. Computational analysis of the *Yap1* gene identified a putative p53 binding site in the intron 1 (Fig 2.9). Consistently, decrease and increase of Yap1 expression was observed after deletion and doxorubicin-induced upregulation of *p53*, respectively (Fig 2.8C and Fig 2.10C). Taken together, these observations indicate that defective Rb/E2F pathway was likely to be sufficient for immediate upregulation of *cIAP1* and *cIAP2,* as well as later overexpression of *Yap1*, thereby avoiding the need for genomic amplification of these genes during mammary carcinogenesis.

To further elucidate the roles of *cIAP1*, *cIAP2* and *Yap1* in mammary carcinomas we used siRNA to knockdown the expression of these genes (Fig 2.11 and Fig 2.12). Downregulation of each gene individually resulted in significant decrease in cell proliferation and increase in apoptosis (Fig 2.11A). The effect was even more pronounced after two or all three genes were inactivated simultaneously. To test tumorigenic properties of cIAP1, cIAP2 and Yap1*,* respective siRNAs were delivered with atelocollagen to mammary carcinoma cells transplanted to the mammary fat pad. Downregulation of each gene, individually, resulted in deceleration of tumor growth. Similarly to cell culture results, suppression of tumor growth was most pronounced by simultaneous downregulation of 2 and particularly all 3 genes. Taken together, these observations demonstrate that *cIAP1*, *cIAP2*, and *Yap1* are important for mammary carcinogenesis associated with p53 deficiency and cooperate to promote neoplastic growth.

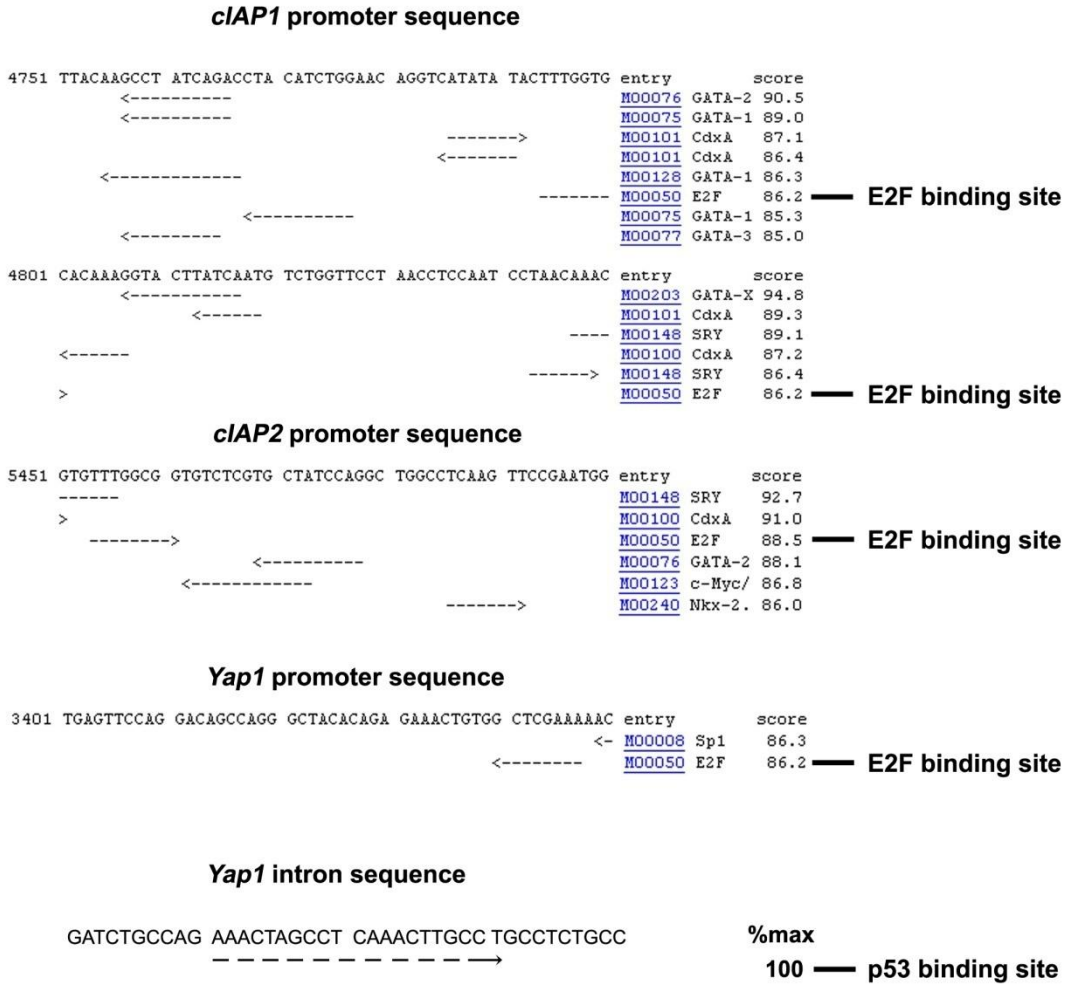

Figure 2.9 Analysis of *cIAP1*, *cIAP2*, and *Yap1* genes for binding sites.

Promoter regions of *cIAP1*, *cIAP2*, and *Yap1* contain E2F binding sites according to TFSEARCH: Searching Transcription Factor Binding Sites (version 1.3), UCSC Genome Browser (http://molsun1.cbrc.aist.go.jp/research/db/TFSEARCH.html). Yap1 gene contains p53 binding site in the intron 1 according to the Program p53MH (http://linkage.rockefeller.edu/ott/p53MH.htm).

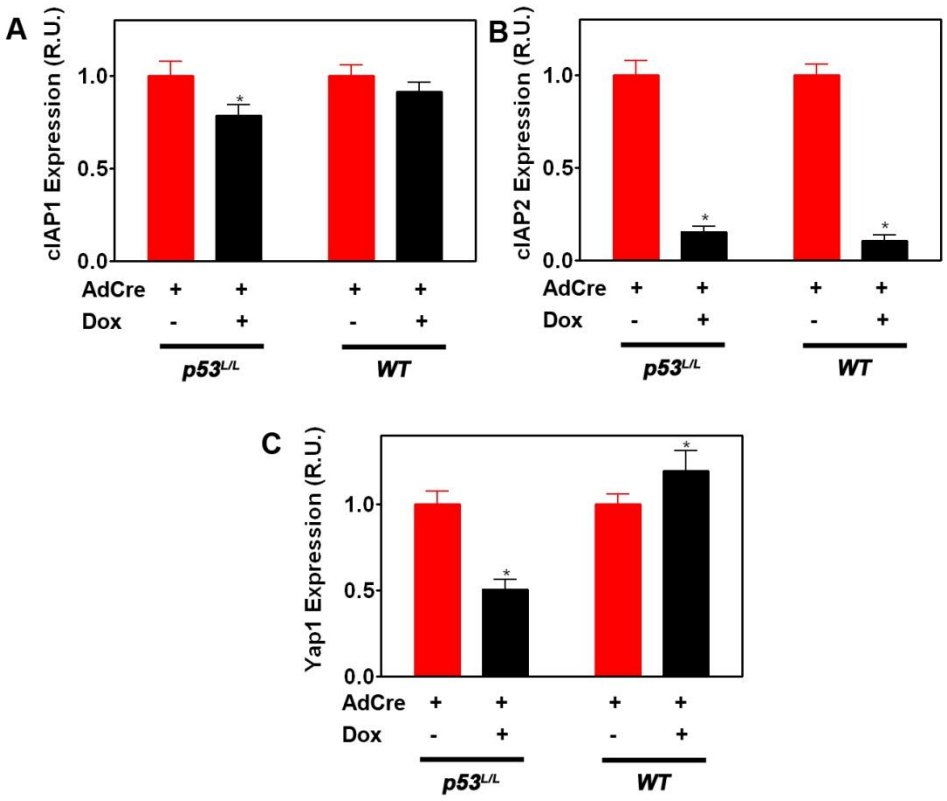

Figure 2.10 Effect of doxorubicin on cIAP1, cIAP2 and Yap1 expression.

Primary mammary epithelium cells from either *p53* floxed ($p53^{L/L}$) or wild-type mouse were exposed to AdCre for 48 hrs followed by treatment with doxorubicin (Dox, 2 µg/ml) for 12 hours (Mean ± SD, n=4 in each group, $P<0.05$, as compared to control, is indicated as*).

Figure 2.11 *cIAP1, cIAP2,* and *Yap1* cooperate in mammary carcinogenesis.

A, Downregulation of either *cIAP1*, *cIAP2* or *Yap1* by siRNA in primary mammary carcinoma cells leads to decreased cell proliferation (left) and increase of apoptosis (right) as compared to scrambled siRNA control. Both effects are more pronounced after inactivation of any two or all three genes. (Mean ± SD, n=4 in each group, $P<0.05$, indicated as*). B, Effect of *cIAP1*, *cIAP2* or *Yap1* knockdown on tumor growth (Mean ± SD, n=4 in each group). According to the tumor volume measurements 17 days after transplantation, downregulation of *cIAP1*, *cIAP2* and *Yap1* by siRNA in mammary carcinoma cells decelerates tumor growth as compared to control (P=0.014, P=0.0056, and P=0.0091, respectively). Combination of *cIAP1* and *cIAP2*, *cIAP1* and *Yap1*, or all three genes further delays the tumor growth (P=0.0022, P=0.0073, and P=0.0069, n=4, respectively).

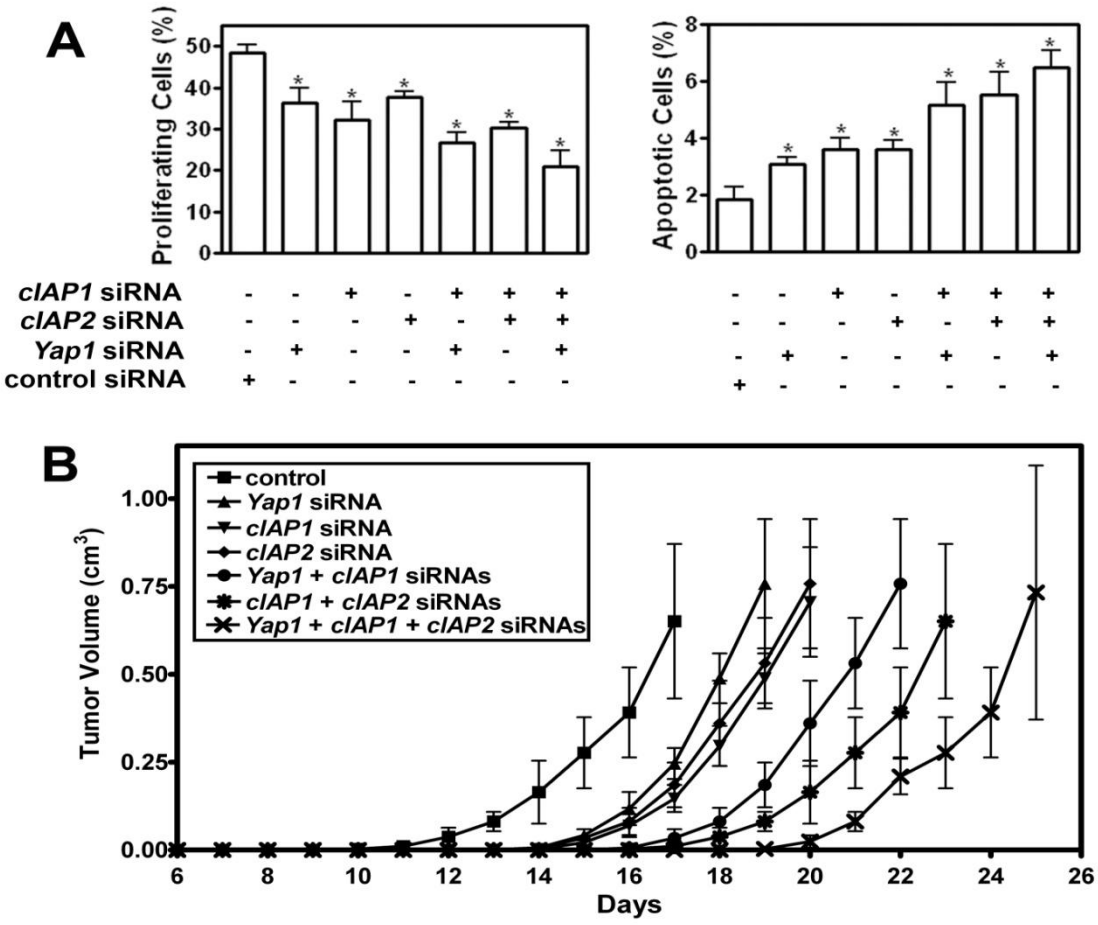
A
Proliferating Cells (%)
Apoptotic Cells (%)
cIAP1 siRNA
cIAP2 siRNA
Yap1 siRNA
control siRNA
B
control
Yap1 siRNA
cIAP1 siRNA
cIAP2 siRNA
Yap1 + cIAP1 siRNAs
cIAP1 + cIAP2 siRNAs
Yap1 + cIAP1 + cIAP2 siRNAs
Tumor Volume (cm3)
Days

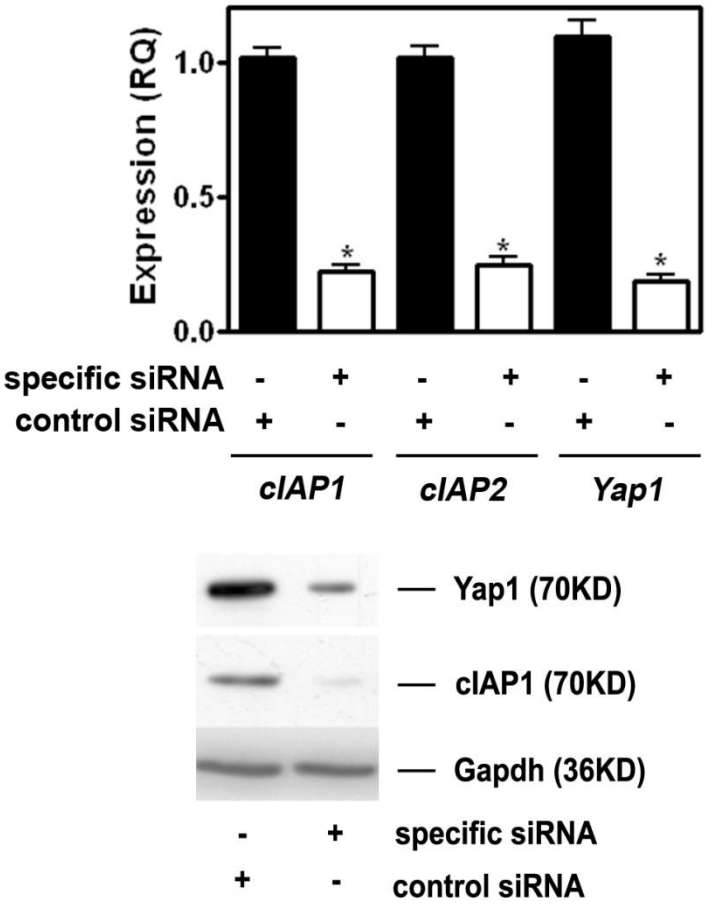

Figure 2.12 Efficacy of *cIAP1*, *cIAp2* and *Yap1* siRNA knock down.

(Top) Relative mRNA expression of cIAP1, cIAP2 and Yap1 decreases from 1 to 0.22 (cIAP1, P = 0.0003), to 0.25 (cIAP2 P =0.0002), and to 0.20 (Yap1, P = 0.0001) after knockdown with respective siRNAs as compared to the control siRNA (Mean ± SD, n=4 in each group, P<0.05, is indicated as *). Western blot analysis (Bottom) demonstrates decreased levels cIAP1 and Yap1 proteins after knockdown with specific siRNA as compared to the control scrambled siRNA.

2.5 Discussion

Human sporadic cancers have a broad repertoire of genetic changes and understanding of their contributions to major pathways defects is of critical importance. Mouse models of human cancer have been shown to serve as useful systems to facilitate identification of genetic alterations essential for carcinogenesis by comparative oncogenomic approaches (Maser et al., 2007; Morrison and Kimble, 2006; Zender et al., 2006). During the past two decades it has become increasingly clear that different cancer phenotypes of mouse models may reflect distinct initiating genetic and epigenetic alterations (Cardiff et al., 2000). Indeed, combination of *p53* and *Brca1* somatic inactivation results in formation of tumors mimicking human BRCA1-mutated ER negative basal-like cancer (Liu et al., 2007). At the same time inactivation of *p53* together with E-cadherin leads to ER negative metastatic lobular mammary carcinoma (Derksen et al., 2006). Mammary neoplasms associated with p53 deficiency alone were reported to be either ER negative (Liu et al., 2007) or both ER negative and positive, depending on *MMTV* or *WAP* promoter used to express Cre in deleter mouse strains (Lin et al., 2004).

Since available mammary epithelium-specific deleter strains express Cre in lymphoid and other tissues, we have established an additional *MMTV-Cre* strain with a highly mammary epithelium-restrictive expression pattern. Interestingly, different from other *MMTV-Cre* based models and likely due to transgene positional effects, the cancers forming in our model are ER positive and have no or very limited non-luminal differentiation typical for such tumor types as adenomyoepthelial, adenosquamous and basal-like carcinomas. Thus interpretation of cancer phenotypes is also likely to be affected by variations in transgene expression patterns and transformation of distinct cell

lineages and their subpopulations.

Based on the expression of markers for luminal differentiation, such as ER and CK8, combined with p53 deficient status, as well as expression of Mad2 and cIAP2 (Frasor et al., 2009), this model may represent an attractive tool for studies of human luminal subtype B breast cancers (Hu et al., 2006; Sorlie et al., 2001). This model is also particularly amenable to further experiments because of responsiveness of mammary carcinomas to an estrogen antagonist as well as availability of established syngeneic mammary carcinoma cell lines. Considering the 50% frequency of mammary carcinomas and long latency period of carcinogenesis in $p53^{ME-/-}$ mice, they are particularly well suited for assessment of other endogenous and exogenous factors which are expected to accelerate carcinogenesis.

Our studies confirmed previous observations that sporadic inactivation of *Rb* alone is insufficient for the initiation of mammary carcinogenesis (Robinson et al., 2001). Furthermore, the use of a *Cre-loxP* approach allowed direct genetic demonstration that *Rb* loss-of-function, without inactivation of p107 and/or p130, leads to acceleration of mammary carcinogenesis associated with *p53* inactivation. At least in part, this effect may be explained by increased proliferation rate of Rb-deficient neoplastic cells.

p53 and Rb pathways are extensively connected and their inactivation frequently cooperates during carcinogenesis presumably by abrogating E2F-induced p53-mediated apoptosis or senescence (Sherr, 2004; Sherr and McCormick, 2002). Our study illuminates genomic instability as another mechanism of p53 and Rb cooperation. Genomic instability is a hallmark of most human cancers. Although much attention has been focused on the role of p53 in the maintenance of genomic stability, an accumulating body of

evidence indicates Rb as another important player (Knudsen et al., 2006). *Rb* inactivation has been shown to promote genomic instability by uncoupling cell cycle progression from mitotic control (Hernando et al., 2004) and by mediating DNA double strand break accumulation (Pickering and Kowalik, 2006) in cell culture models. *In vivo, Rb* loss results in ectopic cell cycle, compromises ploidy control in mouse liver (Mayhew et al., 2005) and promotes hepatocarcinogenesis (Mayhew et al., 2007; Reed et al., 2009). Our study extends these observations by demonstrating higher levels of the E2F downstream target Mad2, higher rates of double strand DNA breaks and centrosome amplification and overall increase in chromosomal structural instability in mammary carcinomas deficient for both p53 and Rb. Further studies should determine if *Rb* loss leads to similar consequences in the normal mammary epithelium. It also remains to be demonstrated whether observed increase in phenotypical diversity and trend towards increase of cellular polymorphism and poorer differentiations in carcinomas of $p53^{ME-/-}$ $Rb^{ME-/-}$ mice are a result of elevated genomic instability associated with Rb deficiency.

Using aCGH, we identified a number of recurrent genetic alterations in our mammary carcinoma models. It is likely that each of these alterations has individual contributions to carcinogenesis. The amplification of 9A1 locus is of a particular interest because it includes protooncogenes, such as *cIAP1*, *cIAP2* and *Yap1*. *cIAP1* and *cIAP2* encoded proteins contain baculoviral IAP repeat (BIR) domain and are key regulators of apoptosis, cytokinesis, and signal transduction. Both genes are commonly amplified in many human cancers (reviewed in LaCasse et al., 2008). Yap1 contains a WW domain and binds to the SRC Homology 3 domain of the tyrosine kinase Yes. It has been

shown to be expressed in common solid tumors (Steinhardt et al., 2008) and to have tumorigenic properties in both liver (Zender et al., 2006) and breast cancer (Overholtzer et al., 2006). Considering the high frequency of 9A1 locus amplification in neoplasms of *p53*$^{ME-/-}$ mice, this model may prove to be very valuable for further studies of mechanisms involved in amplification of human orthologous genes on chromosome 11q22.

Amplification of both *cIAP1* and *Yap1* was observed in 4 out of 7 tumors in a transplantable mouse model of liver cancer based on transduction of p53 deficient fetal hepatoblasts with Myc retrovirus (Zender et al., 2006). At the same time, amplification of *cIAP1* and *cIAP2*, together with matrix metalloproteinase MMP13, was observed in 5 out of 41 osteosarcomas (Ma et al., 2009). *Yap1* amplification was detected in one out of 15 mammary tumors of *MMTV-Cre Brca1*$^{floxP/-}$ *p53*$^{+/-}$ mice. However, amplification of *Yap1* was detected in none of over 100 sporadic human breast cancers (Overholtzer et al., 2006). Our observations of E2F-mediated control of cIAP1, cIAP2 and Yap1 may explain how dysfunctional Rb/E2F pathway may substitute for recurrent amplification of these genes. Since alterations in the Rb pathway are quite common in mouse and human tumors, including mammary carcinomas, this mechanism may also explain differences in frequencies of *cIAP1*, *cIAP2* and *Yap1* amplification among various tumor types.

Our results demonstrate that cIAP1, cIAP2 and Yap1 overexpression is critical for mammary carcinogenesis associated with *p53* mutations. It is of interest that overexpression of cIAP2 has been recently reported to be associated with luminal subtype B of breast cancer (Frasor et al., 2009). Further studies will examine whether tumors of this subtype also overexpress cIAP1 and Yap1. Cooperation among cIAP1, cIAP2 and Yap1 in promoting

tumorigenicity observed in our work is consistent with previously reported cooperation between cIAP1 and Yap1 in hepatocarinogenesis (Zender et al., 2006). Recently a broad variety of IAP molecule antagonists has been developed (LaCasse et al., 2008). Our results indicate that their application may be particularly effective in combination with downregulation of Yap1.

In summary, we established a new mouse model of sporadic ER positive luminal mammary carcinoma associated with *p53* inactivation. We demonstrated that *Rb* deficiency accelerates mammary carcinogenesis and leads to increased genomic instability and to a different spectrum of recurrent genomic alterations. Of particular interest, genes of chromosome band 9A1, namely *cIAP1*, *cIAP2* and *Yap1*, were shown to be important for mammary carcinogenesis. We proposed the E2F-mediated mechanism of their regulation and established cooperation among all three genes in promoting neoplastic growth. These observations provide the basis for further elucidation of cooperation of these genes in human cancers and lay the ground for rational development of therapeutic approaches in preclinical settings.

REFERENCES

Borresen-Dale, A. L. (2003). TP53 and breast cancer. Hum Mutat *21*, 292-300.

Bosco, E. E., Wang, Y., Xu, H., Zilfou, J. T., Knudsen, K. E., Aronow, B. J., Lowe, S. W., and Knudsen, E. S. (2007). The retinoblastoma tumor suppressor modifies the therapeutic response of breast cancer. J Clin Invest *117*, 218-228.

Burkhart, D. L., and Sage, J. (2008). Cellular mechanisms of tumour suppression by the retinoblastoma gene. Nat Rev Cancer *8*, 671-682.

Cardiff, R. D., Anver, M. R., Gusterson, B. A., Hennighausen, L., Jensen, R. A., Merino, M. J., Rehm, S., Russo, J., Tavassoli, F. A., Wakefield, L. M.*, et al.* (2000). The mammary pathology of genetically engineered mice: the consensus report and recommendations from the Annapolis meeting. Oncogene *19*, 968-988.

Chai, Y., Jiang, X., Ito, Y., Bringas, P., Jr., Han, J., Rowitch, D. H., Soriano, P., McMahon, A. P., and Sucov, H. M. (2000). Fate of the mammalian cranial neural crest during tooth and mandibular morphogenesis. Development *127*, 1671-1679.

Davisson, M. T. (1994). Rules and guidelines for nomenclature of mouse genes. International Committee on Standardized Genetic Nomenclature for Mice. Gene *147*, 157-160.

Derksen, P. W., Liu, X., Saridin, F., van der Gulden, H., Zevenhoven, J., Evers, B., van Beijnum, J. R., Griffioen, A. W., Vink, J., Krimpenfort, P.*, et al.* (2006). Somatic inactivation of E-cadherin and p53 in mice leads to metastatic lobular mammary carcinoma through induction of anoikis resistance and angiogenesis. Cancer Cell *10*, 437-449.

Donehower, L. A., Harvey, M., Slagle, B. L., McArthur, M. J., Montgomery, C. A., Jr., Butel, J. S., and Bradley, A. (1992). Mice deficient for p53 are developmentally normal but susceptible to spontaneous tumours. Nature *356*, 215-221.

Flesken-Nikitin, A., Choi, K. C., Eng, J. P., Shmidt, E. N., and Nikitin, A. Y. (2003). Induction of carcinogenesis by concurrent inactivation of p53 and Rb1 in the mouse ovarian surface epithelium. Cancer Res *63*, 3459-3463.

Frasor, J., Weaver, A., Pradhan, M., Dai, Y., Miller, L. D., Lin, C. Y., and Stanculescu, A. (2009). Positive cross-talk between estrogen receptor and NF-kappaB in breast cancer. Cancer Res *69*, 8918-8925.

Geradts, J., and Wilson, P. A. (1996). High frequency of aberrant p16(INK4A) expression in human breast cancer. Am J Pathol *149*, 15-20.

Hernando, E., Nahle, Z., Juan, G., Diaz-Rodriguez, E., Alaminos, M., Hemann, M., Michel, L., Mittal, V., Gerald, W., Benezra, R.*, et al.* (2004). Rb inactivation promotes genomic instability by uncoupling cell cycle progression from mitotic control. Nature *430*, 797-802.

Hu, Z., Fan, C., Oh, D. S., Marron, J. S., He, X., Qaqish, B. F., Livasy, C., Carey, L. A., Reynolds, E., Dressler, L.*, et al.* (2006). The molecular portraits of breast tumors are conserved across microarray platforms. BMC Genomics *7*, 96.

Jacks, T., Remington, L., Williams, B. O., Schmitt, E. M., Halachmi, S., Bronson, R. T., and Weinberg, R. A. (1994). Tumor spectrum analysis in p53-mutant mice. Curr Biol *4*, 1-7.

Jemal, A., Siegel, R., Xu, J., and Ward, E. Cancer Statistics, 2010. CA Cancer J Clin. *in press*.

Jonkers, J., Meuwissen, R., van der Gulden, H., Peterse, H., van der Valk, M.,

and Berns, A. (2001). Synergistic tumor suppressor activity of BRCA2 and p53 in a conditional mouse model for breast cancer. Nat Genet *29*, 418-425.

Knudsen, E. S., Sexton, C. R., and Mayhew, C. N. (2006). Role of the retinoblastoma tumor suppressor in the maintenance of genome integrity. Curr Mol Med *6*, 749-757.

Kuperwasser, C., Hurlbut, G. D., Kittrell, F. S., Dickinson, E. S., Laucirica, R., Medina, D., Naber, S. P., and Jerry, D. J. (2000). Development of spontaneous mammary tumors in BALB/c p53 heterozygous mice. A model for Li-Fraumeni syndrome. Am J Pathol *157*, 2151-2159.

LaCasse, E. C., Mahoney, D. J., Cheung, H. H., Plenchette, S., Baird, S., and Korneluk, R. G. (2008). IAP-targeted therapies for cancer. Oncogene *27*, 6252-6275.

Li, M., Lewis, B., Capuco, A. V., Laucirica, R., and Furth, P. A. (2000). WAP-TAg transgenic mice and the study of dysregulated cell survival, proliferation, and mutation during breast carcinogenesis. Oncogene *19*, 1010-1019.

Lin, S. C., Lee, K. F., Nikitin, A. Y., Hilsenbeck, S. G., Cardiff, R. D., Li, A., Kang, K. W., Frank, S. A., Lee, W. H., and Lee, E. Y. (2004). Somatic mutation of p53 leads to estrogen receptor alpha-positive and -negative mouse mammary tumors with high frequency of metastasis. Cancer Res *64*, 3525-3532.

Liu, X., Holstege, H., van der Gulden, H., Treur-Mulder, M., Zevenhoven, J., Velds, A., Kerkhoven, R. M., van Vliet, M. H., Wessels, L. F., Peterse, J. L.*, et al.* (2007). Somatic loss of BRCA1 and p53 in mice induces mammary tumors with features of human BRCA1-mutated basal-like breast cancer. Proc Natl Acad Sci U S A *104*, 12111-12116.

Liyanage, M., Coleman, A., du Manoir, S., Veldman, T., McCormack, S.,

Dickson, R. B., Barlow, C., Wynshaw-Boris, A., Janz, S., Wienberg, J.*, et al.* (1996). Multicolour spectral karyotyping of mouse chromosomes. Nat Genet *14*, 312-315.

Ma, O., Cai, W. W., Zender, L., Dayaram, T., Shen, J., Herron, A. J., Lowe, S. W., Man, T. K., Lau, C. C., and Donehower, L. A. (2009). MMP13, Birc2 (cIAP1), and Birc3 (cIAP2), amplified on chromosome 9, collaborate with p53 deficiency in mouse osteosarcoma progression. Cancer Res *69*, 2559-2567.

Malkin, D. (1994). Germline p53 mutations and heritable cancer. Annu Rev Genet *28*, 443-465.

Marino, S., Vooijs, M., van Der Gulden, H., Jonkers, J., and Berns, A. (2000). Induction of medulloblastomas in p53-null mutant mice by somatic inactivation of Rb in the external granular layer cells of the cerebellum. Genes Dev *14*, 994-1004.

Maser, R. S., Choudhury, B., Campbell, P. J., Feng, B., Wong, K. K., Protopopov, A., O'Neil, J., Gutierrez, A., Ivanova, E., Perna, I.*, et al.* (2007). Chromosomally unstable mouse tumours have genomic alterations similar to diverse human cancers. Nature *447*, 966-971.

Matoso, A., Zhou, Z., Hayama, R., Flesken-Nikitin, A., and Nikitin, A. Y. (2008). Cell lineage-specific interactions between Men1 and Rb in neuroendocrine neoplasia. Carcinogenesis *29*, 620-628.

Mayhew, C. N., Bosco, E. E., Fox, S. R., Okaya, T., Tarapore, P., Schwemberger, S. J., Babcock, G. F., Lentsch, A. B., Fukasawa, K., and Knudsen, E. S. (2005). Liver-specific pRB loss results in ectopic cell cycle entry and aberrant ploidy. Cancer Res *65*, 4568-4577.

Mayhew, C. N., Carter, S. L., Fox, S. R., Sexton, C. R., Reed, C. A., Srinivasan, S. V., Liu, X., Wikenheiser-Brokamp, K., Boivin, G. P., Lee, J. S.,

et al. (2007). RB loss abrogates cell cycle control and genome integrity to promote liver tumorigenesis. Gastroenterology *133*, 976-984.

Meek, D. W. (2009). Tumour suppression by p53: a role for the DNA damage response? Nat Rev Cancer *9*, 714-723.

Minakuchi, Y., Takeshita, F., Kosaka, N., Sasaki, H., Yamamoto, Y., Kouno, M., Honma, K., Nagahara, S., Hanai, K., Sano, A.*, et al.* (2004). Atelocollagen-mediated synthetic small interfering RNA delivery for effective gene silencing in vitro and in vivo. Nucleic Acids Res *32*, e109.

Morrison, S. J., and Kimble, J. (2006). Asymmetric and symmetric stem-cell divisions in development and cancer. Nature *441*, 1068-1074.

Nikitin, A., and Lee, W. H. (1996). Early loss of the retinoblastoma gene is associated with impaired growth inhibitory innervation during melanotroph carcinogenesis in Rb+/- mice. Genes Dev *10*, 1870-1879.

Overholtzer, M., Zhang, J., Smolen, G. A., Muir, B., Li, W., Sgroi, D. C., Deng, C. X., Brugge, J. S., and Haber, D. A. (2006). Transforming properties of YAP, a candidate oncogene on the chromosome 11q22 amplicon. Proc Natl Acad Sci U S A *103*, 12405-12410.

Padilla-Nash, H. M., Wu, K., Just, H., Ried, T., and Thestrup-Pedersen, K. (2007). Spectral karyotyping demonstrates genetically unstable skin-homing T lymphocytes in cutaneous T-cell lymphoma. Exp Dermatol *16*, 98-103.

Pickering, M. T., and Kowalik, T. F. (2006). Rb inactivation leads to E2F1-mediated DNA double-strand break accumulation. Oncogene *25*, 746-755.

Reed, C. A., Mayhew, C. N., McClendon, A. K., Yang, X., Witkiewicz, A., and Knudsen, E. S. (2009). RB has a critical role in mediating the in vivo checkpoint response, mitigating secondary DNA damage and suppressing liver tumorigenesis initiated by aflatoxin B1. Oncogene *28*, 4434-4443.

Riley, T., Sontag, E., Chen, P., and Levine, A. (2008). Transcriptional control of human p53-regulated genes. Nat Rev Mol Cell Biol *9*, 402-412.

Robinson, G. W., Wagner, K. U., and Hennighausen, L. (2001). Functional mammary gland development and oncogene-induced tumor formation are not affected by the absence of the retinoblastoma gene. Oncogene *20*, 7115-7119.

Roy, P. G., and Thompson, A. M. (2006). Cyclin D1 and breast cancer. Breast *15*, 718-727.

Scambia, G., Lovergine, S., and Masciullo, V. (2006). RB family members as predictive and prognostic factors in human cancer. Oncogene *25*, 5302-5308.

Sherr, C. J. (2004). Principles of tumor suppression. Cell *116*, 235-246.

Sherr, C. J., and McCormick, F. (2002). The RB and p53 pathways in cancer. Cancer Cell *2*, 103-112.

Simin, K., Wu, H., Lu, L., Pinkel, D., Albertson, D., Cardiff, R. D., and Van Dyke, T. (2004). pRb inactivation in mammary cells reveals common mechanisms for tumor initiation and progression in divergent epithelia. PLoS Biol *2*, E22.

Sorlie, T., Perou, C. M., Tibshirani, R., Aas, T., Geisler, S., Johnsen, H., Hastie, T., Eisen, M. B., van de Rijn, M., Jeffrey, S. S., *et al.* (2001). Gene expression patterns of breast carcinomas distinguish tumor subclasses with clinical implications. Proc Natl Acad Sci U S A *98*, 10869-10874.

Sporn, M. B., Dowsett, S. A., Mershon, J., and Bryant, H. U. (2004). Role of raloxifene in breast cancer prevention in postmenopausal women: clinical evidence and potential mechanisms of action. Clin Ther *26*, 830-840.

Steinhardt, A. A., Gayyed, M. F., Klein, A. P., Dong, J., Maitra, A., Pan, D., Montgomery, E. A., and Anders, R. A. (2008). Expression of Yes-associated

protein in common solid tumors. Hum Pathol *39*, 1582-1589.

Wang, T. C., Cardiff, R. D., Zukerberg, L., Lees, E., Arnold, A., and Schmidt, E. V. (1994). Mammary hyperplasia and carcinoma in MMTV-cyclin D1 transgenic mice. Nature *369*, 669-671.

Wijnhoven, S. W., Zwart, E., Speksnijder, E. N., Beems, R. B., Olive, K. P., Tuveson, D. A., Jonkers, J., Schaap, M. M., van den Berg, J., Jacks, T.*, et al.* (2005). Mice expressing a mammary gland-specific R270H mutation in the p53 tumor suppressor gene mimic human breast cancer development. Cancer Res *65*, 8166-8173.

Zender, L., Spector, M. S., Xue, W., Flemming, P., Cordon-Cardo, C., Silke, J., Fan, S. T., Luk, J. M., Wigler, M., Hannon, G. J.*, et al.* (2006). Identification and validation of oncogenes in liver cancer using an integrative oncogenomic approach. Cell *125*, 1253-1267.

Zhou, Z., Flesken-Nikitin, A., Corney, D. C., Wang, W., Goodrich, D. W., Roy-Burman, P., and Nikitin, A. Y. (2006). Synergy of p53 and Rb Deficiency in a Conditional Mouse Model for Metastatic Prostate Cancer. Cancer Res *66*, 7889-7898.

Zhou, Z., Flesken-Nikitin, A., and Nikitin, A. Y. (2007). Prostate cancer associated with p53 and Rb deficiency arises from the stem/progenitor cell-enriched proximal region of prostatic ducts. Cancer Res *67*, 5683-5690.

CHAPTER 3

IDENTIFICATION AND CHARACTERIZATION OF CANCER STEM CELLS

3.1 Abstract

The leading explanation of the molecular and genetic heterogeneity of many cancers, including breast cancer, lies in the existence of a small highly tumorigenic subpopulation of cells called cancer stem cells (CSC). Since CSC represent an appealing target for development of more selective and efficient therapies their identification and characterization are critical for further advances of cancer research. To test if CSC exist in our model of mammary carcinoma associated with p53 and Rb deficiency cells expressing mammary stem cell markers CD24 and CD49f have been isolated and functionally characterized. As compared to $CD24^{-}CD49f^{-}$ cell population far fewer of $CD24^{+}CD49f^{+}$ cells were required for orthotopic transplantation into the cleared mammary fat pad. Furthermore, as expected from CSC, $CD24^{+}CD49f^{+}$ cells yielded carcinomas much earlier and were able to reconstitute all tumor populations more efficiently than $CD24^{-}CD49f^{-}$ cells in secondary and tertiary transplantations. Thus, $CD24^{+}CD49f^{+}$ cells were identified as CSC in our model. As compared to cancer non stem cells (CnSC, $CD24^{-}CD49f^{-}$) CSC had more stable genome according to lower percentage of comet tail positive cell, lower expression of Mad2, and less DNA damage after γ irradiation. Phenotypic characterization of CSC identified high levels of cIAP1 and Aldh1 which allowed determining their location by double immunostaining of tissue sections. To study the role of stem cell compartment in carcinogenesis and CSC initiation, we have isolated populations of mammary stem cells

(mammary repopulating units, MRU; $CD24^{med}CD49f^{high}$), and their progeny mammary colony-forming cells (Ma-CFC, $CD24^{high}CD49f^{low}$). We found that loss of *p53* leads to an increase in the number and proliferation rate of Ma-CFC but not MRU. Both parameters are further increased in Ma-CFC cell pool deficient for both p53 and Rb. Taken together, we demonstrate existence of CSC in our model and provide their initial characterization. Our study also identifies the mammary progenitor cells as the principle targets for malignant transformation, which subsequently leads to appearance of CSC, and suggests expansion of progenitor cell pool as a novel cooperative effect of *p53* and *Rb* inactivation on carcinogenesis.

3.2 Introduction

Cancers, whether solid or hematopoietic, from different patients often exhibit heterogeneity in morphology, genetic lesions, molecular profile, cell surface markers, cell proliferation kinetics, and response to therapy (Buerger et al., 1999a; Buerger et al., 1999b; Heppner and Miller, 1983). This heterogeneity may be due to cells with stem cell properties that can differentiate to yield different cell types within a tumor. Since the 19^{th} century, it has been proposed that a subpopulation of neoplastic cells called cancer stem cells (CSC) may be responsible for initiating and propagating tumors (Nafus & Nikitin, 2009). CSC have stem cell-like properties that are thought to be responsible for the growth, progression, and recurrence of tumors (Clarke and Fuller, 2006). In 2003, Al-Hajj et al., first reported the isolation of cancer stem cells ($CD44^{+}$ $CD24^{-}$) from human breast cancer (Al-Hajj et al., 2003). This study also demonstrates that human breast cancer have a small proportion of cells that have the capacity to form a new tumor when serially xenografted in

NOD/SCID mice. To date, in humans, CSC have been identified in a number of malignancies, including leukemia (Bonnet and Dick, 1997; Lapidot et al., 1994), prostate cancer (Collins et al., 2005), brain tumors (Bao et al., 2006), ovarian cancer (Alvero et al., 2009; Szotek et al., 2006; Zhang et al., 2008b) and colon cancer (O'Brien et al., 2007; Ricci-Vitiani et al., 2007).

The CSC subpopulation has been described in several mouse models of mammary carcinogenesis using different cell surface markers(Cho et al., 2008; Vaillant et al., 2008; Zhang et al., 2008a). For example, in the *MMTV-Wnt1* mouse model of mammary cancer, a $Thy1^{+}CD24^{+}$ cancer cell population was found to be highly enriched for CSC relative to the non $Thy1^{+}CD24^{+}$ population (Cho et al., 2008). Vaillant and colleagues (2008) reported a different set of markers (CD29, CD24, and CD61) that can be used to isolate a CSC population which possesses a 20-fold enrichment tumor-initiating capacity in *MMTV–Wnt1* mammary tumors (Vaillant et al., 2008). In addition, it is worth to note that CSC were not found in all mouse models of mammary tumors. In the well established *MMTV–Erbb2* strain, no CSC subset could be identified using multiple different cell surface markers, suggesting a clonal evolution or stochastic model of carcinogenesis (Vaillant et al., 2008). In the *p53*-null mammary tumor model described by Zhang and colleagues (Zhang et al., 2008a), most of the tumors coexpressed luminal cell markers (CK8) and myoepithelial cell marker (CK14). A subpopulation of cells expressing high levels of CD24 and CD29 ($Lin^{-}CD24^{H}CD29^{H}$), which accounts for 5-10% of total mammary epithelial cell population, has been identified as CSC by limiting dilution in cell culture mammosphere assays and subsequent transplantation *in vivo* (Zhang et al., 2008a). However, it should be noted that all experiments in this study were performed on tumors derived by

transplantation of p53-null mammary epithelium cells into cleared mammary fat pads. Thus, it remains to be demonstrated if the observed results can be reproduced in an autochthonous sporadic mouse model of mammary carcinogenesis.

Alterations in p53 and Rb tumor suppressors or their pathways are common in human breast cancer. In addition, both p53 and Rb have important functions in stem cells. *p53* has been shown to mediate the onset of senescence of endothelial progenitor cells, to negatively regulate proliferation and survival of neural stem cells, and to induce differentiation of embryonic stem cells (reviewed in Stingl and Caldas, 2007). *Rb* and its pathway are involved in control of stem cell cycle progression, senescence and tissue homeostasis (reviewed in Galderisi et al., 2006). Notably, p16/Rb and ARF/p53 pathways are extensively connected and may be coordinately regulated by Bmi-1. Bmi-1 has been shown to be required for maintenance and self-renewal of hematopoietic and neural stem and progenitor cells in mice and is involved in control of cell proliferation, survival and differentiation (reviewed in Valk-Lingbeek et al., 2004). Furthermore, it has been demonstrated that in a conditional mouse model of prostate cancer associated with p53 and Rb deficiency cancer cells show a heterogeneous phenotype and arise from the prostate stem cell compartment (Zhou et al., 2006; Zhou et al., 2007). However, it remains unclear whether mammary stem cells (MaSC) represent a preferential target for malignant transformation associated with p53 and/or Rb mutation.

As discussed in Chapter 2, we generated mouse models of mammary carcinoma associated with p53 and Rb deficiency and demonstrated that these neoplasms are similar to human luminal type B, ER positive and

raloxifene-responsive breast cancer (Chapter 2). In this study, by using negative selection for cell lineage markers CD31, CD45 Ter119, CD140a, and positive selection for mammary stem cell markers CD24 and CD49f, we demonstrate that the mammary neoplasms in our model contain CSC. As compared to cancer non-stem cells (CnSC), CSC have a more stable genome. We further demonstrate that CSC have high expression of cIAP1 (cellular inhibitor of apoptosis 1) and Aldh1 and can be localized by double immunofluorescence on tissue sections. Finally, we demonstrate that p53 and Rb cooperatively control mammary progenitor cell proliferation and inactivation of these genes may result in carcinogenesis due to expansion of mutant progenitor cells.

3.3 Materials and methods

Mouse. Generation of $p53^{ME-/-}$, $Rb^{ME-/-}$, and $p53^{ME-/-}$ $Rb^{ME-/-}$ mice was described in *Materials and Methods* of Chapter 2. *MMTV-Neu* mice *(Guy et al., 1992)* were obtained from the Jackson laboratory. The efficiency and tissue specificity of *Cre*-mediated recombination was examined by crossing *MMTVCre* transgenic founders with *Tg(ACTB-Bgeo/GFP)21Lbe (*Z/EG) mice (Novak et al., 2000) which express EGFP after Cre administration.

Isolation of primary mammary epithelial cells and tumor cells. Normal mammary glands were dissected from 5 months old healthy FVB/N females. Mammary tumor tissue was from mouse model of mammary tumor with p53 and/or Rb deficiency. Procedure of isolation of primary mammary epithelial cells and tumor cells was described in *Materials and Methods* of Chapter 2.

Cell labeling and Fluorescence Activated Cell Sorting (FACS)

analysis. Lineage positive cells were magnetically removed with CD31 (endothelial cell), CD45 (hematopoietic cells), Ter119 (hematopoietic cells), and CD140a (stromal cells) antibodies using CELLection Biotin Binder Kit (Invitrogen, Carlsbad, CA, USA) after treatment of dissociated cells with respective biotinylated antibodies at concentration 1µg / 10^6 cell. The remaining cells were stained with PE-conjugated anti-CD24 antibody (BD, Franklin Lakes, NJ, USA) and FITC-conjugated anti-CD49f antibody (BD) or PE-conjugated and FITC-conjugated isotype control antibodies for 30 min on ice. Cells were washed twice with FACS buffer and resuspended into FACS buffer for cell sorting. Cell sorting was performed on a FACS Aria cell sorter (BD).

Tumor cell transplantation and raloxifene treatment. This procedure was described in *Materials and Methods* of Chapter 2.

Serial transplantations. To prove the self-renewal of CD24+ and CD49f+ population, sorted cells were serially transplanted following FACS and mammary fat pad transplantation described above. CD24+CD49f+ and CD24-CD49f- cell fractions will be transplanted into the cleared mammary fat pad and grafts were collected after surgery, dissociated and subjected to sorting and transplantation as before. These experiments were accompanied by performing serial dilutions of transplanted cells in order to estimate number of clonogenic cells. Limiting dilution analysis was conducted by L-Calc™ software. The user guide of L-Calc™ can be found in http://www.stemcell.com/technical/lcalc02.pdf.

Matrigel culture. Assay media was prepared by adding 49 ml of growth media (EpiCult-B, StemCell Technologies, Vancouver, BC, Canada) and 1 mL of matrigel (BD), and then cells were diluted to 1 x 10^4 cells/mL with assay

media. 500 µL of cell suspension was added to each well of the 48 well plate containing Matrigel, and then incubated at 37°C in a CO^2 incubator. Clones were counted four days after culture.

Immunohistochemical analyses. This procedure was described in *Materials and Methods* of Chapter 2. Primary antibodies used include: CK5 (Covance, Berkeley, CA, USA, 1:1000), CK6, (Covance, 1:300), CK8 (Developmental Studies Hybridoma Bank, University of Iowa, IW, USA, 1:50), SMA (Spring Bioscience, Fermont, CA, USA 1:300), and Phospha-Histone H2A.X (Ser139) (Cell signaling, Danvers, MA, USA, 1:100). All quantitative analyses were performed on digitally captured images as described in (Zhou et al., 2006).

Western blot analysis. This procedure was described in *Materials and Methods* of Chapter 2. Primary antibody used include cIAP1 (Abcam, Cambridge, MA, USA, 1:300), Mad2 (Santa Cruz, Santa Cruz, CA, USA, 1:200), and Gapdh (Advanced immunochemical Inc, Long Beach, CA, USA, 1:1000).

Neutral comet, Irradiation and H2AX staining assays. This procedure of neutral comet assay was described in *Materials and Methods* of Chapter 2. For tumor cell irradiation, isolated primary tumor cells were irradiated (10 Gray, PRIMUS Linear Accelerator, SIEMENS, Malvern, PA, USA), and then checked for DNA damage 6, 12, or 24 hours after irradiation by Phospha-Histone H2A.X (Ser139) staining.

Real-time PCR. This procedure of real-time PCR was described in *Materials and Methods* of Chapter 2. *cIAP1* and *Mad2* TaqMan probes were from Applied Biosystems (Carlsbad, CA, USA).

Cell proliferation and survival. For the proliferation assay, mice were

injected by i.p. with 5mg/ml bromodeoxyueidine (BrdU, Sigma, St. Louis, MO, USA) 20µl/g body weight. One hour after injection, mammary glands were dissected and processed for FACS sorting as described above. Sorted cells were spun onto microscope slides and stained for BrdU immunostaining as described previously (Flesken-Nikitin et al., 2003; Zhou et al., 2006; Zhou et al., 2007). For the apoptosis assay, Lin- cells were incubated with Annexin V-FITC (BD), CD24-PE and CD49f-PE-Cy5 in dark for 30 min at 4^{o}C and analyzed by FACS. A total of at least 50,000 cells were analyzed per sample.

Statistical Analyses. All statistical analyses in this study were done using InStat 3.06 and Prism 5.01 software (GraphPad, Inc., San Diego, CA, USA) as described previously (Zhou et al., 2006).

3.4 Results

Identification of tumorigenic subpopulations with stem cell properties. According to flow cytometry analysis of mammary carcinomas from *p53*$^{ME-/-}$ and *p53*$^{ME-/-}$*Rb*$^{ME-/-}$ mice (10 in each group), 8.8 ± 4.9% vs 11.8 ± 5.6% for each group of total tumor cell population were CD24^{+}CD49f^{+} cells, (Fig 3.1A). No significant differences were observed regarding to the percentage of CD24^{+}CD49f^{+} cells in carcinomas from *p53*$^{ME-/-}$ and *p53*$^{ME-/-}$ *Rb*$^{ME-/-}$ mice. When 5 x 10^{3} cells of CD24^{+}CD49f^{+} or CD24^{-}CD49f^{-} were cultured in Matrigel for 4 days, the CD24^{+}CD49f^{+} population generated 4 folds more clones than CD24^{-} CD49f^{-} population (Fig 3.1C, D). We further tested the tumorigenic ability of these populations by transplanting cells into cleared mammary fat pad of 3 week old FVB mice. Transplantation of as few as one CD24^{+}CD49f^{+} cell resulted in tumors formation 3 of 8 transplants, whereas no tumors were observed from 10^{3} CD24^{-}CD49f^{-} cells (0 of 4 transplants) (Table

3.1). Twenty days after transplantation, 10^4 $CD24^+CD49f^+$ cells formed much larger tumors (Fig 3.1B left) than those of 10^4 $CD24^-CD49f^-$. Quantitative assessment showed that significant tumor volume difference (Fig 3.1B right, 1.0 ± 0.18 cm^3 VS 0.05 ± 0.08 cm^3, $CD24^+CD49f^+$ VS $CD24^-CD49f^-$, Mean±SD, P<0.0001. 6 transplantation per group). According to calculations with L-Calc software and the data from Table 3.1, the frequency of tumorigenic cells was 1 in 9 in $CD24^+CD49f^+$ cell population, and 1 in 19,380 in $CD24^-CD49f^-$ cell population. Since self-renewal is a unique property of stem cells, it was tested by serial orthotopic transplantations of cell subpopulations. $CD24^+CD49f^+$ cells from the first round transplantation were able to reconstitute all tumor populations far more efficiently than $CD24^-$ $CD49f^-$ cells in secondary and tertiary transplantations (Table 3.1). In addition, transplant tumors generated by $CD24^+CD49f^+$ population displayed similar pathology and marker expression (CK8, SMA, CK5, and CK6) as compared with the original tumors (Fig 3.2), suggesting that these cells were able to generate the heterogeneous characteristics of the original tumor. Taken together these results demonstrate that $CD24^+CD49f^+$ cells meet the definition of CSC.

Phenotypical properties of CSC. To evaluate functional status of isolated CSC population we have tested a number of markers. Cytosolic aldehyde dehydrogenase (Aldh), an enzyme implicated in retinoid metabolism and resistance of hematopoietic stem cells to alkylating agents such as cyclophosphamide (Hess et al., 2006). Aldh may have a role in early differentiation of stem cells through its role in oxidizing retinol to retinoic acid (Chute et al., 2006). It has been shown that mouse and human hematopoietic and neural stem and progenitor cells have high Aldh activity (Armstrong et al., 2004; Hess et al., 2004).

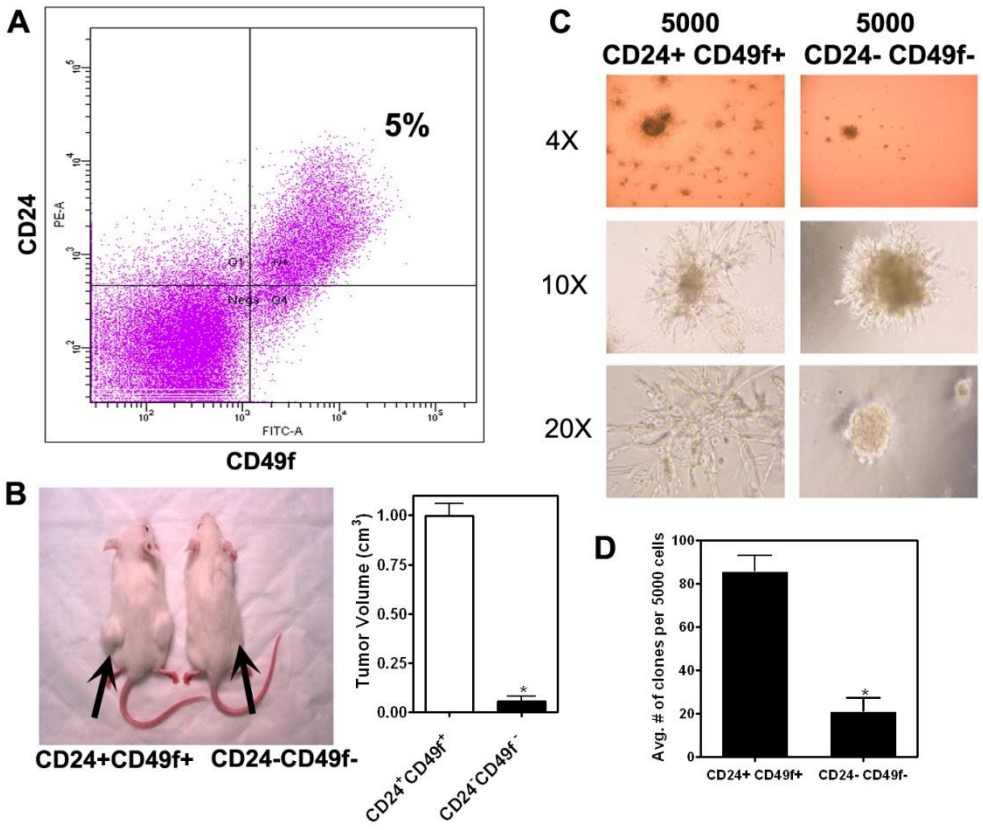

Figure 3.2 Identification of cancer stem cell.

A. Representative flow cytometry profiles of CD24 (PE) and CD49f (FITC) expression in freshly isolated mouse mammary tumor cells from *p53*$^{ME-/-}$ or *p53*$^{ME-/-}$*Rb*$^{ME-/-}$ mice. B. Cleared mammary fat pad transplantation with 10^4 CD24$^+$CD49f$^+$ (Left mouse) and CD24$^-$CD49f$^-$ (Right mouse). 20 days after transplantation, double positive tumor cells form much larger tumors than that of double negative tumor cells. C and D. CD24$^+$CD49f$^+$ cell population form more clones than CD24$^-$CD49f$^-$ cells in Matrigel (Mean ± SD, 86 ± 7 vs 21 ± 6, n=5, P=0.0003, * indicates P<0.05).

Table 3.2 CSC and CnSC transplantation with serial dilution.

#	First round transplantation		Second round transplantation		Third round transplantation	
	CSC	CnSC	CSC	CnSC	CSC	CnSC
10^4	~14 days 6/6 mice	~30 days 2/6 mice	N/A	N/A	N/A	N/A
5×10^3	N/A	~25 days 1/4 mice	N/A	N/A	N/A	N/A
2×10^3	~12 days 4/4 mice	~35 days 1/4 mice	~12 days 4/4 mice	~25 days 2/4 mice	~10 days 4/4 mice	~18 days 2/4 mice
10^3	N/A	~40 days 0/4 mice	~15 days 4/4 mice	~35 days 1/4 mice	~12 days 4/4 mice	~25 days 1/4 mice
3×10^2	~22 days 4/4 mice	N/A	N/A	N/A	N/A	N/A
10^2	~25 days 4/4 mice	N/A	~25 days 3/4 mice	~45 days 0/4 mice	~18 days 3/4 mice	~45 days 0/4 mice
20	~ 30 days 3/4 mice	N/A	N/A	N/A	N/A	N/A
1	~30 days 3/8 mice	N/A	~30 days 2/4 mice	N/A	~25 days 2/4 mice	N/A

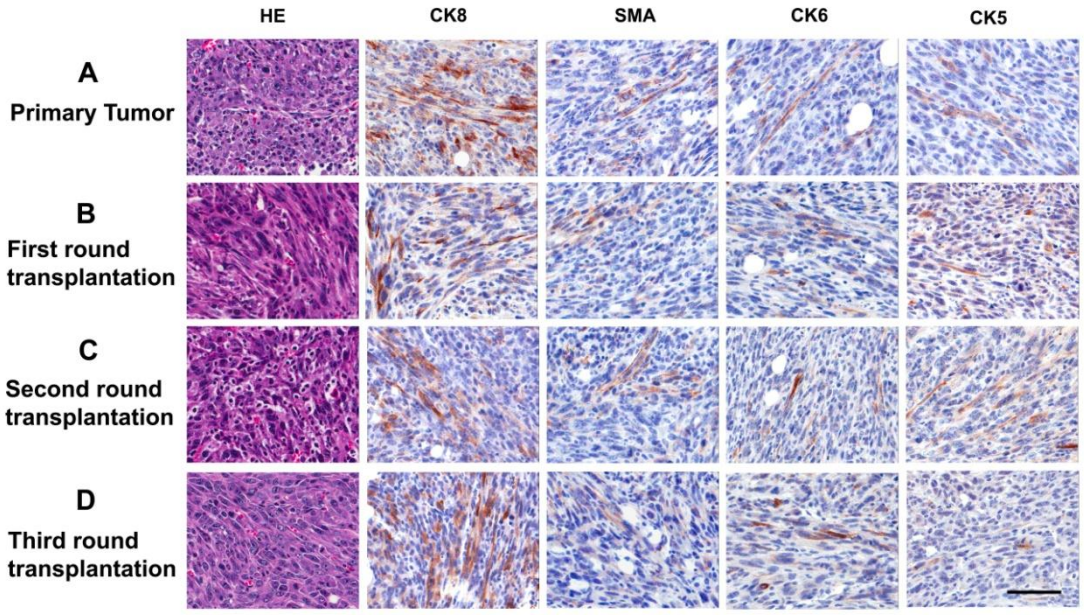

Figure 3.3 Immunohistochemical evaluation of mammary tumors after serial orthotopic transplantation.

Histological sections of mammary tumors: (A) primary tumor, (B) first, (C) second, and (D) third round of transplantation of $2X10^3$ $CD24^+CD49f^+$ cells were stained with hematoxylin and eosin (HE), CK8, SMA, CK6 and CK5. CK8, SMA, CK6 and CK5, ABC method, counterstaining with hematoxylin. Calibration bar for all images: 100 µm.

Recently, ALDH1 expression and activity have been reported as markers of normal and malignant human mammary stem cells and a predictor of poor clinical outcome (Ginestier et al., 2007). In our study, over 90% $CD24^+$ $CD49f^+$ tumor cells were positive for Aldefluor, an indicator of Aldh1 enzymatic activity (Fig 3.3A), in all carcinoma analyzed (8 tumors from $p53^{ME-/-}$ and 8 tumor from $p53^{ME-/-}Rb^{ME-/-}$ mice). Thus our results confirmed Aldh as a CSC marker.

cIAP1 (also known as Birc2) is a member of inhibitor of apoptosis (IAP) family. IAP family members are important regulators of cell death, and overexpression of IAPs predicts poor patient outcome in several types of cancer. cIAP1, containing the baculoviral IAP repeat domain, is an endogenous apoptosis inhibitor that interacts with caspases, suppressing apoptosis by preventing procaspase activation and inhibition of the enzymatic activities of caspases (Deveraux and Reed, 1999; LaCasse et al., 2008). Our studies demonstrated that overexpression of cIAP1 is essential for mammary carcinogenesis (Chapter 2). Interestingly we determined that particularly high levels of cIAP1 are present in CSC on both mRNA and protein level (Fig 3.3B and C). Therefore, cIAP1 can be used as a novel marker for CSC. Both CSC and CnSC are ER positive and CSC express well known stem cell regulators Gli2 and Wnt1 (Fig 3.3C).

Localization of CSC population. Studies of brain tumors have demonstrated that specialized perivascular niches contribute to the CSC long term growth and self-renewal by secreting factors (Calabrese et al., 2007; Charles et al.). To study if breast cancer also have similar vascular niche, we used blood vessel endothelial cell marker CD31 in combination with Aldh1

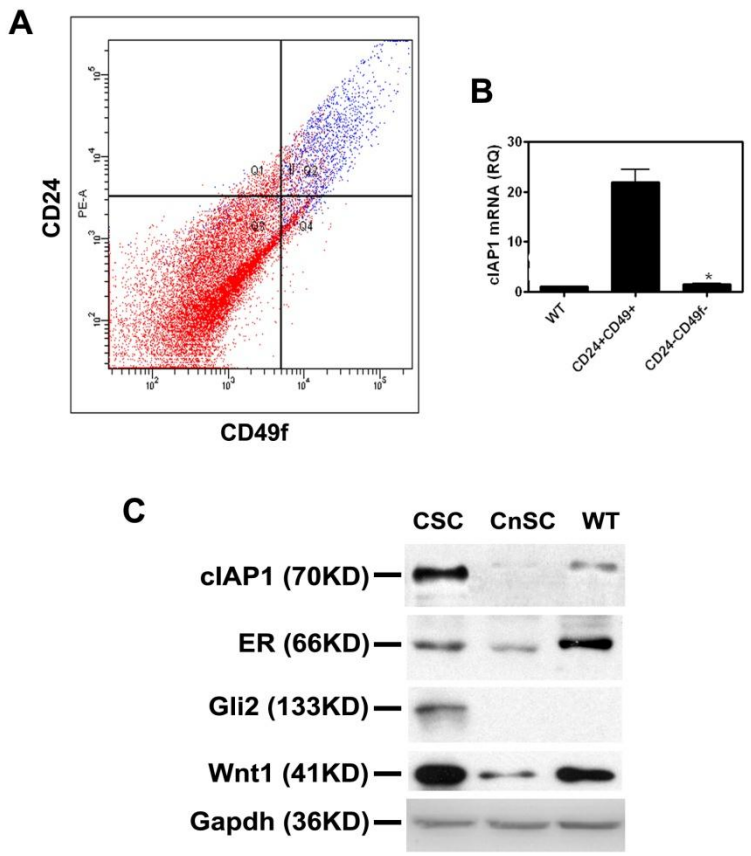

Figure 3.4 Characterization of cancer stem cells.

A. Representative flow cytometry profiles of CD24 (PE) and CD49f (FITC) expression in freshly isolated mouse mammary tumor cells from *p53*$^{ME-/-}$ and *p53*$^{ME-/-}$ *Rb*$^{ME-/-}$ mice. Over 90% of CD24+CD49f+ tumor cells are Aldefluor positive. B. Real time PCR analysis demonstrated that cIAP1 mRNA are overexpressed in CSC (Mean ± SD, 22.8 ± 3.1 (CSC) vs 1.9 ± 0.1 (CnSC), n=5, P=0.0002, * indicates P<0.05). C. Protein expression of cIAP1, ER, Gli2 and Wnt1 in CSC, CnSC and normal mammary epithelia cells (WT). cIAP1 protein is overexpressed in CSC, as compared to CnSC and WT. Both CSC and CnSC are ER positive. Gli2 and Wnt1 are highly expressed in CSC as compared to CnSC.

Figure 3.5 Localization of cancer stem cells.

A. Double fluorescence staining with Aldh1 and CD31. Location of Aldh1 positive cells is associated with CD31 positive cells (Top and Middle). Aldh1 negative cells are not associated with CD31 positive cells (Bottom). B. Double fluorescence staining with cIAP1 and CD31. Location of cIAP1 positive cells is associated with CD31 positive cells (Top and Middle). cIAP1 negative cells are not associated with CD31 positive cells (Bottom). C. Double fluorescence staining with Aldh1 and cIAP1. Aldh1 overexpressed cells are co-localized with cIAP1 overexpressed cells very well. Arrows show positive cells.

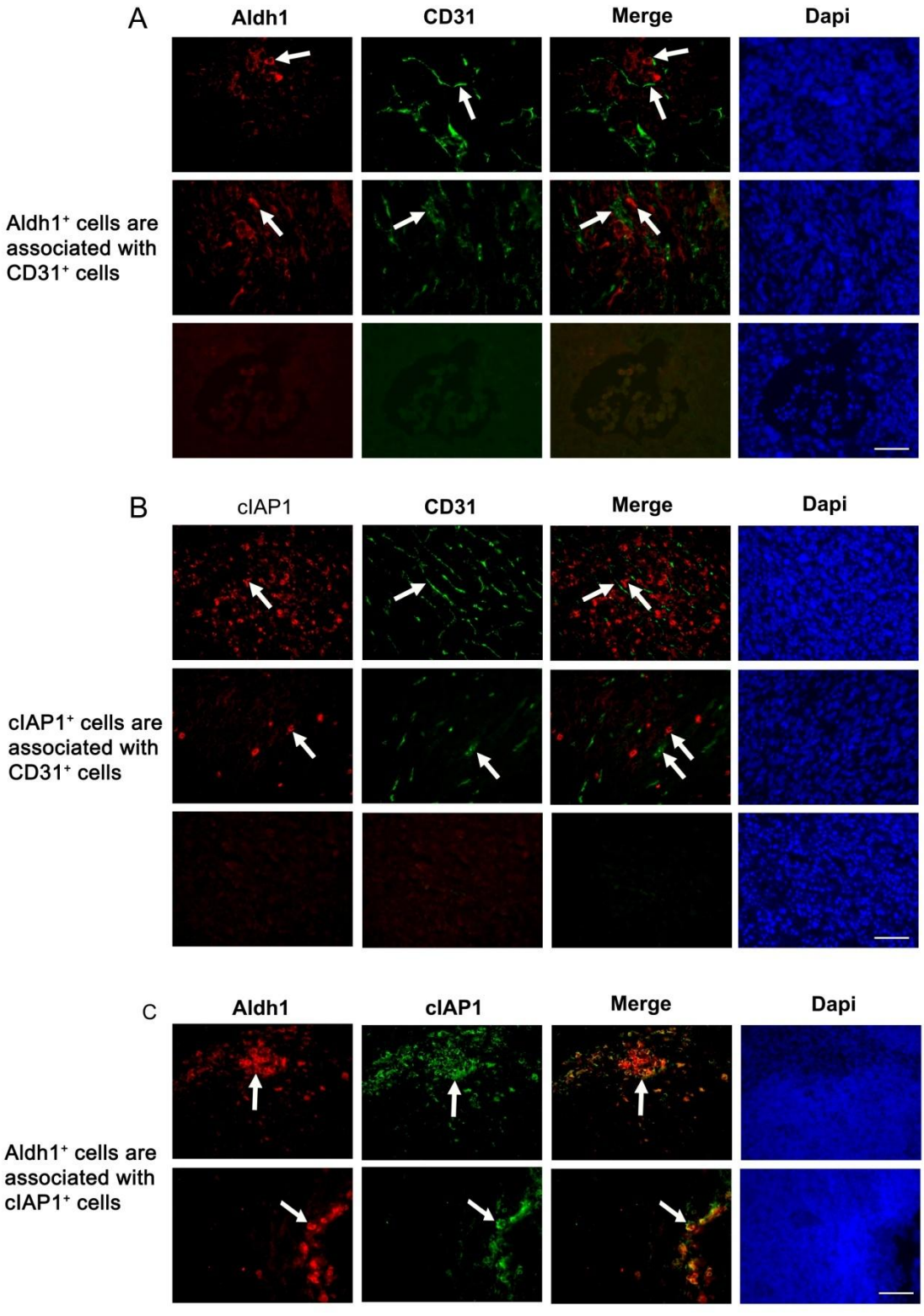
A
Aldh1
CD31
Merge
Dapi
Aldh1+ cells are associated with CD31+ cells
B
cIAP1
CD31
Merge
Dapi
cIAP1+ cells are associated with CD31+ cells
C
Aldh1
cIAP1
Merge
Dapi
Aldh1+ cells are associated with cIAP1+ cells

and/or cIAP1 antibodies. Double fluorescence staining with Aldh1 and CD31, or cIAP1 and CD31 showed that Aldh1 or cIAP1 positive cells are associated with CD31 positive cells (Fig 3.4A and B). While Aldh1 or cIAP1 negative cells are not associated with CD31 positive cells (Fig 3.4A and B). As expected, Aldh1 and cIAP1 positive cells are co-localized (>75%) in the most of cases (Fig 3.4C). Total 6 tumors were analyzed. These observations may indicate that breast CSC have a similar vascular niche to that in brain tumors.

CSC have higher genomic stability as compared to CnSC. Similar to normal stem cells CSC may have higher levels of resistance to genotoxic factor. Indeed it has been reported that CSC are frequently more resistant to irradiation and chemotherapy (reviewed in Rich and Bao, 2007). To test if CSC have higher genomic stability as compared to CnSC, we examined Mad2 expression and performed comet tail assay. Mad2 has been shown to mediate DNA double strand break accumulation and contribute to mitotic defects and genomic instability (Hernando et al., 2004; Pickering and Kowalik, 2006). Neutral comet tail assay is used to identify DNA double strand break. CSC had significantly lower Mad2 expression on both mRNA and protein level, and less comet tail positive cells (Fig 3.5A, B and C). Therefore, our observations indicate that CSC have relatively more stable genome than CnSC.

To test CSC DNA damage response to γ irradiation primary mammary carcinoma cells were exposed to a dose of 10 Gray. 6, 12 and 24 hours after irradiation to separate CSC and CnSC populations, and stained for Phosphorylated H2AX, a marker for DNA damage. CSC have lower percentage of phosphorylated H2AX positive cells than CnSC at 0 hour (Fig 3.5D). Percentage of H2AX positive CSC has no change until 12 hours after irradiation, while increased percentage of H2AX positive CnSC is detected

Figure 3.6 CSC have higher genomic stability as compared to CnSC.

CSC have lower Mad2 expression than CnSC in both mRNA (A, (Mean ± SD, 2.45 ± 0.12 VS 3.78 ± 0.11, n=4, P=0.001, * indicated P<0.05).) and protein level (B). C. CSC have lower percentage of comet tail positive cells than CnSC (Mean ± SD, 15.1 ± 1.2 VS 17.8 ± 1.3, n=4, P=0.043, * indicated P<0.05). D. Cells treated with irradiation will cause DNA damage. Without irradiation, CSC have less DNA damage than CnSC, as indicated by less percentage of positive phosphorylated H2AX cells (12 ± 2 VS 21 ± 3.6, n=4, p=0.013). After irradiation, percentage of positive phosphorylated H2Ax cell is 9 ± 1 VS 37 ± 4.6 (CSC VS CnSC, Mean ± SD, n=4, P=0.0083), 20 ± 1.7 VS 49 ± 6 (P=0.0023), and 46.7 ± 11.9 VS 63.3 ± 2.9 (P=0.026) at 6 hours, 12 hours and 24 hours, respectively.

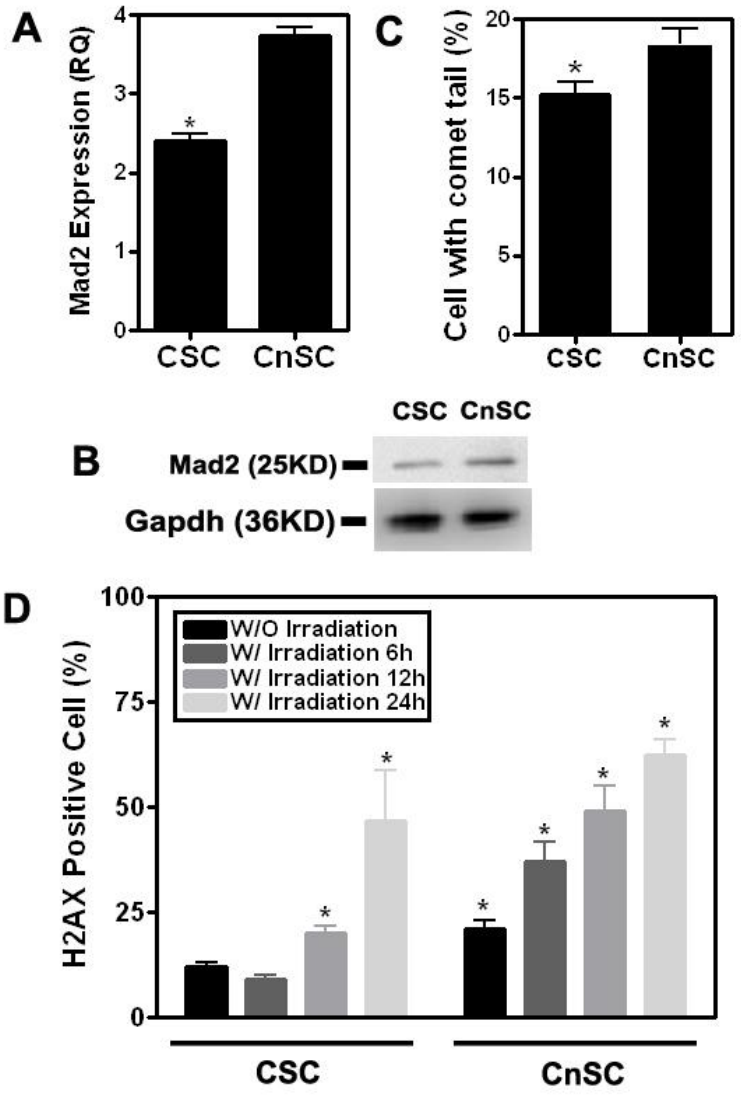
A
Mad2 Expression (RQ)
4
3
2
1
0
*
CSC
CnSC
C
Cell with comet tail (%)
20
15
10
5
0
*
CSC
CnSC
CSC CnSC
B
Mad2 (25KD)
Gapdh (36KD)
D
H2AX Positive Cell (%)
100
75
50
25
0
W/O Irradiation
W/ Irradiation 6h
W/ Irradiation 12h
W/ Irradiation 24h
*
CSC
CnSC

already at 6 hours after irradiation. Eventually, Percentage of H2AX positive CSC increased at 12 and 24 hours after irradiation, but was less pronounced than that of CnSC at all time points, indicating that CSC are likely to be more resistant to irradiation therapy.

***Cre* expression in mammary stem and colony-forming cells.** Recently it has been demonstrated that mammary stem cells, mammary repopulating units (MRU) and their progeny mammary colony-forming cells (Ma-CFC) can be successfully isolated by negative selection for lineage markers (Lin-) of hematopoietic (CD45 and Ter119), endothelial (CD31) and stromal (CD140a) cells followed by positive selection for mammary stem cell markers CD24 and CD49f or CD29 (reviewed in Stingl and Caldas, 2007). We were able to reproduce those experiments and confirmed that MRU, and to some extent Ma-CFC were able to form mammary gland after transplantation into the cleared mammary fad pat (Fig 3.6).

To study the role of stem cells in mammary carcinogenesis, we first assessed efficiency of *Cre*-mediated recombination in MRU and Ma-CFC. *MMTVCre* mice were crossed with Z/EG reporter mice, in which the EGFP expression indicates *Cre* activity. According to tri-color FACS analysis of mammary epithelial cells about 2.8% of MRU ($CD24^{med}CD49f^{high}$) and 3.4% of Ma-CFC ($CD24^{high}CD49f^{low}$) were EGFP positive in *MMTV-Cre EGL* mice (Fig 3.7). Therefore, *Cre* is expressed in both MRU and Ma-CFC.

Inactivation of *p53* and *Rb* cooperate in increasing Ma-CFC population. To determine the role of *p53* and *Rb* in control of MRU and Ma-CFC, MRU and Ma-CFC were isolated from *FVB*, *MMTV-Neu*, $p53^{ME-/-}$, $Rb^{ME-/-}$ and $p53^{ME-/-}$ $Rb^{ME-/-}$ 4 to 6 months old female mice and subjected to quantitative flow cytometry analysis (Fig 3.8). There was no significant

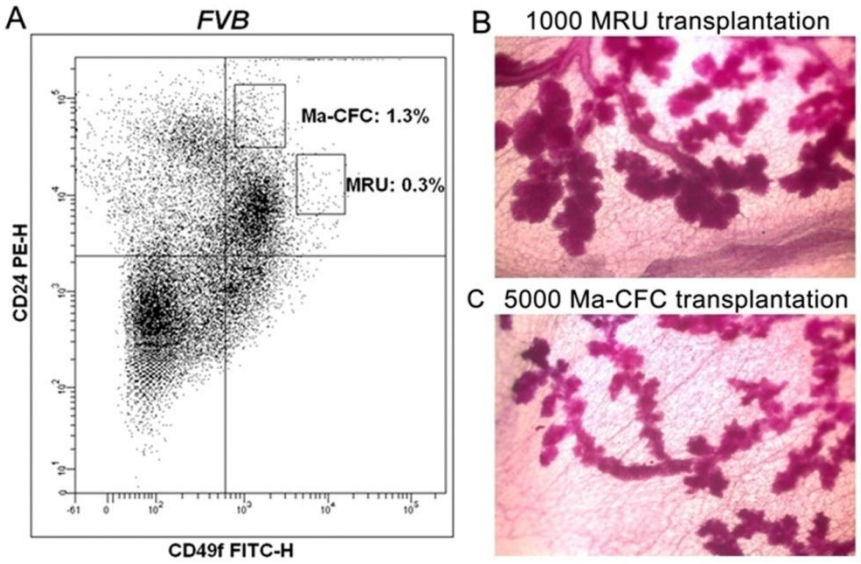

Figure 3.7 Isolation and characterization of MRU and Ma-CFC.

A. Representative flow cytometry profiles of CD24 (PE) and CD49f (FITC) expression in freshly isolated mouse mammary epithelia cells. MRU and Ma-CFC account for 0.3% and 1.3% of total cell population, respectively. B and C. Whole mount staining of the mammary gland generated within 4 weeks by transplantation of 1000 MRU and 5000 Ma-CFC, respectively, into the cleared mammary fat pad.

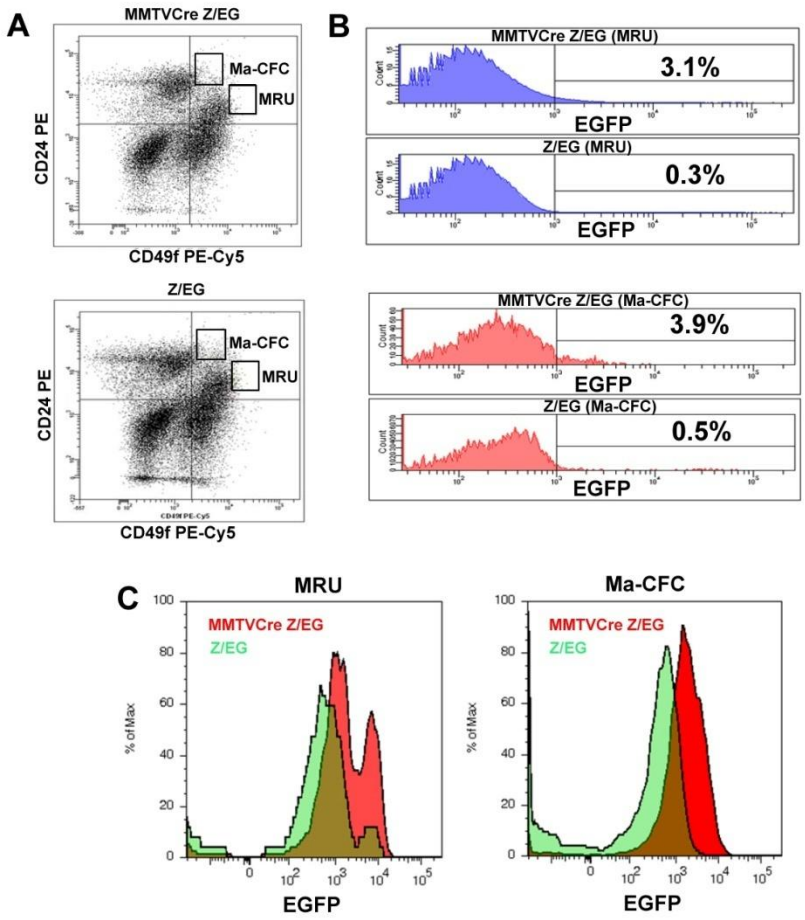

Figure 3.8 *Cre* expression in MRU and Ma-CFC.

A, Flow cytometry profiles of CD24 (PE) and CD49f (PE-Cy5) expression in freshly isolated mouse mammary cells from *MMTVCre* Z/EG (Top) and Z/EG (Bottom) mice. B, Comparison of EGFP expression in MRU (Top) and Ma-CFC (Bottom) of *MMTVCre* Z/EG and Z/EG nulliparous mice. C, EGFP expression profiles in MRU (Left) and Ma-CFC (Right) of *MMTVCre* Z/EG and Z/EG nulliparous mice. All experiments were performed twice.

Figure 3.9 Effects of p53 and Rb inactivation on MRU and Ma-CFC pools in the mammary epithelium.

A, Examples of flow cytometric staining patterns of freshly isolated mouse mammary cells in FVB, *MMTV*-Neu, $p53^{ME-/-}$, $Rb^{ME-/-}$, and $p53^{ME-/-}Rb^{ME-/-}$ mice. MRU, green gates; Ma-CFC, black gates. B, Percentage of MRU (Left) and Ma-CFC (Right) in mouse mammary glands (Mean ± SD). No significant differences were found among all MRU groups (two-tailed $P > 0.05$, $n \geq 3$). As compared to FVB control (n=7) more Ma-CFC were found in mammary glands from $p53^{ME-/-}$ (n=4, $P<0.0001$), $Rb^{ME-/-}$ (n=3, $P=0.0003$) and $p53^{ME-/-}Rb^{ME-/-}$ (n=6, $P<0.0001$). Star, statistically significant differences.

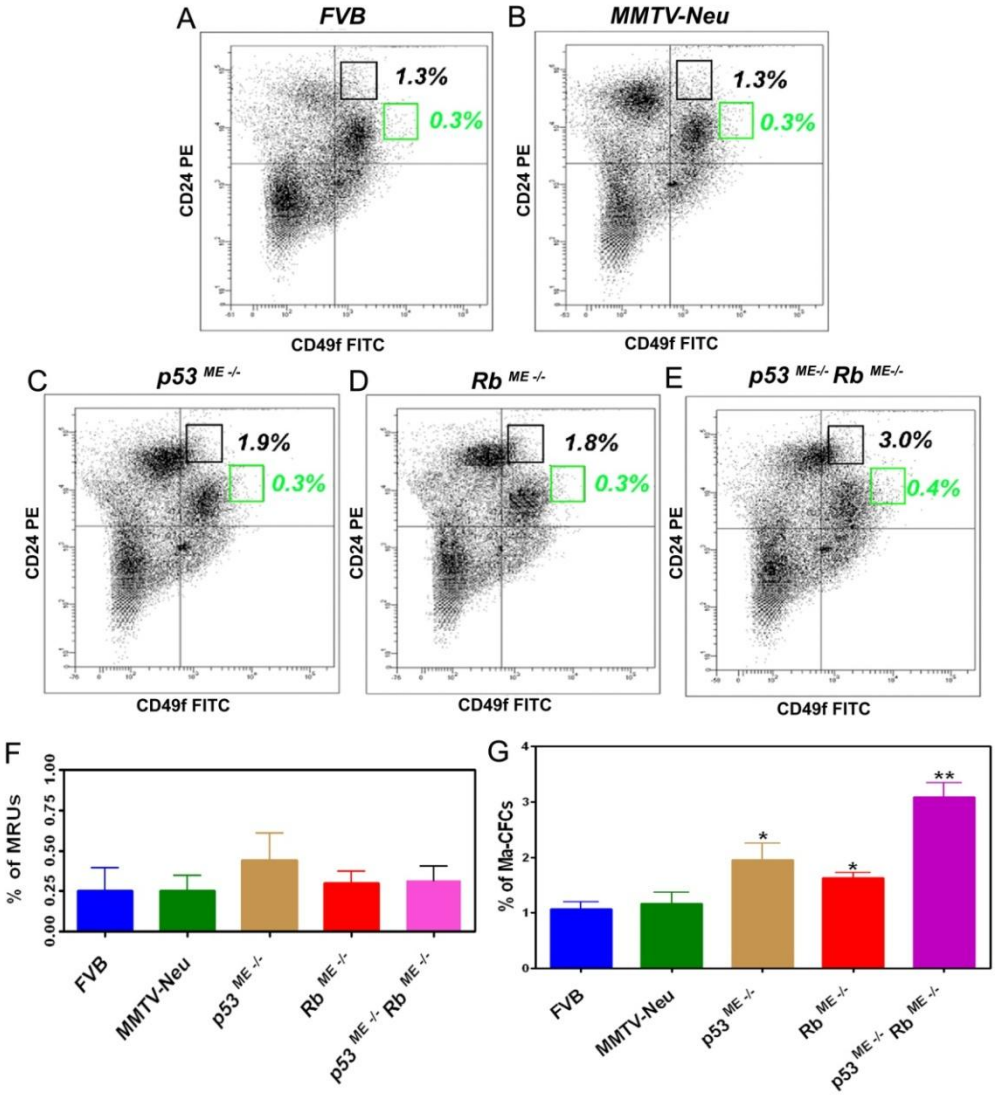
A
FVB
1.3%
0.3%
CD24 PE
CD49f FITC
B
MMTV-Neu
1.3%
0.3%
CD24 PE
CD49f FITC
C
p53 ME -/-
1.9%
0.3%
CD24 PE
CD49f FITC
D
Rb ME -/-
1.8%
0.3%
CD24 PE
CD49f FITC
E
p53 ME-/- Rb ME-/-
3.0%
0.4%
CD24 PE
CD49f FITC
F
% of MRUs
0.00 0.25 0.50 0.75 1.00
FVB
MMTV-Neu
p53 ME -/-
Rb ME -/-
p53 ME -/- Rb ME -/-
G
% of Ma-CFCs
0 1 2 3 4
*
*
**
FVB
MMTV-Neu
p53 ME -/-
Rb ME -/-
p53 ME -/- Rb ME -/-

difference in the number of MRU in all tested groups. In agreement with previous results indicating that *Neu* usually targets more differentiated luminal cells (Li et al., 2003; Liu et al., 2004; Liu et al., 2007), the number of Ma-CFC isolated from *MMTV-Neu* was close to that of Ma-CFC isolated from *FVB* mice. However, inactivation of either *p53* or *Rb* significantly increased the number of Ma-CFC compared to *FVB* and *MMTV-Neu* mice ($p < 0.05$). Loss of both *p53* and *Rb* led to further elevation in number of Ma-CFC. Thus, *p53* and *Rb* are likely to cooperate in controlling the size of Ma-CFC but not MRU population.

Loss of *p53* and *Rb* preferentially increases Ma-CFC proliferation. To further investigate the mechanisms of by which *p53* and *Rb* increase the number of Ma-CFC, cell proliferation (BrdU incorporation, Fig. 3.9A) and cell apoptosis (Annexin V staining, Fig. 3.9B) assays were preformed on sorted MRU and Ma-CFC cells. Inactivation of *p53* and/or *Rb* did not affect MRU proliferation. However, loss of either *p53* or *Rb* led to 3-fold increased in Ma-CFC proliferation ($P=0.0004$ and $P=0.001$, respectively). Inactivation of both *p53* and *Rb* elevated Ma-CFC proliferation by 5 times ($P=0.0024$). At the same time, loss of p53 or *Rb* alone or together had no effects on apoptosis of MRU and Ma-CFC. Thus, lack of *p53* and *Rb* leads to increase in size of Ma-CFC population mainly by elevating cell proliferation.

3.5 Discussion

During recent years there have been extensive efforts to identify, isolate, and target CSC in human cancers. However, such fundamental questions as specific contributions of stem cell-related molecular mechanisms to pathogenesis of various cancers, the role of normal stem cell compartment

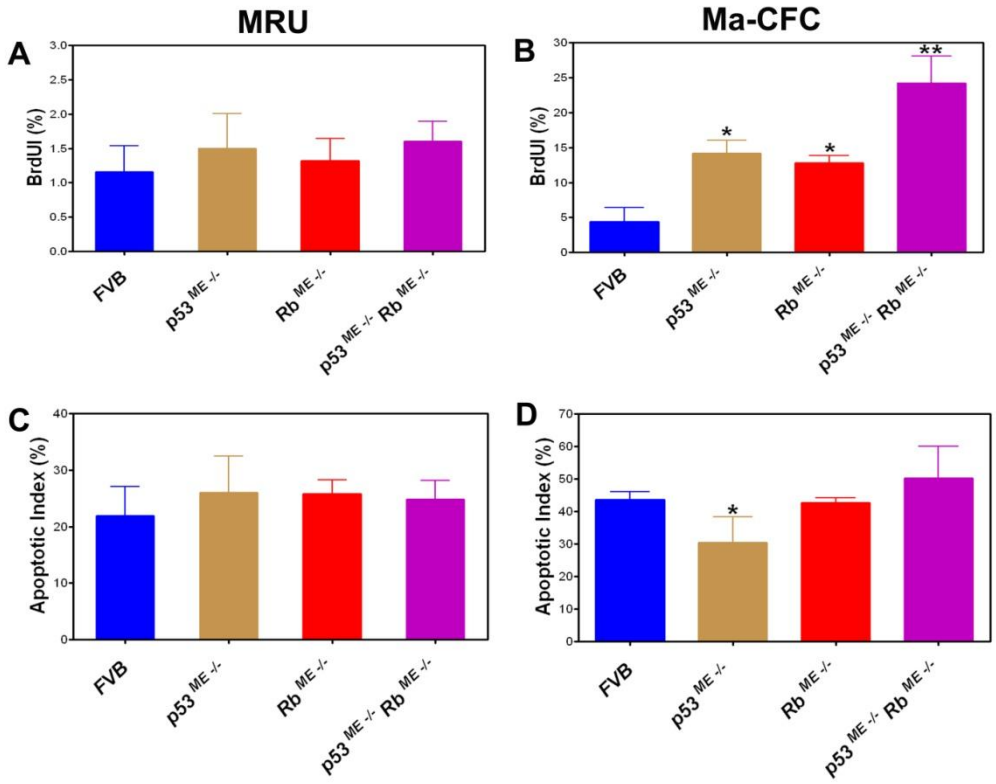

Figure 3.10 Quantitative assessment of proliferation and apoptotic rates of MRU and Ma-CFC.

No significant differences (two-tailed P > 0.05, n≥3) among groups were found in proliferation rates of MRU (A) and apoptotic rates of MRUs (B) and Ma-CFC (D). C, As compared to FVB control (n=4) more proliferating Ma-CFC were found in mammary glands from *p53*$^{ME-/-}$ (n=4, P=0.0004), *Rb*$^{ME-/-}$ (n=4, P=0.001) and *p53*$^{ME-/-}$*Rb*$^{ME-/-}$ (n=4, P=0.0024). Star, statistically significant differences.

in cancer initiation and effects of immune system and microenvironment on stem cells during carcinogenesis have only just begun to be addressed.

Our autochthonous sporadic mouse models of breast cancer have similar hisopathological features to the human breast cancer (Luminal type B, ER positive and raloxifene responsive), and are expected to recapitulate the genetics and molecular characteristics as well as therapeutic responses of human breast cancer (Chapter 2). Using CD24 and CD49f ($Lin^-CD24^+CD49f^+$), we identified and functionally tested CSC by both Matrigel cell culture assay and cleared mammary fat pad transplantation *in vivo* assay. Furthermore, we have found that CSC show more stable genome and exhibit γ-irradiation-induced DNA damage as compared to CnSC. Our observations are consistent with many other studies demonstrating that traditional therapies do not efficiently target CSC, and cancer commonly relapses after first round of treatment. For example, it was observed that glioma stem cells (CD133+) were enriched after irradiation (Bao et al., 2006). The CD133+ cells had higher DNA damage checkpoint activation and more efficient DNA repair relative to the CD133− cells. In addition, the radioresistance of CD133+ cells can be restored by inhibiting the cell cycle checkpoint, using a Chk1/Chk2 inhibitor. Another group reported that CD133+ glioma cells are more resistant than CD133− cells to several chemotherapeutic agents (Liu et al., 2006). They showed that this resistance could be attributed to increases in anti-apoptotic factors, including FLIP, BCL-2 and BCL-XL. Consistently, we have found that CSC overexpress protooncogene cIAP1, the key regulator of apoptosis, cytokinesis, and signal transduction and are commonly amplified in many cancers (reviewed in LaCasse et al., 2008). CSC also have Mad2 down-

regulation, which mediate DNA double strand break accumulation and contribute to mitotic defects and genomic instability (Pickering and Kowalik, 2006). Furthermore, some other studies have shown that CSC possess low levels of reactive oxygen species (ROS), which normally catalyze apoptosis following radiotherapy (Diehn et al., 2009; Rich & Bao, 2007). Targeting the DNA damage checkpoint response and ROS pathways in CSC may overcome radioresistance and provide a therapeutic model for cancer.

The maintenance of stem cell prosperities is critically affected by the microenvironment called the niche. The niche is composed of surrounding cells in a special location that functions to maintain the stem cells. The cells of the niche generate extrinsic factors that control stem cell number, proliferation and differentiation (Sneddon and Werb, 2007). In recent years, niches have been identified for mammalian stem cells in the intestinal, neural, epidermal, and hematopoietic systems (Sneddon and Werb, 2007). It was reported that niches may be involved in CSC regulation, tumor invasion and metastasis, oxidative stress response (Iwasaki and Suda, 2009). Work in the hematopoietic system demonstrated that specialized microenvironments of bone marrow endothelial cells appear to be required for the homing and engraftment of both normal hematopoietic stem cells and leukemic cells (Sipkins et al., 2005). Recently, in solid tumors, perivascular niche was reported in which endothelial cells in brain tumors contribute to the CSC long term growth and self-renewal by secreting factors, such as nitric oxide (Calabrese et al., 2007; Charles et al.). Nitric oxide secreted from endothelial cells promotes a stem cell-like character in cells present in the perivascular niche (Charles et al.). In addition, by an ectopic transplantation assay, it has been demonstrated that microenvironment may play an essential role in

controlling cancer formation in the prostatic stem cell compartment (Zhou et al., 2007). We localized mammary CSC by using two markers, Aldh1 and cIAP1. Localization of CSC in tumor provides a tool to further study the CSC niche, and effects of microenvironment on self-renewal and differentiation of CSC.

CSC and normal stem cells share several other important properties, including their active expression of telomerase, the activation of antiapoptotic pathways, and an increased ability to migrate and metastasize. In addition, CSC resemble the normal stem cells of corresponding tissue of origin. For example, mammary CSC express CD24 and CD29/CD49f that mark normal mammary stem cells (Zhang et al., 2008a). Interestingly, our results indicate that expansion of mammary precursor cells (Ma-CFC) but not stem cells (MRU) precedes development of overt neoplasms associated with p53 and Rb deficiency. Such an expansion may represent an essential step for accumulation of secondary mutations necessary for further progression and selection of neoplastic traits. Importantly, cooperation p53 and Rb in control of Ma-CFC population may represent an additional tumor suppressive mechanism which may explain frequent coincidence of alterations in these genes or their respective pathways.

Expression of Ma-CFC markers is associated with colony-forming cells of the luminal lineage (reviewed in Stingl and Caldas, 2007). Notably, our mouse models of mammary carcinoma have hisopathological features that are similar to those of the human luminal type B breast cancer. Thus, they may be particularly well suited for future studies to determine how p53 and Rb may specifically control luminal-restricted progenitors.

In summary, we demonstrated that in addition to previously established

similarities with human disease, our mouse model of mammary carcinoma contains CSC which are likely to arise from the expanded pool of luminal progenitors. We also developed tools for detection of CSC in tissues and demonstrated that CSC have higher genomic stability as compared to CnSC. Thus our mouse model is well suited for development of therapeutics that directly target CSC.

REFERENCES

Al-Hajj, M., Wicha, M. S., Benito-Hernandez, A., Morrison, S. J., and Clarke, M. F. (2003). Prospective identification of tumorigenic breast cancer cells. Proc Natl Acad Sci USA 100, 3983-3988.

Alvero, A. B., Chen, R., Fu, H. H., Montagna, M., Schwartz, P. E., Rutherford, T., Silasi, D. A., Steffensen, K. D., Waldstrom, M., Visintin, I., and Mor, G. (2009). Molecular phenotyping of human ovarian cancer stem cells unravels the mechanisms for repair and chemoresistance. Cell Cycle 8, 158-166.

Armstrong, L., Stojkovic, M., Dimmick, I., Ahmad, S., Stojkovic, P., Hole, N., and Lako, M. (2004). Phenotypic characterization of murine primitive hematopoietic progenitor cells isolated on basis of aldehyde dehydrogenase activity. Stem Cells 22, 1142-1151.

Bao, S., Wu, Q., McLendon, R. E., Hao, Y., Shi, Q., Hjelmeland, A. B., Dewhirst, M. W., Bigner, D. D., and Rich, J. N. (2006). Glioma stem cells promote radioresistance by preferential activation of the DNA damage response. Nature 444, 756-760.

Bonnet, D., and Dick, J. E. (1997). Human acute myeloid leukemia is organized as a hierarchy that originates from a primitive hematopoietic cell. Nat Med 3, 730-737.

Buerger, H., Otterbach, F., Simon, R., Poremba, C., Diallo, R., Decker, T., Riethdorf, L., Brinkschmidt, C., Dockhorn-Dworniczak, B., and Boecker, W. (1999a). Comparative genomic hybridization of ductal carcinoma in situ of the breast-evidence of multiple genetic pathways. J Pathol 187, 396-402.

Buerger, H., Otterbach, F., Simon, R., Schafer, K. L., Poremba, C., Diallo, R.,

Brinkschmidt, C., Dockhorn-Dworniczak, B., and Boecker, W. (1999b). Different genetic pathways in the evolution of invasive breast cancer are associated with distinct morphological subtypes. J Pathol 189, 521-526.

Calabrese, C., Poppleton, H., Kocak, M., Hogg, T. L., Fuller, C., Hamner, B., Oh, E. Y., Gaber, M. W., Finklestein, D., Allen, M., et al. (2007). A perivascular niche for brain tumor stem cells. Cancer Cell 11, 69-82.

Charles, N., Ozawa, T., Squatrito, M., Bleau, A. M., Brennan, C. W., Hambardzumyan, D., and Holland, E. C. Perivascular nitric oxide activates notch signaling and promotes stem-like character in PDGF-induced glioma cells. Cell Stem Cell 6, 141-152.

Cho, R. W., Wang, X., Diehn, M., Shedden, K., Chen, G. Y., Sherlock, G., Gurney, A., Lewicki, J., and Clarke, M. F. (2008). Isolation and molecular characterization of cancer stem cells in MMTV-Wnt-1 murine breast tumors. Stem Cells 26, 364-371.

Chute, J. P., Muramoto, G. G., Whitesides, J., Colvin, M., Safi, R., Chao, N. J., and McDonnell, D. P. (2006). Inhibition of aldehyde dehydrogenase and retinoid signaling induces the expansion of human hematopoietic stem cells. Proc Natl Acad Sci U S A 103, 11707-11712.

Clarke, M. F., and Fuller, M. (2006). Stem cells and cancer: two faces of eve. Cell 124, 1111-1115.

Collins, A. T., Berry, P. A., Hyde, C., Stower, M. J., and Maitland, N. J. (2005). Prospective identification of tumorigenic prostate cancer stem cells. Cancer Res 65, 10946-10951.

Deveraux, Q. L., and Reed, J. C. (1999). IAP family proteins--suppressors of apoptosis. Genes Dev 13, 239-252.

Flesken-Nikitin, A., Choi, K. C., Eng, J. P., Shmidt, E. N., and Nikitin, A. Y.

(2003). Induction of carcinogenesis by concurrent inactivation of p53 and Rb1 in the mouse ovarian surface epithelium. Cancer Res 63, 3459-3463.

Galderisi, U., Cipollaro, M., and Giordano, A. (2006). The retinoblastoma gene is involved in multiple aspects of stem cell biology. Oncogene 25, 5250-5256.

Ginestier, C., Hur, M. H., Charafe-Jauffret, E., Monville, F., Dutcher, J., Brown, M., Jacquemier, J., Viens, P., Kleer, C. G., Liu, S., et al. (2007). ALDH1 is a marker of normal and malignant human mammary stem cells and a predictor of poor clinical outcome. Cell Stem Cell 1, 555-567.

Guy, C. T., Webster, M. A., Schaller, M., Parsons, T. J., Cardiff, R. D., and Muller, W. J. (1992). Expression of the neu protooncogene in the mammary epithelium of transgenic mice induces metastatic disease. Proc Natl Acad Sci U S A 89, 10578-10582.

Heppner, G. H., and Miller, B. E. (1983). Tumor heterogeneity: biological implications and therapeutic consequences. Cancer Metastasis Rev 2, 5-23.

Hernando, E., Nahle, Z., Juan, G., Diaz-Rodriguez, E., Alaminos, M., Hemann, M., Michel, L., Mittal, V., Gerald, W., Benezra, R., et al. (2004). Rb inactivation promotes genomic instability by uncoupling cell cycle progression from mitotic control. Nature 430, 797-802.

Hess, D. A., Meyerrose, T. E., Wirthlin, L., Craft, T. P., Herrbrich, P. E., Creer, M. H., and Nolta, J. A. (2004). Functional characterization of highly purified human hematopoietic repopulating cells isolated according to aldehyde dehydrogenase activity. Blood 104, 1648-1655.

Hess, D. A., Wirthlin, L., Craft, T. P., Herrbrich, P. E., Hohm, S. A., Lahey, R., Eades, W. C., Creer, M. H., and Nolta, J. A. (2006). Selection based on CD133 and high aldehyde dehydrogenase activity isolates long-term reconstituting human hematopoietic stem cells. Blood 107, 2162-2169.

Iwasaki, H., and Suda, T. (2009). Cancer stem cells and their niche. Cancer Sci 100, 1166-1172.

LaCasse, E. C., Mahoney, D. J., Cheung, H. H., Plenchette, S., Baird, S., and Korneluk, R. G. (2008). IAP-targeted therapies for cancer. Oncogene 27, 6252-6275.

Lapidot, T., Sirard, C., Vormoor, J., Murdoch, B., Hoang, T., Caceres-Cortes, J., Minden, M., Paterson, B., Caligiuri, M. A., and Dick, J. E. (1994). A cell initiating human acute myeloid leukaemia after transplantation into SCID mice. Nature 367, 645-648.

Li, Y., Welm, B., Podsypanina, K., Huang, S., Chamorro, M., Zhang, X., Rowlands, T., Egeblad, M., Cowin, P., Werb, Z., et al. (2003). Evidence that transgenes encoding components of the Wnt signaling pathway preferentially induce mammary cancers from progenitor cells. Proc Natl Acad Sci U S A 100, 15853-15858.

Liu, B. Y., McDermott, S. P., Khwaja, S. S., and Alexander, C. M. (2004). The transforming activity of Wnt effectors correlates with their ability to induce the accumulation of mammary progenitor cells. Proc Natl Acad Sci U S A 101, 4158-4163.

Liu, G., Yuan, X., Zeng, Z., Tunici, P., Ng, H., Abdulkadir, I. R., Lu, L., Irvin, D., Black, K. L., and Yu, J. S. (2006). Analysis of gene expression and chemoresistance of CD133+ cancer stem cells in glioblastoma. Mol Cancer 5, 67.

Liu, X., Holstege, H., van der Gulden, H., Treur-Mulder, M., Zevenhoven, J., Velds, A., Kerkhoven, R. M., van Vliet, M. H., Wessels, L. F., Peterse, J. L., et al. (2007). Somatic loss of BRCA1 and p53 in mice induces mammary tumors with features of human BRCA1-mutated basal-like breast cancer. Proc Natl

Acad Sci U S A 104, 12111-12116.

Novak, A., Guo, C., Yang, W., Nagy, A., and Lobe, C. G. (2000). Z/EG, a double reporter mouse line that expresses enhanced green fluorescent protein upon Cre-mediated excision. Genesis 28, 147-155.

O'Brien, C. A., Pollett, A., Gallinger, S., and Dick, J. E. (2007). A human colon cancer cell capable of initiating tumour growth in immunodeficient mice. Nature 445, 106-110.

Pickering, M. T., and Kowalik, T. F. (2006). Rb inactivation leads to E2F1-mediated DNA double-strand break accumulation. Oncogene 25, 746-755.

Ricci-Vitiani, L., Lombardi, D. G., Pilozzi, E., Biffoni, M., Todaro, M., Peschle, C., and De Maria, R. (2007). Identification and expansion of human colon-cancer-initiating cells. Nature 445, 111-115.

Rich, J. N., and Bao, S. (2007). Chemotherapy and Cancer Stem Cells. Cell Stem Cell 1, 353-355.

Sipkins, D. A., Wei, X., Wu, J. W., Runnels, J. M., Cote, D., Means, T. K., Luster, A. D., Scadden, D. T., and Lin, C. P. (2005). In vivo imaging of specialized bone marrow endothelial microdomains for tumour engraftment. Nature 435, 969-973.

Sneddon, J. B., and Werb, Z. (2007). Location, location, location: the cancer stem cell niche. Cell Stem Cell 1, 607-611.

Stingl, J., and Caldas, C. (2007). Molecular heterogeneity of breast carcinomas and the cancer stem cell hypothesis. Nat Rev Cancer 7, 791-799.

Szotek, P. P., Pieretti-Vanmarcke, R., Masiakos, P. T., Dinulescu, D. M., Connolly, D., Foster, R., Dombkowski, D., Preffer, F., Maclaughlin, D. T., and Donahoe, P. K. (2006). Ovarian cancer side population defines cells with stem cell-like characteristics and Mullerian Inhibiting Substance responsiveness.

Proc Natl Acad Sci U S A 103, 11154-11159.

Vaillant, F., Asselin-Labat, M. L., Shackleton, M., Forrest, N. C., Lindeman, G. J., and Visvader, J. E. (2008). The mammary progenitor marker CD61/beta3 integrin identifies cancer stem cells in mouse models of mammary tumorigenesis. Cancer Res 68, 7711-7717.

Valk-Lingbeek, M. E., Bruggeman, S. W., and van Lohuizen, M. (2004). Stem cells and cancer; the polycomb connection. Cell 118, 409-418.

Zhang, M., Behbod, F., Atkinson, R. L., Landis, M. D., Kittrell, F., Edwards, D., Medina, D., Tsimelzon, A., Hilsenbeck, S., Green, J. E., et al. (2008a). Identification of tumor-initiating cells in a p53-null mouse model of breast cancer. Cancer Res 68, 4674-4682.

Zhang, S., Balch, C., Chan, M. W., Lai, H. C., Matei, D., Schilder, J. M., Yan, P. S., Huang, T. H., and Nephew, K. P. (2008b). Identification and characterization of ovarian cancer-initiating cells from primary human tumors. Cancer Res 68, 4311-4320.

Zhou, Z., Flesken-Nikitin, A., Corney, D. C., Wang, W., Goodrich, D. W., Roy-Burman, P., and Nikitin, A. Y. (2006). Synergy of p53 and Rb Deficiency in a Conditional Mouse Model for Metastatic Prostate Cancer. Cancer Res 66, 7889-7898.

Zhou, Z., Flesken-Nikitin, A., and Nikitin, A. Y. (2007). Prostate cancer associated with p53 and Rb deficiency arises from the stem/progenitor cell-enriched proximal region of prostatic ducts. Cancer Res 67, 5683-5690.

CHAPTER 4

THE ROLE OF MIR-376B/MIR-467B-CIAP1/2 PATHWAY IN MAMMARY CANCER STEM CELLS

4.1 Abstract

Cancer stem cells (CSC) are a subpopulation of tumor cells that are derived from transformed stem cells, progenitor cells, or more differentiated proliferating cells. These cells possess both the ability to self-renew to repopulate tumors and to differentiate to form heterogeneous populations of cells. MicroRNAs are a class of small RNAs whose ability to regulate gene expression makes them crucial in many cellular processes, which led us to ask whether miRNAs may be involved in the regulation of CSC. CSC were isolated from a mouse model of mammary carcinoma associated with *p53* and/or *Rb* deficiency by using the CD24 and CD49f cell surface markers. Microarray analysis identified that miR-376b and miR-467b, downregulated in both CSC and Mammary Stem Cells (MaSC) as compared to Cancer non Stem Cells (CnSC) and normal differentiated mammary epithelial cells. Using bioinformatics and luciferase reporter assay, we identified proto-oncogenes *Cellular Inhibitors of Apoptosis (cIAP) 1 and 2* as targets of both miRNAs. It was determined that cIAP1/2 are overexpressed in CSC as compared to CnSC, and miR-376b and miR-467b reconstitution leads to decreased levels of cIAP1/2 according to quantitative real time PCR and western blotting. Accordingly, miR-376b and miR-467b reconstitution, as well as cIAP1/2 siRNA-mediated knockdown decrease mammosphere formation. These studies indicate that miR-376b/ miR-467b - cIAP1/2 pathway is important for

CSC self-renewal and may represent a new target for development of new therapeutic approaches.

4.2 Introduction

Cancer stem cells (CSC) are a subpopulation of tumor cells that are derived from transformed stem cells, progenitor cells, or more differentiated proliferating cells. The CSC hypothesis postulates that tumors are maintained by a population of neoplastic cells with stem cell properties such as the ability to self-renew and to produce a progenitor cell that can proliferate and differentiate in one asymmetric cell division (Wicha et al., 2006). Human CSC have been identified in a variety of cancer types, including breast cancer. There are still questions about the molecular mechanisms of CSC formation and self-renewal as well as CSC interaction with their microenvironment. Mouse models that remove the potential cross-species barriers to xenotransplantation represent an important tool for studying these questions. In the context of mammary tumors, the CSC subpopulation has been described in several mouse models of mammary carcinogenesis using different cell surface markers (Cho et al., 2008; Vaillant et al., 2008; Zhang et al., 2008).

MicroRNAs (miRNA) are small (around 22 nucleotides) linear fragments of RNA that serve as post-transcriptional regulators of gene expression. Initially thought to represent a rare class of regulatory molecules, the number of metazoan miRNA is now predicted to be upwards of 500 unique molecules (Bartel, 2009). Many miRNAs have been implicated in various human cancers. Tumor cells seem to undergo a general change of global miRNA expression, which promotes transformation. miR-15a and miR-16-1 loss has been found in

chronic lymphocytic leukemia, prostate cancer and myeloma, resulting in induce apoptosis and inhibit carcinogenesis (Cimmino et al., 2005). The loss of the miR-34 family which induces apoptosis has been found in pancreatic, colon, breast and liver cancers. Additionally, the loss of let-7, miR-29, miR-145, miR-221, miR-222, miR-21, miR-372 and miR-373 are common in human cancers, and inhibit carcinogenesis (reviewed in (Croce, 2009)). Furthermore, overexpression of miRNAs has been observed in various human cancers. The first miRNAs that were found to be overexpressed in cancers were miR-155 and miR-17-92 cluster in B cell lymphomas. Importantly, some miRNAs have both oncogenes and tumor suppressor gene function, depending on tissue or cell type. For example, miR-221 and miR-222 target an oncogene, *KIT*, and inhibit the growth of erythroblastic leukaemia, and function as tumor suppressors in erythroblastic cells. However they also target at least four tumor suppressors- PTEN, p27, p57 and TIMP3, and function as oncogenes (Croce, 2009).

MicroRNAs have been shown to influence stem cell self-renewal. Firstly, dicer, an endoribonuclease, cleaves pre-microRNA into short double strand RNA. Mouse dicer mutants were embryonic lethal and exhibited embryonic stem (ES) cell division and proliferation defects. Furthermore, many miRNA have been identified as “ES specific” indicating that these miRNA may play a unique role in maintaining the pluripotency of stem cells (Zhang et al., 2006). miRNAs have also been implicated in the maintenance of mammary epithelial progenitor cells. 50 miRNAs were shown to be differentially expressed between progenitors and differentiated cells. In particular, *miR-let7c* causes a decrease in the self-renewing compartment of mammary epithelial cells. Furthermore, the self-renewing compartment generated much fewer

mammospheres after treatment with precursor *miR-let-7c* molecules (Ibarra et al., 2007). *miR-10b* has been implicated as a causal contributor to breast cancer invasion and metastasis. Regulated by the transcription factor TWIST, high *miR-10b* expression correlates to greater metastasis via the upregulation of the pro-metastatic gene *RHOC (Ma et al., 2007).* In addition, a set of miRNAs have been recently identified that are not expressed in either mammary epithelial stem cells or in enriched breast cancer stem cells (Shimono et al., 2009). The same group also found that overexpression of miR-200c either in normal stem cells or in cancer stem cells, reduced their clonogenic and tumor initiating activities.

To identify and understand the function of specific microRNAs that may be important for CSC functions we used a mouse model of mammary carcinoma associated with p53 deficiency. In this model, mammary neoplasms are similar to human Luminal B type, ER positive, and raloxifene responsive breast cancer (Chapter 2). Previously, CSC ($CD24^{+}CD49f^{+}$) have been identified and characterized in these tumors (Chapter 3). Given the above mouse model, we first isolated CSC and CnSC via FACS followed by characterization of the miRNA expression profile via microarray analysis. miR-376b and miR-467b were among the most down-regulated miRNAs, and were selected to further study. After verifying the expression of these miRNAs using real time PCR, we determined that miR-376b and miR-467b may regulate cIAP1 and cIAP2 by bioinformatics approach. This possibility has been further confirmed by measurement of mRNA and protein levels of target genes after reconstitution of miRNAs and use of luciferase vectors that carry the putative miRNA binding site within the 3' UTR of target genes. Finally, we performed proliferation, apoptosis and self-renewal to determine the role of miR-376b and

miR467b, and their target genes cIAP1 and cIAP2 in CSC.

4.3 Materials and methods

Isolation of primary mammary epithelial cells and tumor cells. The procedure was described in *Materials and Methods* of Chapter 2 and 3.

Cell culture. The procedure was described in *Materials and Methods* of Chapter 2.

Cell labeling and Fluorescence Activated Cell Sorting (FACS) analysis. The procedure was described in *Materials and Methods* of Chapter 3.

Mammosphere assay. Dissociated mammary epithelial cells are counted by hemocytometer and suspended in 1:1 Matrigel (BD, Franklin Lakes, NJ, USA) /mammary epithelial growth medium (MEGM, Lonza, Basel, Switzerland) in a total volume of 100 µl. Samples are plated around the rims of wells in a 12-well plate and allowed to solidify at 37°C for 10 minutes. After that, 1 ml of MEGM is added to each well and replenished every 3 days. Ten days after plating, spheres with a diameter over 40 µm are counted.

RNA isolation and enrichment of small RNA. RNA was isolated from the FACS sorted cells using the mirVana™ miRNA Isolation Kit from Ambion/Applied Biosystems (Foster City, CA, USA). The protocol was followed according to manufacturers' recommendations. The concentration of RNA was measured using a Nanodrop (Nanodrop Technologies, Wilmington, DE). RNA was stored at -80^{o}C until needed. For further study of the microRNA population, Flash PAGE (Ambion) was used to enrich small RNAs (<70 bp). Total RNA was migrated through a miniature electrophoretic acrylamide gel, and the small RNAs, which migrated first out of the gel, were collected. The

concentration of small RNAs was checked using Nanodrop and RNA was prepared for microarray analysis.

Microarray. The small RNAs were labeled using Mirus *LabelIT* miRNA labeling kit (Mirus, Madison, WI, USA). The fluorescent dye used in the labeling reaction was Cy5™. Manufacturer's protocol was followed, ensuring that a minimum of 50 ng of small RNAs were used for each reaction. Labeled RNA was provided to the Microarray Core Facility at Cornell University. CombiMatrix MicroRNA 4X2K microarrays (CombiMatrix, Mukilteo, WI, USA), containing probes against mouse miRNAs (release 8.1 of the Sanger database) were used for hybridization. Array data was analyzed by Cornell Microarray Core Facility.

Real-time PCR. Total cDNA was made using an oligo-dT primed reverse transcription reaction. The Superscript™ III First Strand RT kit (Invitrogen, Carlsbad, CA, USA) was used to make cDNA from the poly-adenylated mRNA population, as described by the protocol. Generating cDNA from very small fragments of RNA required a special RT system, developed by Applied Biosystems. A stem-loop sequence-specific primer hybridized to the 3' end of the miRNA and first strand cDNA was synthesized. TaqMan™ Gene Expression Assays were purchased from ABI for each gene of interest as well as our miRNA of interest. The endogenous controls used for miRNA and mRNA calibration were *RNU6B* and *Gapdh*, respectively (ABI). The manufacturer's protocol was followed precisely. Each sample was replicated four times. Optical 96-well plates (ABI) were used for real-time quantification of PCR using a 7500 Real Time PCR System (ABI). Fold change in gene expression was calculated as per the $2^{-\Delta\Delta Ct}$ method.

miRNA precursors. Precursor molecules (pre-miRNA) for *miR-376b*,

miR-467b, and *miR-scramble* were purchased (Ambion). The miR-scramble represents a precursor miRNA molecule that is processed within the cell, but does not target any identified 3'UTRs. These molecules (20 nM into each well of a 24-well plate) were transfected into cells using Lipofectamine2000™ (Invitrogen) reagent, in order to upregulate the cellular concentration of the miRNA of interest. Following 48 hours of this treatment, the expression levels of target mRNA were checked using qPCR, the levels of cellular proteins were checked using western blotting, proliferation and apoptosis were measured using BrdU incorporation and caspase-3 staining respectively.

Western blot analysis. The procedure was described in *Materials and Methods* of Chapter 2. Primary antibody used include cIAP1 (Abcam, Cambridge, MA, USA, 1:300), Mad2 (Santa Cruz, Santa Cruz, CA, USA, 1:200), and Gapdh (Advanced immunochemical Inc, Long Beach, CA, USA, 1:1000).

Luciferase assays. Luciferase vectors (Ambion) contained multiple cloning sites (MCSs) at the 3' end of the luciferase gene. This enabled us to clone 3' UTRs of our genes of interest into the MCS of the luciferase vector. Upon cloning, the luciferase vector + 3'UTR was transfected into cells using Lipofectamine2000™ along with the precursor miRNA molecules. If the miRNA were able to target a specific 3'UTR, a decrease in luciferase expression due to translational inhibition is observed.

Cloning. The luciferase vector (pMIR-REPORT™ miRNA Expression Reporter Vector System, Ambion) was provided as a glycerol stock solution in *E. coli* (Fig. 4.1). The plasmid was isolated from the bacteria using Midi preps (QIAGEN, Germantown, MD, USA) to yield a large quantity of plasmid. The luciferase vector was double digested with SpeI and MluI (NEB) in NEB Buffer

2 with added BSA for 3 hours at 37^{o}C. Simultaneously, PCR was performed on genomic wild-type DNA (from mouse FVB/N mammary epithelial cells) in order to clone the 3'UTRs of *Birc2, and Birc3*. Primers were designed, using IDTDNA primer design software, with insertions of the SpeI (ACTAGT) and MluI (ACGCGT) restriction sequences (Table 1). The PCR products were then double digested with MluI and SpeI at 37^{o}C for 3 hours. Digested products were run on a 1% agarose gel with EtBr and extracted using a Gel Purification kit (QIAGEN). The gel purified products were used in a ligation reaction overnight at room temperature. Ligated vectors were transformed into TOP10 *E. coli* (Invitrogen, Carlsbad, CA) as per manufacturer's protocol and plated onto LB agar plates with 100 µg/mL of ampicillin overnight at 37^{o}C. Four colonies were picked for each ligation reaction. DNA was also sequenced for each of the four colonies for the three 3'UTRs (12 samples total) using the following primer: 5'– AGGCGATTAAGTTGGGTA–3'. This primer sequenced the 3'UTR of each insert from the 3' to 5' end of the 3' UTR. Plasmid DNA and primer were combined and provided to the DNA Sequencing facility. Sequencing was performed using Big Dye terminator chemistry on an ABI 3730 Automated DNA Analyzer. Sequence results were analyzed with Chromas (Technelysium, Holland Park, Australia) software.

Luciferase screening. 24-well plates were used to culture tumor cells to 50% confluence in complete medium. Transfections were carried out according to the protocol provided for Lipofectamine 2000™ (Invitrogen) transfection using OptiMEM™ medium (Invitrogen). After 48 hours of treatment, the media was aspirated from the 24 well plates and cells were washed with 1xPBS. PBS was aspirated and cells were lysed using the lysis buffer provided in the Luciferase Assay System (Promega, Madison, WI). 10

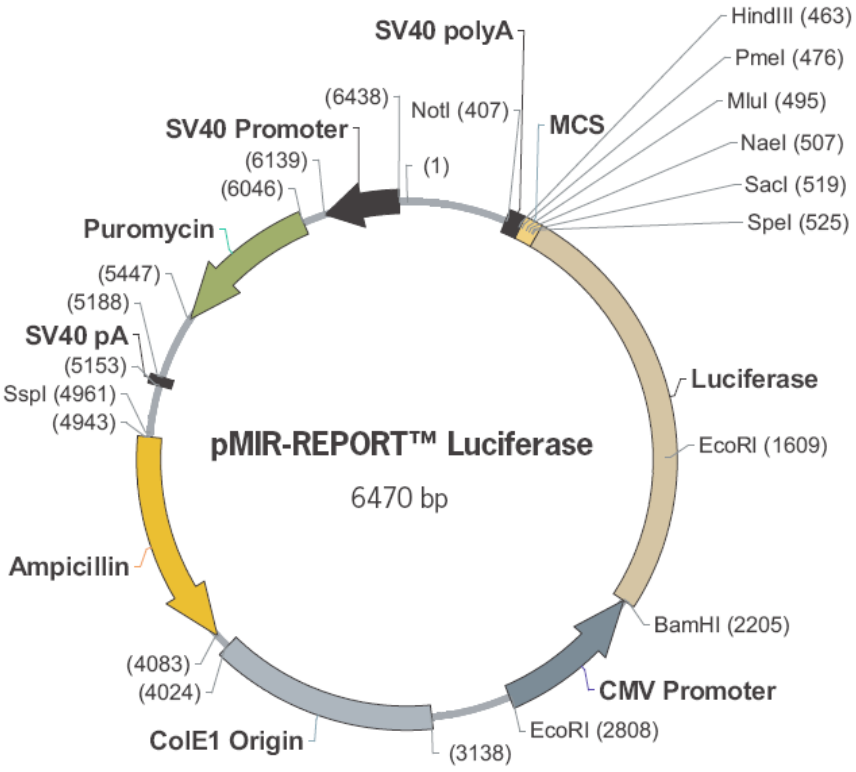

Figure 4.11 Luciferase expression vector driven by CMV promoter.

Total size is 6470 bp without 3' UTR inserts at the 3' end of the *luciferase* gene. Plasmid encodes ampicillin and puromycin resistance.

Table 4.1 PCR Primers for 3' UTR amplification.

Gene	Sequence
Birc2 Forward	5' AAA**ACTAGT**TGGTCTGAAAGTATTGTTGGACA 3'
Birc2 Reverse	5' AAA**ACGCGT**GCATACATCCCTGCACACAC 3'
Birc3 Forward	5' AAA**ACTAGT**TCAGCCAGGAGGAAGTTCAC 3'
Birc3 Reverse	5' AAA**ACGCGT**TCATATCCCTAAAATGTCATCCAA 3'
E2F2 Forward	5' AAA**ACTAGT**GCTCTCTTCCAGCCTTCCTT 3'
E2F2 Reverse	5' AAA**ACGCGT**CTTTGGGACAGTGGGTGTTT 3'

Primers used to amplify the 3' UTR of Birc2, Birc3, and E2F2 respectively. The SpeI sequence is in blue, the MluI sequence is in red.

µL of lysed cells were added to 100 µL of luciferase reagent, causing luciferase to catalyze its substrate into a light emitting compound. The intensity of light emitted was measured using a luminometer (Turner Biosystems, Sunnyvale, CA, USA). Each reaction was conducted in triplicate, yielding three theoretically identical readings for each sample.

Proliferation assay and apoptosis assay. Both procedures were described in *Materials and Methods* of Chapter 2.

Bioinformatics. Bioinformatics analysis was performed using a variety of online software algorithms. Of utmost importance was the Sanger Institute's mirBase website release 12.0. This database contained the pre-miR and mature miRNA sequences along with genome information and citations for known miRNA. miRNA target searches were employed to identify genes that were potentially targeted by our miRNA of interest. These included Miranda, Targetscan, and Targetrank.

Statistical Analyses. All statistical analyses in this study were done using InStat 3.06 and Prism 5.01 software (GraphPad, Inc., San Diego, CA, USA) as described previously (Zhou et al., 2006).

4.4 Results

Microarray analysis. The results of the microarray analysis yielded five most upregulated and downregulated miRNA in the CSC population as compared to the CnSC population (Table 4.2). Two of the most downregulated miRNAs, *miR-376b* and *miR-467b* were chosen for further study (Table 4.3). The results of the microarray were validated using stem-loop reverse transcription and real time PCR (Fig. 4.2A). The results were in line with expectations; *miR-376b* was downregulated about 6 fold in the CSC

population and *miR-467b* was downregulated about 3 fold. Both results were statistically significant. Furthermore, we studied the expression of these two miRNAs in normal mammary stem cell (MRU), progenitor (Ma-CFC) and differentiated epithelia cell (MEC). Both miRNAs are overexpressed in normal cells than that in cancer cells. In addition, both miRNAs are downregulated in normal mammary stem cell and progenitor populations (Fig. 4.2A). The highest expression of both miRNAs was seen in differentiated mammary epithelial cells.

Targets of miR-376b and miR-467b. Bioinformatics analysis of the potential gene targets of *miR-376b* and *miR-467b* yielded several oncogenes and "stemness"-related genes (Table 4.3). Inhibitors of apoptosis *cIAP1* and *cIAP2* (also known as *Birc2* and *Birc3* respectively) were chosen for further study. Reverse bioinformatics confirmed that *miR-376* could target *cIAP1* and that *cIAP2* could be targeted by *miR-467b.* The expression of cIAP1 and cIAP2, the potential targets of these miRNAs, was examined. Corresponding to the low expression of *miR-376b* and *miR-467b,* cIAP1 and cIAP2 were expressed higher in CSC as compared to CnSC (Fig 4.2B). Upon treatment of precursor miRNA molecules, the mRNA levels of each gene following precursor miRNA treatment were measured using real time PCR. cIAP1 mRNA decreased about 50% upon treatment with *pre-miR-376b. pre-miR-467b* had a similar effect on tumor cells decreased upon treatment with *pre-miR-376b.* The effect of *pre-miR-467b* was not as profound (Fig. 4.3B).

To directly prove the regulation of miRNAs to cIAPs, we use luciferase assays. We made luciferase expression vectors with either normal or mutated 3'UTRs of the putative target genes. Transfection of Luc-3'UTR and pre-miR molecules into tumor cells, and subsequent luciferase measurement

Table 4.2 Upregulation and downregulation of miRNAs in the CSC.

	miRNA	Fold Change (CSC over CnSC)	p-value *
Significantly upregulated miRNA	*mmu-miR-19a*	5.47	0.086
	mmu-miR-9a	4.17	0.040
	mmu-miR-183	4.09	0.032
	mmu-miR-30e	3.90	0.24
	mmu-miR-29c	3.86	0.028
Significantly downregulated miRNA	*mmu-miR-698*	-4.073	0.125
	mmu-miR-485	-4.92	0.129
	mmu-miR-207	-4.96	0.100
	mmu-miR-467b	-5.28	0.066
	mmu-miR-376b	-7.37	0.041

Table 4.3 List of genes targeted by *miR-376b* and *miR-467b*.

miRNA	Targets	Function of these target genes
miR-376b	Sox21/6/11/9	Stemness regulatory transcription factor
	Klf4/6	Stemness regulatory transcription factor
	cIAP1 (Birc2)	Inhibitor of Apoptosis 1
	TGFβ Receptor 1	Proliferative transduction pathway
	Rab11a	Oncogene
	Met	Oncogene
miR-467b	Histone Deacetylase 9	Downregulates gene expression
	Wnt3a	Promotes proliferation
	cIAP2	Inhibitor of Apoptosis 2
	E2F2	Proliferative Transcription Factor
	FoxP2	Oncogene
	Sox2	Stemness regulatory transcription factor
	Klf9	Stemness regulatory transcription factor

Figure 4.12 Expression of miR-376b and miR-467b in CSC and mammary stem cells (MaSC).

A. Stem-loop reverse transcription qPCR illustrates that miR-376b and miR-467b are downregulated in the CSC population (P=0.0012 and P=0.0073, respectively), as compared to cancer non stem cells (CnSC). When comparing the expression of miR-376b and miR-467b in normal mammary epithelial cells (MEC), mammary progenitors (Ma-CFC) and mammary stem cells (MRU), expression of miR-376b and miR-467b is lowest in MRU and Ma-CFC populations (P=0.0024 and P=0.0089, respectively). B. Expression of cIAP1 and cIAP2 is much higher in CSC than in CnSC (P=0.0001 and P=0.0012, respectively). * $P<0.05$. R.U., Relative Units. n = 4. Mean ± SD.

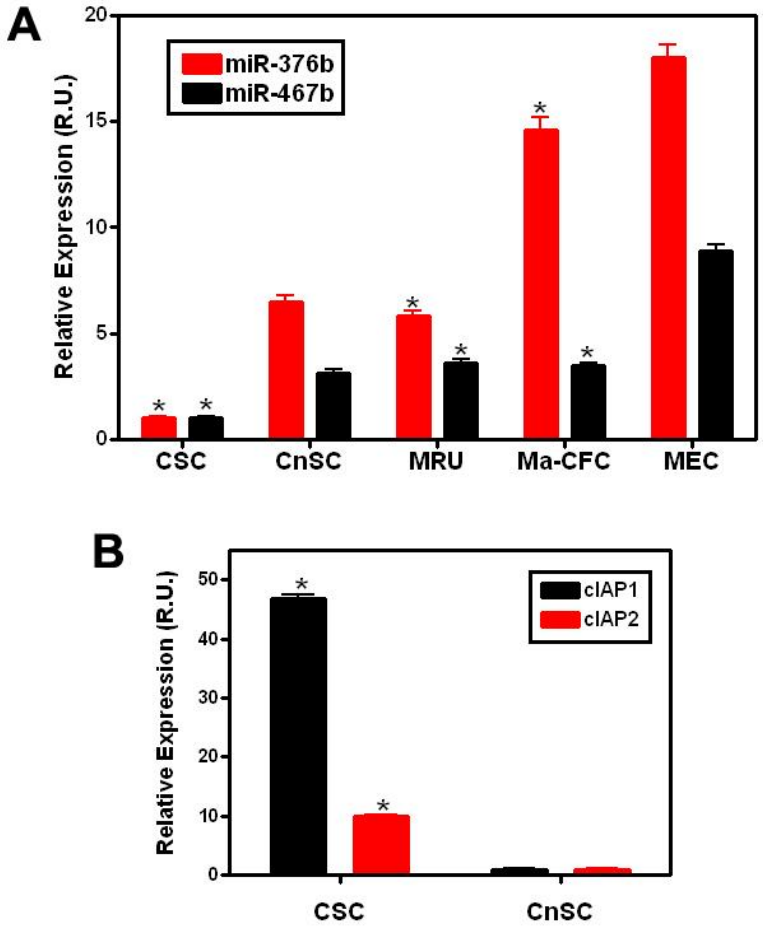
A
Relative Expression (R.U.)
miR-376b
miR-467b
CSC
CnSC
MRU
Ma-CFC
MEC
B
Relative Expression (R.U.)
cIAP1
cIAP2
CSC
CnSC

supported the observation that *miR-376b* and *miR-467b* target the 3'UTRs of *cIAP2*. Interestingly, *miR-376b* treatment also decreased *cIAP2* mRNA by about 20%. In addition, *miR-467b* treatment also affected *cIAP1* mRNA levels, decreasing its expression by the same magnitude as *miR-376b* (Fig. 4.3A). Using western blotting, we observed that the cIAP1 protein was decreased after *miR-376b* treatment (Fig. 4.3B). According to luciferase assays (Fig 4.3C and D), the downregulation was observed with *pre-miR-376b* on both *cIAP1* and *cIAP2.* This 50% to 60% decrease in luciferase expression in *cIAP1* and *cIAP2* upon treatment with *miR-376b* indicates that these genes possess *miR-376b* recognition sites. *pre-miR-467b* only caused a significant decrease in luciferase expression in *cIAP2*. These results indicate that the miRNAs of interest possess overlapping gene targets.

Role of miR-376b/467b and cIAPs pathway in CSC and CnSC. To assess potential role of miR-376b/467b and cIAPs pathway in CSC self-renewal, we used mammosphere formation assay. Mammosphere formation CSC was significantly inhibited by either *pre-miR-376b,* or *pre-miR-467b*, or both miRNAs. Both miRNAs treatments had cooperative effect on reducing mammosphere formation by CSC (Fig 4.4A). Similarly, knocking down either cIAP1, or cIAP2, or both genes, decreased mammosphere formation. (Fig 4.4A).

To further investigate the mechanism of mammosphere formation decreasing by miR-376b/467b and cIAPs pathway, we checked cell proliferation and apoptosis of CSC and CnSC. Proliferation of CSC and CnSC was significantly inhibited by either *pre-miR-376b,* or *pre-miR-467b*, or both, as measured by BrdU incorporation. Both miRNAs treatment have cooperative effect on decreasing cell proliferation (Fig 4.4B). Correspondingly, knock down

Figure 4.13 miR-376b and miR-467b directly target cIAPs.

A. As compared to negative control, miR-376b and miR-467b decrease the mRNA amount of cIAP1 (P=0.004 and P=0.0041, respectively) and cIAP2 (P=0.018 and P=0.0088, respectively) in p53 deficient MCN1 cancer cell line. B. Both miR-376b and miR-467b decrease levels of cIAP1 protein. C.D. Luciferase assay results of MCN1 (p53-/-) cancer cells transfected with vectors (0.4 µg) and pre-miRNA molecule (20 nM). Vector cIAP1 N has predicted miR-376b binding seed sequence in 3'-UTR of cIAP1, and cIAP2 N has predicted miR-467b binding seed sequence in 3'-UTR of cIAP2. Vectors (cIAP1 M and cIAP2 M) have mutated miRNA binding sequences. miR-376b specifically inhibit expression of cIAP1 (P=0.0039), while both miR-376b and miR-467b can inhibit expression of cIAP2 (P=0.0018 and P=0.0056, respectively). R.U., Relative Luciferase Units. * P<0.05. N=3. Mean ± SD.

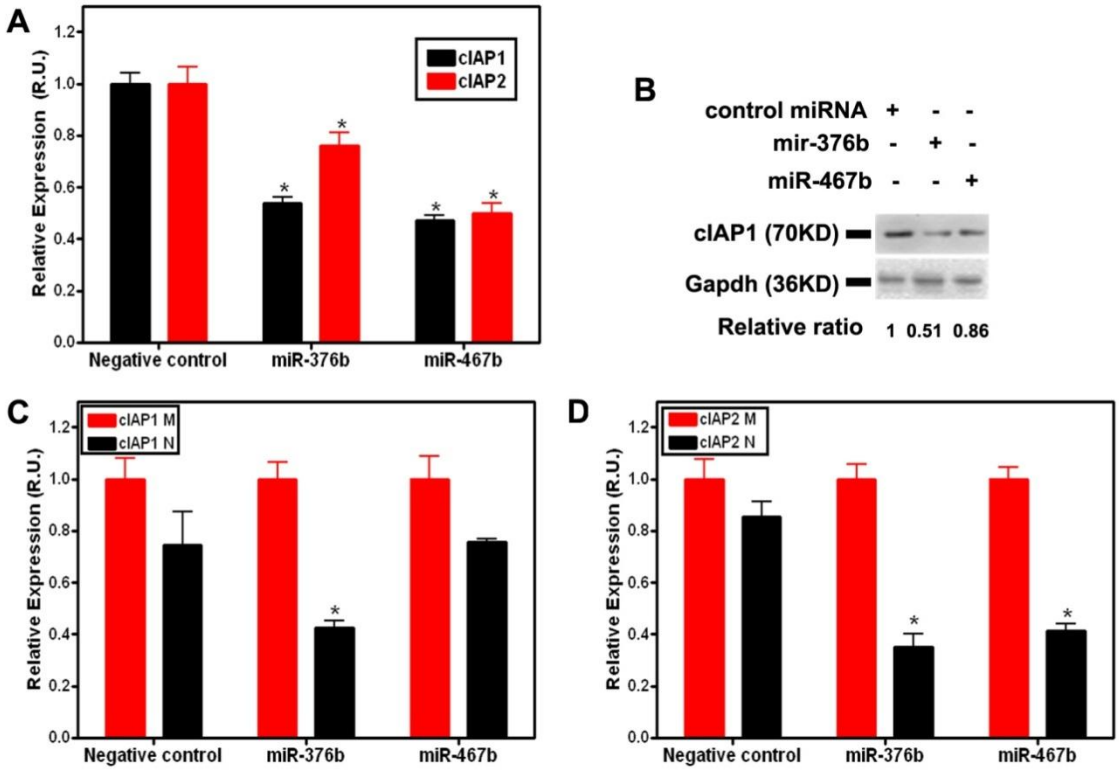
A
Relative Expression (R.U.)
cIAP1
cIAP2
Negative control
miR-376b
miR-467b
B
control miRNA + - -
mir-376b - + -
miR-467b - - +
cIAP1 (70KD)
Gapdh (36KD)
Relative ratio 1 0.51 0.86
C
cIAP1 M
cIAP1 N
D
cIAP2 M
cIAP2 N

of the either cIAP1, or cIAP2, or both genes, decreased proliferation of both CSC and CnSC. Interestingly, miRNAs treatments had more apparent effects on CSC and CnSC proliferation than downregulation of cIAP1 and cIAP2, indicating that other targets of miRNAs contributed to the cell proliferation decreasing (Fig 4.4B).According to staining for the apoptosis marker cleaved caspase-3, after treatment with either *pre-miR-376b,* or *pre-miR-467b,* or both miRNAs, CSC and CnSC apoptosis was lowest in the cells treated with scrambled miRNA (negative control), which is biologically inert. The highest rate of apoptosis in CSC and CnSC was observed in cells treated with both *pre-miR-376b* and *pre-miR-467b* (Fig. 4.4C). Consistently, knock down of either cIAP1, or cIAP2, or both genes, led to increase in CSC and CnSC apoptosis. The highest rate of apoptosis in CSC and CnSC was observed in cells with both cIAP1 and cIAP2 knockdown (Fig. 4.4C). Taken together, these results demonstrate that effects of miR-376b and miR-467b on increasing cell proliferation and decreasing cell apoptosis may go through the cIAP1 and cIAP2 pathway.

4.5 Discussion

miR-376b and *miR-467b* were significantly downregulated in CSC. We have proved that cIAP1 and cIAP2 are among their downstream targets. These two inhibitors of apoptosis (IAP) family members were upregulated in CSCs and show parallel upregulation in the Ma-CFCs. IAP family consists of eight members, which collude to suppress apoptosis by directly inhibiting both initiator and effector caspase activity. The defining characteristic of IAPs is a baculovirus IAP repeat (BIR) domain, which is directly involved in caspase inhibition. We have demonstrated in Chapter 2 that downregulation of *cIAP1*

Figure 4.14 Effects of miR-376b, miR-467b and cIAPs on CSC.

Primary p53 deficient cancer cells were treated with either miR-376b or miR-467b, or cIAPs, and then sorted for CSC and CnSC. A. Culturing the CSC mammosphere demonstrated that both miR-376b and miR-467b treatments decrease the mammosphere formation (P=0.0012 and P=0.048, respectively), while miR-376 has the most significant effect. Both siR-cIAP1 and siR-cIAP2 treatments decrease the mammosphere formation (P=0.024 and P=0.0026, respectively), and knocking down both cIAP1 and cIAP2 has cooperative effect on mammosphere formation (P=0.0004). B. Significant decreases of cell proliferation were observed in CnSC treated with miR-376b (P=0.0225), miR-467b (P=0.0097) and both miRNAs (P=0.0083) and in CSC treated with miR-376b (P=0.0011), miR-467b (P=0.0128) and both miRNAs (P=0.0001). Significant decreases of cell proliferation were observed in CnSC treated with siR-cIAP1 (P=0.042), miR-467b (P=0.038) and both miRNAs (P=0.0283) and in CSC treated with miR-376b (P=0.048), miR-467b (P=0.0428) and both miRNAs (P=0.0189). C. Significant increases of cell apoptosis were observed in CnSC treated with miR-376b (P=0.0024), miR-467b (P=0.0073), and both were observed in CnSC treated with siR-cIAP1 (P=0.018), miR-467b (P=0.013), and both miRNAs (P=0.0023) and in CSC treated with miR-376b (P=0.012), miR-467b (P=0.018) and both miRNAs (P=0.037). *P<0.05. R.U., Relative Units. N= 3. Mean ± SD.

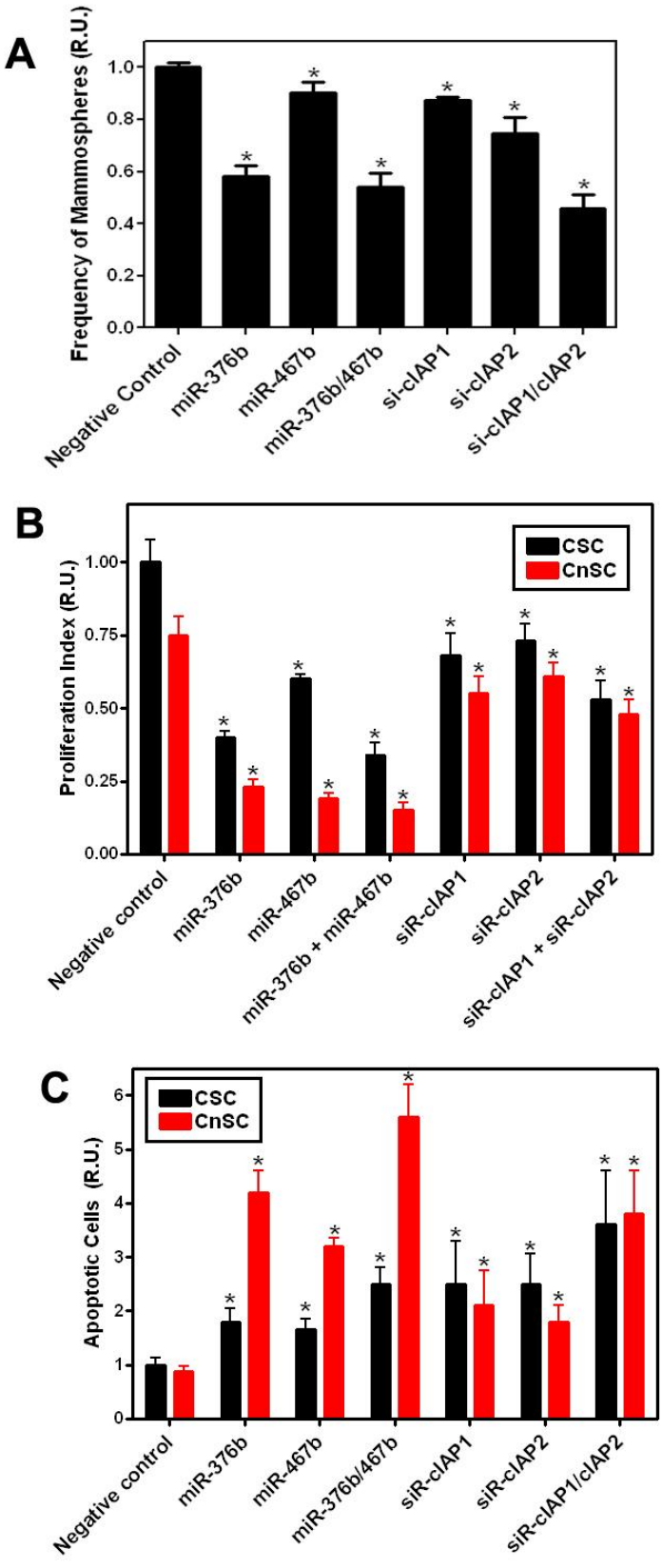
A
Frequency of Mammospheres (R.U.)
1.0
0.8
0.6
0.4
0.2
0.0
Negative Control
miR-376b
miR-467b
miR-376b/467b
si-cIAP1
si-cIAP2
si-cIAP1/cIAP2
B
Proliferation Index (R.U.)
1.00
0.75
0.50
0.25
0.00
CSC
CnSC
Negative control
miR-376b
miR-467b
miR-376b + miR-467b
siR-cIAP1
siR-cIAP2
siR-cIAP1 + siR-cIAP2
C
Apoptotic Cells (R.U.)
6
5
4
3
2
1
0
CSC
CnSC
Negative control
miR-376b
miR-467b
miR-376b/467b
siR-cIAP1
siR-cIAP2
siR-cIAP1/cIAP2

and *cIAP2* is able to decrease cell proliferation and increase apoptosis. Elevated levels of *cIAPs* are fairly common in cancer cells, and in some models, is a requisite step in the initiation of transformation. In brain tumor stem cells, it was observed that elevated levels of *cIAPs* correlated with multidrug and chemotherapeutic resistance (Liu et al., 2006).

miR-376b has a mature sequence of 5'A**UCAUAGA**GGAACAUCCACUU 3' (seed sequence given in bold). *miR-376b* is a member of a large cluster of 40 miRNAs that is found on chromosome 12 in *Mus musculus* and conserved on *Homo sapiens* chromosome 14.q32.31. The human version of *miR-376b* maintains the same seed sequence as in the mouse, but has different nucleotides at the 3' end. Furthermore, this cluster appears to be imprinted to the maternal chromosome, with little or no expression of genes from the paternal chromosome (Lin et al., 2003). It is expected that this cluster is expressed under control of the neighboring *Gtl2* promoter as a poly-cistronic primary transcript. *Gtl2* is known to be actively transcribed in embryos, providing a contextual clue that the miRNA cluster, which includes *miR-376b* and would most likely be co-expressed with *Gtl2*, plays a role in regulating embryonic development (Seitz et al., 2004). Deletion of maternal imprinting results in embryonic lethality, emphasizing the importance of the genes controlled under the maternal *Gtl2* promoter. Parallel to this observation, paternal uniparental disomy 12 are also embryonic lethal since the *Gtl2* promoter is methylated and therefore inhibited (Schuster-Gossler et al., 1998). It was shown that *miR-376b* is expressed in mouse embryos, and is surprisingly over-represented in mouse teratocarcinomas. Furthermore, the seed sequence, as mentioned earlier, is conserved between mice, rats, and humans (Landgraf et al., 2007).

miR-467b has a mature sequence of 5' G**UAAGUGC**CUGCAUGUAUAUG 3' (seed sequence given in bold). *miR-467b* is part of a large cluster of about 50 miRNAs that are within the 10th intron of the gene *Sfmbt2,* which is found on mouse chromosome 2. Therefore, the expression of miRNA within this cluster is linked tightly to the expression of *Sfmbt2* and the activity of its promoter and enhancers(Sun et al., 2009). The chromosome 2 cluster has been linked with promoting self-renewal and pluripotence(Calabrese et al., 2007). The expression of this cluster was found to be highest in ES cells, but decreases upon retinoic acid-induced differentiation. In particular, *Sox2* was proposed as a target of *miR-467b*, implicating *miR-467b* in a feedback loop that tightly regulates ES cell self-renewal(Gu et al., 2008).

Sfmbt2 is a member of the *Polycomb Group* (*PcG*) genes, which, as described earlier, are crucial regulators of *homeobox* gene expression and are often predictive of a CSC phenotype. It was shown that SFMBT2 forms a complex with the transcription factor YY1 to maintain the stem cell population in ES cells. Additionally, it was shown that *Sfmbt2* is paternally imprinted in early embryonic development (Kuzmin et al., 2008), leading us to infer that the associated intronic miRNA cluster is also paternally imprinted. Interestingly, *Yaf2,* also known as *YY1-associated factor 2,* was mentioned as a putative target of unedited *miR-376b (Kawahara et al., 2007)*. This suggests a complex loop of feedback regulation where co-expression of *miR-376b* and *miR-467b* results in decreased SFMBT2 activity due to inhibition of YAF2/YY1. If both miRNA are downregulated, as we observe in our CSCs, we would expect increased SFMBT2 activity, resulting in increased stem cell maintenance. This is one instance of many possible cross-talk pathways between *miR-376b* and

miR-467b.

Additionally, we have shown that both *pre-miR-376b and pre-miR-467b* can induce apoptosis and inhibit proliferation in mammary carcinoma cells. We have demonstrated the important role of cIAP1/2 in mammary carcinogenesis (Chapter 2). Therefore, these observations can be attributed, in part, to the inhibition of *cIAP1/2* translation. Reconstitution of *miR-376b and miR-467b* expression results in lower cellular concentrations of *cIAP1/2* signaling. Therefore, downregulation of the *miR-376* family may be one of the key events during mammary carcinogenesis in our model.

It should be noted that the ability of CSC to form mammosphere is likely to be controlled by *miR-376b/467b-cIAP1/2* pathway*.* Consistently, *miR-376b* and *miR-467b* expression is lowest, and cIAP1 and cIAP2 expression is highest in MRU and Ma-CFC, consistent with the expectation of high frequency of mammosphere formation in MaSC and high proliferation in their progeny. Apoptosis is also suppressed in stem cells, consistent with our hypothesis, which suggests that *cIAP1* and *cIAP2* are upregulated, in part, due to the decrease in their negative regulator *miR-376b* and *miR-467b.*

These observations would allow us to draw parallels between *miR-376b/467b* and *miR-15/16.* These miRNAs target the anti-apoptotic protein Bcl2. Absence of these miRNA leads to a decrease in the rate of apoptosis, resulting in a massive expansion of the B cell population. We observe that in our model of mammary cancer, associated with *p53* and/or *Rb* deficiency, there is a decrease in *miR-376b* and *miR-467b* expression in CSCs. Consequently, increased levels of *cIAP1* and *cIAP2* result in decreased apoptosis, which has been correlated to irradiation resistance, consistent with previously established theories of CSCs.

Taken together, the above studies indicate that the CSC phenotype may be, in part, due to lower expression of *miR-376b* and *miR-467b* and high expression of cIAP1 and cIAP2. The connections between the primary mutations, loss of *p53* and *Rb*, and the downstream observation that *miR-376b* and *miR-467b* are specifically downregulated in the CSCs, remain to be elucidated. It is unclear if loss of *p53* and *Rb* directly influences the expression of *miR-376b* and *miR-467b*. Rather, *p53* and *Rb* loss may occur in cells that already maintain low expression of these two miRNA (as shown by real time PCR of wild type MRU and Ma-CFC) in order to preserve stemness. In this case, the tumorigenic effect of *p53* and *Rb* loss, in conjunction with the previously existent stem cell gene expression profile, results in the formation of CSC. If this hypothesis is true, then it would not be unexpected to find downregulation of *miR-376b* and *miR-467b* in other putative stem cell and CSC models.

As described earlier, it is imperative to focus on treating not only rapidly dividing cells, but also the relatively quiescent CSC that are capable of metastasizing and seeding new tumors. If *miR-376b* and *miR-467b* directly inhibit stemness, proliferative, and anti-apoptotic genes, reconstitution of their expression can be a vital biological approach to treating CSC. Furthermore, chemical inhibitors of *IAP* family proteins have been a recent area of focus. These drugs hold great promise in promoting apoptosis in conjunction with ionizing radiation treatment or chemotherapy (LaCasse et al., 2008). Thus, our studies provide an essential basis for development of CSC-specific therapeutic approaches targeting 376b/ miR-467b - cIAP1/2 pathway.

REFERENCES

Bartel, D. P. (2009). MicroRNAs: target recognition and regulatory functions. Cell *136*, 215-233.

Calabrese, J. M., Seila, A. C., Yeo, G. W., and Sharp, P. A. (2007). RNA sequence analysis defines Dicer's role in mouse embryonic stem cells. Proc Natl Acad Sci U S A *104*, 18097-18102.

Cho, R. W., Wang, X., Diehn, M., Shedden, K., Chen, G. Y., Sherlock, G., Gurney, A., Lewicki, J., and Clarke, M. F. (2008). Isolation and molecular characterization of cancer stem cells in MMTV-Wnt-1 murine breast tumors. Stem Cells *26*, 364-371.

Cimmino, A., Calin, G. A., Fabbri, M., Iorio, M. V., Ferracin, M., Shimizu, M., Wojcik, S. E., Aqeilan, R. I., Zupo, S., Dono, M.*, et al.* (2005). miR-15 and miR-16 induce apoptosis by targeting BCL2. Proc Natl Acad Sci U S A *102*, 13944-13949.

Croce, C. M. (2009). Causes and consequences of microRNA dysregulation in cancer. Nat Rev Genet *10*, 704-714.

Gu, P., Reid, J. G., Gao, X., Shaw, C. A., Creighton, C., Tran, P. L., Zhou, X., Drabek, R. B., Steffen, D. L., Hoang, D. M.*, et al.* (2008). Novel microRNA candidates and miRNA-mRNA pairs in embryonic stem (ES) cells. PLoS One *3*, e2548.

Ibarra, I., Erlich, Y., Muthuswamy, S. K., Sachidanandam, R., and Hannon, G. J. (2007). A role for microRNAs in maintenance of mouse mammary epithelial progenitor cells. Genes Dev *21*, 3238-3243.

Kawahara, Y., Zinshteyn, B., Sethupathy, P., Iizasa, H., Hatzigeorgiou, A. G., and Nishikura, K. (2007). Redirection of silencing targets by adenosine-to-

inosine editing of miRNAs. Science *315*, 1137-1140.

Kuzmin, A., Han, Z., Golding, M. C., Mann, M. R., Latham, K. E., and Varmuza, S. (2008). The PcG gene Sfmbt2 is paternally expressed in extraembryonic tissues. Gene Expr Patterns *8*, 107-116.

LaCasse, E. C., Mahoney, D. J., Cheung, H. H., Plenchette, S., Baird, S., and Korneluk, R. G. (2008). IAP-targeted therapies for cancer. Oncogene *27*, 6252-6275.

Landgraf, P., Rusu, M., Sheridan, R., Sewer, A., Iovino, N., Aravin, A., Pfeffer, S., Rice, A., Kamphorst, A. O., Landthaler, M.*, et al.* (2007). A mammalian microRNA expression atlas based on small RNA library sequencing. Cell *129*, 1401-1414.

Lin, S. P., Youngson, N., Takada, S., Seitz, H., Reik, W., Paulsen, M., Cavaille, J., and Ferguson-Smith, A. C. (2003). Asymmetric regulation of imprinting on the maternal and paternal chromosomes at the Dlk1-Gtl2 imprinted cluster on mouse chromosome 12. Nat Genet *35*, 97-102.

Liu, G., Yuan, X., Zeng, Z., Tunici, P., Ng, H., Abdulkadir, I. R., Lu, L., Irvin, D., Black, K. L., and Yu, J. S. (2006). Analysis of gene expression and chemoresistance of CD133+ cancer stem cells in glioblastoma. Mol Cancer *5*, 67.

Ma, L., Teruya-Feldstein, J., and Weinberg, R. A. (2007). Tumour invasion and metastasis initiated by microRNA-10b in breast cancer. Nature *449*, 682-688.

Schuster-Gossler, K., Bilinski, P., Sado, T., Ferguson-Smith, A., and Gossler, A. (1998). The mouse Gtl2 gene is differentially expressed during embryonic development, encodes multiple alternatively spliced transcripts, and may act as an RNA. Dev Dyn *212*, 214-228.

Seitz, H., Royo, H., Bortolin, M. L., Lin, S. P., Ferguson-Smith, A. C., and

Cavaille, J. (2004). A large imprinted microRNA gene cluster at the mouse Dlk1-Gtl2 domain. Genome Res *14*, 1741-1748.

Shimono, Y., Zabala, M., Cho, R. W., Lobo, N., Dalerba, P., Qian, D., Diehn, M., Liu, H., Panula, S. P., Chiao, E.*, et al.* (2009). Downregulation of miRNA-200c links breast cancer stem cells with normal stem cells. Cell *138*, 592-603.

Sun, Y., Wu, J., Wu, S. H., Thakur, A., Bollig, A., Huang, Y., and Liao, D. J. (2009). Expression profile of microRNAs in c-Myc induced mouse mammary tumors. Breast Cancer Res Treat *118*, 185-196.

Vaillant, F., Asselin-Labat, M. L., Shackleton, M., Forrest, N. C., Lindeman, G. J., and Visvader, J. E. (2008). The mammary progenitor marker CD61/beta3 integrin identifies cancer stem cells in mouse models of mammary tumorigenesis. Cancer Res *68*, 7711-7717.

Wicha, M. S., Liu, S., and Dontu, G. (2006). Cancer stem cells: an old idea--a paradigm shift. Cancer Res *66*, 1883-1890; discussion 1895-1886.

Zhang, B., Pan, X., and Anderson, T. A. (2006). MicroRNA: a new player in stem cells. J Cell Physiol *209*, 266-269.

Zhang, M., Behbod, F., Atkinson, R. L., Landis, M. D., Kittrell, F., Edwards, D., Medina, D., Tsimelzon, A., Hilsenbeck, S., Green, J. E.*, et al.* (2008). Identification of tumor-initiating cells in a p53-null mouse model of breast cancer. Cancer Res *68*, 4674-4682.

Zhou, Z., Flesken-Nikitin, A., Corney, D. C., Wang, W., Goodrich, D. W., Roy-Burman, P., and Nikitin, A. Y. (2006). Synergy of p53 and Rb Deficiency in a Conditional Mouse Model for Metastatic Prostate Cancer. Cancer Res *66*, 7889-7898.

CHAPTER 5

SUMMARY

5.1 Summary of findings

We generated *MMTV-Cre*105Ayn mice to inactivate *p53* and/or *Rb* strictly in the mammary epithelium and determined recurrent genomic changes associated with deficiencies of these genes. *p53* inactivation led to formation of estrogen receptor positive raloxifene-responsive mammary carcinomas with features of luminal subtype B. Rb deficiency was insufficient to initiate carcinogenesis but promoted genomic instability and growth rate of neoplasms associated with *p53* inactivation. Genome-wide analysis of mammary carcinomas by aCGH identified a recurrent amplification at chromosome band 9qA1, a locus orthologous to human 11q22, which contains protooncogenes *cIAP1, cIAP2* and *Yap1.* Interestingly, this amplicon was preferentially detected in carcinomas carrying wild-type *Rb*. However, all three genes were overexpressed in carcinomas with *p53* and *Rb* inactivation, likely due to E2F-mediated transactivation and cooperated in carcinogenesis according to gene knockdown experiments. In addition, knock-down of *cIAP1, cIAP2* and *Yap1*, has cooperative effects on decreasing cell proliferation and increasing cell apoptosis in cell culture, and slowing down the tumor growth *in vivo*. These findings establish a mouse model of human luminal subtype B mammary carcinoma, identify critical role of cIAP1, cIAP2 and Yap co-expression in mammary carcinogenesis and provide an explanation for the lack of recurrent amplifications of *cIAP1*, *cIAP2* and *Yap1* in some tumors with frequent Rb-deficiency, such as mammary carcinoma.

The cancer stem cells (CSC) hypothesis postulates that tumors are maintained by a population of neoplastic cells with stem cell properties such as the ability to self-renew and to produce a progenitor cell that can proliferate and differentiate, presumably after one asymmetric cell division (Wicha et al., 2006). We have isolated CSC from a mouse model of mammary carcinoma associated with *p53* and/or Rb deficiency by using the mammary stem cell markers CD24 and CD49f. CSC have higher frequency of colony formation in Matrigel, exhibited higher tumorigeneicity and were able to reconstitute all tumor cell populations after serial orthotopic transplantations as compared to CnSC. Our studies also determined that CSC have higher level genomic stability and exhibit less of DNA damage as compared to CnSC. We have also studied the role of mammary stem cells in carcinogenesis, and found that loss of either *p53* or *Rb* leads to an increase in the number and proliferation rate of Ma-CFCs (mammary progenitor cells) but not MRUs (mammary stem cells). Both parameters are further increased in Ma-CFC pool deficient for both p53 and Rb. The mammary progenitor cells may be the principle targets for malignant transformation, and suggest expansion of progenitor cell pool as a novel cooperative effect of *p53* and *Rb* inactivation on carcinogenesis.

Finally, microarray analysis have identified miR-376b and miR-467b as the most downregulated miRNAs in both CSC and mammary stem cells, as compared to CnSC and normal differentiated mammary epithelial cells. Using bioinformatics and luciferase reporter assay, we have determined that cIAP1 and cIAP2 proto-oncogenes as targets of both miRNAs. It has been further demonstrated that cIAP1/2 are overexpressed in CSC as compared to CnSC, and miR-376b and miR-467b reconstitution leads to decreased levels of cIAP1/2 according to quantitative RT-PCR and western blotting. Luciferase

reporter assay has directly confirmed that miR-376b and miR-467b may regulate cIAP1/2 expression. Accordingly, miR-376b and miR-467b reconstitution, as well as cIAP1/2 siRNA-mediated knockdown decrease the mammosphere formation from CSC, inhibiting cell proliferation and promote cell apoptosis. These studies indicate that miR-376b/ miR-467b - cIAP1/2 pathway is important for CSC function and may represent a new target for development of new therapeutic approaches.

In summary (Fig 5.1), our studies have demonstrated that deregulation of miR-376b/miR-467b-cIAP1/2 pathway has an important role in mammary carcinoma associated with p53 or p53 and Rb deficiency. Overexpression of cIAP1/2 is ensured by gene amplification in neoplasms associated with p53 deficiency. Rb loss induces transcription factor E2F expression, which transactivates cIAP1 and cIAP2 expression, thereby eliminating the need for amplification of these genes. Additionally, mammary carcinomas have decreased levels of miR-376b/miR-467b, which have been proven to directly suppress expression of cIAP1/2. At least a part of miR-376b/miR-467b-cIAP1/2 pathway's effects on carcinogenesis may be explained by its role in self-renewal of CSC. It should be noted that cIAP1/2 are negative regulators of both classic and alternative NF-κB signaling (Mahoney et al., 2008), which has a key role in many physiological processes, including cell proliferation, differentiation, death, and inflammation, etc (Baud and Karin, 2009). It is known that p53 induces differentiation of mouse embryonic stem cells by suppressing *Nanog* expression (Lin et al., 2005). Nanog maintains pluripotency of mouse embryonic stem cells by inhibiting NF-κB (Torres and Watt, 2008). As discussed below, involvement of NF-κB in CSC will be explored in the future.

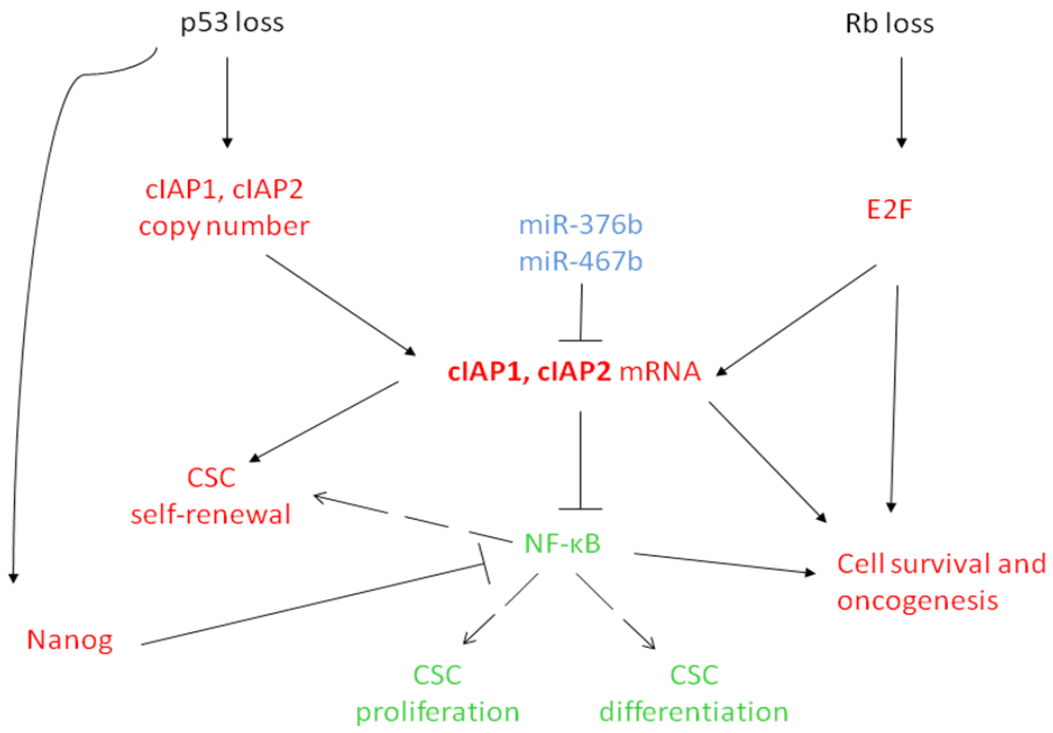

Figure 5.15 Proposed model for miR-376b/miR-467b-cIAP1/2 pathway in mammary carcinogenesis.

p53 loss leads to cIAP1/2 DNA copy number increase, which causes the overexpression of cIAP1/2. Rb loss leads to E2F expression, which transactives cIAP1/2. miR-376b/miR-467b are downregulated in mammary carcinoma associated with *p53* and/or *Rb* inactivation. cIAP1/2 are downregulated by miR-376b/miR-467b. miR-376b/miR-467b and cIAP1/2 are likely involved in regulation of CSC self-renewal. NF-κB signaling may be the downstream target of miR376b/467b-cIAP1/2 pathway.

5.2 Future research

Further characterization of CSC. Our experiments have demonstrated that mammary carcinomas can be reproducibly initiated by *p53* inactivation alone and their formation can be accelerated by inactivation of *Rb*. Our studies also demonstrated presence of CSC in these tumors and indicated that these cells express high levels cIAP1 as compared to CnSC and all types of cells in the normal mammary epithelium. Based on these observations we intend to identify CSC at sequential stages of mammary carcinogenesis and determine time of appearance of *cIAP1* expressing cells by standard immunohistochemistry analysis. In addition, we intend to investigate properties of CSC, such as their proximity to the invasive front of tumor and vessels, their motility, proliferation and apoptosis and response to hypoxia, and chemotherapeutic agents.

Further study of the connection between expanded mutant mammary progenitor (Ma-CFC) and CSC. In chapter 3, we identified and characterized CSC, and also found that expansion of mammary precursor cells (Ma-CFC) but not stem cells (MRU) in development of mammary neoplasms associated with p53 and/or Rb deficiency. One of interesting questions that has not yet been answered is the relationship of expanded Ma-CFC population and CSC. Are Ma-CFC the cell origin of CSC? The limitation of the current mouse model for addressing this question is low efficiency of *Cre*-mediated recombination in MRU and Ma-CFC. Only 2.8% of MRU and 3.4% of Ma-CFC have Cre expression. Therefore we intend to use additional available lines of MMTV-Cre transgenic mice, such as MMTV-Cre line F (Wagner et al., 1997). According to our preliminary results around 50% Ma-CFC and MRU have Cre expression in this line. As a future additional

important tool, mice with temporal regulation of Cre are planned to be generated. By using crosses of these *MMTV-Cre* mice with $p53^{L/L}$, $Rb^{L/L}$ and $p53^{L/L}Rb^{L/L}$ mice, it should be possible to further investigate roles of p53 and Rb in control of mammary stem and progenitor cells and to determine if expanded pool of mutant Ma-CFC gives rise to CSC.

Investigation of mechanism of E2F-mediated regulation of cIAP1, cIAP2 and Yap1, and p53-mediated regulation of Yap1. Our results in Chapter 2 demonstrated that knock down of E2F leads to the decrease of cIAP1, cIAP2 and Yap1 expression. According to bioinformatics, the promoter regions of these genes have E2F binding sites. It would be important to confirm if this is the mechanism of E2F-mediated regulation of cIAP1, cIAP2 and Yap1. To that end we are going to use Chromatin immunoprecipitation (ChIP) assay, which is a powerful tool for identifying proteins associated with specific regions of the genome by using specific antibodies that recognize a specific protein. In addition, according to computational analysis, Yap1 intron 1 contains 100% matching p53 binding site. Consistently, decrease and increase of Yap1 expression is observed after p53 deletion and doxorubicin-induced p53 upregulation, respectively. It will be of particular interest to identify mechanisms substituting for p53-mediated Yap1 transcriptional activation in p53 deficient tumors. Answers to these questions will help us further understand the mechanisms of mammary carcinogenesis associated with p53 and Rb inactivation.

Mechanism of chemoresistance and radioresistence of CSC. Recent studies have shown that CSC are resistant to chemo- and radiation therapy (An and Ongkeko, 2009; Bao et al., 2006; Chiou et al., 2008). It has also been demonstrated that overexpression of cIAP1 causes resistance to

drug treatments in certain types of breast cancer (Wang et al., 2009). As discussed in the dissertation, we found that overexpression of cIAP1 is associated with downregulation of miR-376b. Therefore, we want to test if the resistance of CSC to therapy is due to the overexpression of cIAP1 and/or downregulation of miR-376b. The simple test will be knockdown the cIAP1 expression or reconstitute miR-*376b* in CSC, treat CSC with therapeutic drugs or γ irradiation, and determine if downregulation of cIAP1 or normalization of miR-376b levels sensitizes CSC to chemo- and radiation therapy. Furthermore, to make our model even more relevant to human cancer, we are going to isolate CSC from these cell human breast cancer cell lines, and check cIAP1 and miR-376b expression. High expressing cIAP1 and low expressing miR-376b cell lines will be selected for chemo- and radiation treatments, and the response of CSC to therapeutic drugs or irradiation with or without cIAP1 knockdown or *pre-miR-376b* treatment will be compared.

Effects of cIAP1 overexpression and deficiency on regulation of normal mammary stem, progenitor and differentiated cells, as well as CSC and CnSC in vivo. Our results demonstrated that recurrent amplification of human cancer-related genes cIAP1, cIAP2 and Yap was detected in mouse mammary carcinomas associated with inactivation of *p53* alone or together with *Rb*. Notably these genes are upregulated specifically in cancer stem cells. Effects of cIAP1 deficiency on regulation of CSC have been studied in cell culture. We need to further study the deficiency of cIAP1 in normal mammary stem, progenitor and differentiated cells. To evaluate effects of cIAP1 on regulation of all these cells in vivo, we plan to use mice deficient for cIAP1 and cIAP2. We also propose to test if overexpression of these genes may represent an early and essential step towards selection of a subset of highly

tumorigenic CSC.

To evaluate effects of cIAP1 deficiency, mammary epithelial cells carrying inactivated cIAP1 will be isolated from young (60 days old) female mice resulting from crosses of $p53^{ME-/-}Rb^{ME-/-}$ mice with $cIAP1^{-/-}$ mice and either processed for cell isolation followed by FACS and/or cell culture or directly implanted into cleared mammary fat pad. At the same time, mammary cells of $p53^{floxP/floxP}Rb^{floxP/floxP}$ mice and $p53^{floxP/floPx}Rb^{floxP/floxP}$ $cIAP1^{-/-}$ mice will be initially isolated, placed in cell culture or sorted with FACS and exposed to either Ad*CMV*Cre or lentivirus Cre. After each approach, cells will be tested for proliferation, survival, self-renewal, senescence, differentiation and malignant transformation. Furthermore, effects of cIAP1 overexpression will be studied by introduction of *cIAP1* expression constructs into primary mammary cells sorted for stem cell markers. Furthermore, transgenic mice with conditional expression of *cIAP1*will be generated and crossed to $p53^{ME-/-}$ and/or $Rb^{ME-/-}$ mice and effect of cIAP1 on progression and metastasis of mammary neoplasms in the context of either p53 or Rb deficiency will be established.

Further study of the function of miR-376b and miR467b in mammary stem cells and CSC self-renewal. The role of miR-376b and miR-467b in MaSC and CSC, especially in *in vivo* has not been fully addressed in my study. To fill this void, MaSC and CSC will be infected with microRNA lentivirus vector, which can continuously express miR-376b and/or miR-467b. Infected MaSC or CSC will then be transplanted to cleared mammary fat pad to observe the effects of these miRNAs on either mammary gland tree formation or mammary carcinoma formation. MaSC and CSC from transplant tissues will be separated by FACS sorting to have the second and third round transplantation. We predict that these miRNAs could delay or reduce the

ability of MaSC to form mammary gland tree, and could affect CSC form mammary carcinoma *in vivo*. If these expectations have been met, generation of mice carrying floxed copies of miR-376b and miR-467b will be initiated.

Role of NF-κB signaling pathway in CSC regulation. Recently, it has been shown that cIAP1/2 are negative regulators of both classic and alternative NF-κB signaling (Mahoney et al., 2008). Our results have shown overexpression of cIAP1/2 preferential overexpression of cIAP1/2 in CSC, but role of NF-κB signaling in CSC remains unknown. NF-κB signaling pathway is often altered in human cancers, including both solid and hematopoietic malignances (Baud and Karin, 2009). NF-κB pathway is involved in diverse biological processes, including embryo development, hematopoiesis, immune regulation, and neuronal functions through the transcriptional activation of genes associated with these processes (Baud and Karin, 2009). In addition, it has been found that Nanog maintains pluripotency of mouse embryonic stem cells by inhibiting NF-kB (Torres and Watt, 2008), and the activity of NF-κB is increased during differentiation of embryonic stem cells (Kim et al., 2008). Activation of NF-κB could trigger the proliferation of adult neural stem cells (Widera et al., 2006). Therefore, it is of interest to determine if NF-κB signaling plays a role in CSC regulation.

First of all, we will study the NF-κB activity in CSC as compared to CnSC. If the result is consistent with our predication, we will further investigate the role of NF-κB in CSC self-renewal by either knocking down or overexpressing individual components of NF-κB pathway in cell culture and *in vivo* experiments.

REFERENCES

An, Y., and Ongkeko, W. M. (2009). ABCG2: the key to chemoresistance in cancer stem cells? Expert Opin Drug Metab Toxicol *5*, 1529-1542.

Bao, S., Wu, Q., McLendon, R. E., Hao, Y., Shi, Q., Hjelmeland, A. B., Dewhirst, M. W., Bigner, D. D., and Rich, J. N. (2006). Glioma stem cells promote radioresistance by preferential activation of the DNA damage response. Nature *444*, 756-760.

Baud, V., and Karin, M. (2009). Is NF-kappaB a good target for cancer therapy? Hopes and pitfalls. Nat Rev Drug Discov *8*, 33-40.

Chiou, S. H., Kao, C. L., Chen, Y. W., Chien, C. S., Hung, S. C., Lo, J. F., Chen, Y. J., Ku, H. H., Hsu, M. T., and Wong, T. T. (2008). Identification of CD133-positive radioresistant cells in atypical teratoid/rhabdoid tumor. PLoS One *3*, e2090.

Kim, Y. E., Kang, H. B., Park, J. A., Nam, K. H., Kwon, H. J., and Lee, Y. (2008). Upregulation of NF-kappaB upon differentiation of mouse embryonic stem cells. BMB Rep *41*, 705-709.

Lin, T., Chao, C., Saito, S., Mazur, S. J., Murphy, M. E., Appella, E., and Xu, Y. (2005). p53 induces differentiation of mouse embryonic stem cells by suppressing Nanog expression. Nat Cell Biol *7*, 165-171.

Mahoney, D. J., Cheung, H. H., Mrad, R. L., Plenchette, S., Simard, C., Enwere, E., Arora, V., Mak, T. W., Lacasse, E. C., Waring, J., and Korneluk, R. G. (2008). Both cIAP1 and cIAP2 regulate TNFalpha-mediated NF-kappaB activation. Proc Natl Acad Sci U S A *105*, 11778-11783.

Torres, J., and Watt, F. M. (2008). Nanog maintains pluripotency of mouse

embryonic stem cells by inhibiting NFkappaB and cooperating with Stat3. Nat Cell Biol *10*, 194-201.

Wagner, K. U., Wall, R. J., St-Onge, L., Gruss, P., Wynshaw-Boris, A., Garrett, L., Li, M., Furth, P. A., and Hennighausen, L. (1997). Cre-mediated gene deletion in the mammary gland. Nucleic Acids Res *25*, 4323-4330.

Wang, M. Y., Chen, P. S., Prakash, E., Hsu, H. C., Huang, H. Y., Lin, M. T., Chang, K. J., and Kuo, M. L. (2009). Connective tissue growth factor confers drug resistance in breast cancer through concomitant up-regulation of Bcl-xL and cIAP1. Cancer Res *69*, 3482-3491.

Wicha, M. S., Liu, S., and Dontu, G. (2006). Cancer stem cells: an old idea--a paradigm shift. Cancer Res *66*, 1883-1890; discussion 1895-1886.

Widera, D., Mikenberg, I., Elvers, M., Kaltschmidt, C., and Kaltschmidt, B. (2006). Tumor necrosis factor alpha triggers proliferation of adult neural stem cells via IKK/NF-kappaB signaling. BMC Neurosci *7*, 64.